Universität Zürich[UZH]

Department of Geography

Assessing destabilization patterns of active rock glaciers in the Turtmann Valley incorporating a general typology for destabilized rock glaciers

GEO 511 Master's Thesis

Author: Claudio Steffen, 19-110-725

Supervised by: Dr. Isabelle Gärtner-Roer

Faculty representative: Prof. Dr. Andreas Vieli

26.04.2025

Abstract

Rock glacier destabilization is a complex process that has gained increasing scientific attention, yet its classification and underlying mechanisms remain insufficiently understood. This thesis contributes to the understanding of destabilized rock glaciers by developing a general typology that integrates topographic setting with morphological and kinematic indicators. The typology serves to define diagnostic characteristics, which are applied to assess the long-term evolution of nine selected rock glaciers in the Turtmann Valley, Swiss Alps, using true orthophotos and elevation models from 1968 to 2023. Horizontal displacement is reconstructed using CIAS, vertical changes are quantified through DEM of Difference analysis, and surface disturbance evolution is examined through image interpretation.

The results show that destabilization affects nearly half of the studied rock glaciers, extending beyond previously known cases. Distinct patterns of acceleration, mass redistribution, and surface disturbance confirm that destabilization is a gradual and spatially heterogeneous process. A comparison with other Alpine regions highlights both parallels and regional particularities, supporting the hypothesis that local topographic and internal factors modulate the response of rock glaciers to climatic forcing.

The typology developed in this study offers a transferable framework for the classification of destabilized rock glaciers. Future research should focus on deepening the understanding of the processes driving destabilization, particularly in the context of ongoing climate change.

List of Content

1. List of Figures

2. List of Tables

3. List of Abbreviations

AROSICS	Automated and Robust Open-Source Image Co-Registration Software
a.s.l.	above sea level
b/w	black and white
CIAS	Correlation Image Analysis Software
DEM	Digital Elevation Model
DoD	DEM of Difference
DSM	Digital Surface Model
DTM	Digital Terrain Model
IPCC	Intergovernmental Panel on Climate Change
LiDAR	Light Detection and Ranging
PERMOS	Swiss Permafrost Monitoring Network
RGIK	IPA Action Group: Rock glacier inventories and kinematics
RMSE	Root Mean Square Error

4. Introduction

4.1. Research context and relevance

Climate change is one of the defining challenges of the 21st century, with profound implications for all components of the Earth system. As highlighted in the Sixth Assessment Report of the Intergovernmental Panel on Climate Change (IPCC, 2023), the cryosphere is particularly sensitive to global warming and the ongoing temperature increase is causing fundamental changes in periglacial environments. Among the landforms most directly affected are rock glaciers.

In recent years, increasing attention has been paid to the response of rock glaciers to climate change. A growing number of studies (e.g. Delaloye et al., 2010; Kellerer-Pirklbauer et al., 2024; Marcer et al., 2021) have documented a general trend of surface velocity increase in many active rock glaciers across the European Alps over the past decades, which is widely interpreted as a consequence of rising ground temperatures associated with climate warming. In addition to this acceleration some rock glaciers undergo more profound morphological transformations, including the development of cracks, crevasses and scarps. This is commonly referred to as rock glacier destabilization.

Several destabilized rock glaciers have been studied in detail (e.g. Bodin et al., 2017; Buchli et al., 2018; Delaloye et al., 2013; Delaloye & Morard, 2011; Ghirlanda et al., 2016; Lambiel, 2011; Roer et al., 2008; Scotti et al., 2016; Vivero et al., 2022). However, the terminology and criteria for classifying rock glacier destabilization remain inconsistent in the literature. Recent work by Marcer et al. (2019) and Schoeneich et al. (2015) represents an important step toward establishing more consistent frameworks for identifying and classifying destabilized rock glaciers. Nevertheless, a comprehensive typology that accounts for topographic setting, the interplay of kinematic and morphological anomalies as well as temporal evolution is still lacking. There is a particular need for approaches that go beyond individual case studies and allow for systematic comparison across multiple rock glaciers within a defined region.

The Turtmann Valley in the Swiss Alps provides an ideal setting to address these knowledge gaps. It hosts a large number of active rock glaciers, several of which have been previously studied in terms of their kinematics and thermal properties (Roer et al., 2005, 2008). Notably, the Furggwanghorn rock glacier has been identified as

destabilized and is among the best-documented cases in the region (Buchli et al., 2013, 2018; Springman et al., 2013). While also Gruob rock glacier has been determined as destabilized (Roer et al., 2008), a systematic classification and comparative evaluation of other rock glaciers in the valley related to destabilization has not yet been undertaken.

The relevance of studying rock glacier destabilization extends beyond academic interest, as destabilized rock glaciers increasingly interact in hazard cascade processes. As they degrade, they often accumulate loose debris at their fronts, which may be remobilized under given meteorological conditions, triggering debris flows or rockfalls (Kummert et al., 2017). The Matter Valley, adjacent to the Turtmann Valley, has experienced increased debris-flow activity in certain channels (e.g., Ritigraben) due to the destabilization of rock glaciers overlying these channels (Delaloye et al., 2013; Saarbach R., personal communication 2024). In France, the destabilization of the Lou rock glacier enabled a debris flow that caused damage exceeding €100,000 in the village of Lanslevillard (Marcer et al., 2020). With climate change expected to further increase the frequency and intensity of such processes (Springman et al., 2013), a better understanding of the mechanisms and indicators of rock glacier destabilization is essential for anticipating hazards and improving risk management.

4.2. Objectives

This thesis aims to improve the scientific understanding of destabilized rock glaciers by systematically analysing their long-term development in the Turtmann Valley. The phenomenon of destabilization remains ambiguously defined and inconsistently classified. A first objective of this work is therefore to synthesise existing definitions and classification approaches in order to develop a more coherent and operational framework. Particular emphasis is placed on distinguishing between different manifestations of destabilization.

Building on this conceptual foundation, the study investigates the extent to which destabilization occurs among the active rock glaciers of the Turtmann Valley. Previous research has identified the Furggwanghorn and Gruob rock glacier as destabilized and general acceleration trends have been observed throughout the valley. This raises the question of whether other rock glaciers in the region show similar signs of destabilization, or whether Furggwanghorn and Gruob represent isolated cases.

In addition to the development of a classification framework for destabilized rock glaciers, this thesis is guided by the following research questions:

- To what extent do active rock glaciers in the Turtmann Valley exhibit signs of destabilization over the study period?
- How do the observed developments in the Turtmann Valley compare to those reported from other Alpine regions, and what implications arise for the broader understanding of rock glacier evolution in a changing climate?

To address these research questions, the following hypotheses are tested:

- An increasing number of rock glaciers exhibit signs of destabilization over the study period.
- The observed development of active rock glaciers in the Turtmann Valley partially aligns with trends from other Alpine regions but also shows region-specific characteristics that limit generalisation.

5. Theoretical Background Rock Glaciers

To study destabilized rock glaciers, it is essential to first define "normal" rock glaciers and understand their fundamental characteristics and processes. Rock glaciers are found worldwide in high mountain regions with cold, dry, and continental climates, as well as in Arctic and Antarctic areas (Barsch, 1992). The following chapters on definition and form are globally applicable. However, the sections on structure, processes, and current development are mainly based on studies from the Alps. The observed trends are specific to the European Alps and should not be directly applied to other regions.

5.1. Definition

Barsch (1996) defines active rock glaciers as "*lobate or tongue-shaped bodies of perennially frozen unconsolidated material supersaturated with interstitial ice and ice lenses that move downslope or downvalley by creep as a consequence of the deformation of ice contained in them and which are, thus, features of cohesive flow*". This definition is widely regarded as comprehensive and well-respected in scientific literature.

Another prominent definition by Barsch (1996), following Haeberli's (1985) approach, describes active rock glaciers as "*the visible expression of steady-state creep of ice-supersaturated mountain permafrost bodies in unconsolidated material. They display the whole spectrum of forms created by cohesive flows*." This formulation is more process-oriented. Similarly, Haeberli et al. (2006) define rock glaciers as "*steadily creeping perennially frozen and ice-rich debris on non-glacierised mountain slopes*".

The Rock Glacier Inventories and Kinematics (RGIK) Action Group, an IPA initiative comprising over 200 permafrost scientists, adopts a different approach. Their focus is on inventorying rock glaciers, for which they employ a morphological definition. According to RGIK guidelines, rock glaciers are defined as *"debris landforms generated by the former or current creep of frozen ground (permafrost), detectable in the landscape with the following morphologies: front, lateral margins and optionally ridge-and-furrow surface topography"*. This definition is specifically

tailored for operational use and deliberately bypasses the ongoing controversy surrounding rock glacier genesis (RGIK, 2023).

While several definitions of rock glaciers exist, some researchers argue that the phenomenon cannot be precisely defined due to the complex interactions and gradual transitions to other landforms, such as debris cones, protalus ramparts, or even moraines. This has led to what Haeberli & Vonder Mühll (1996) describe as a "*seemingly endless discussion in the geomorphological literature*". Indeed, the debate over the definition of rock glaciers persists even decades later. Berthling (2011) discusses different approaches to defining rock glaciers, either by their genesis or appearance. He advocates for a generic definition, describing rock glaciers as "*the visible expression of cumulative deformation by long-term creep of ice/debris mixtures under permafrost conditions",* and suggests abandoning purely morphological definitions.

The aforementioned definitions illustrate the diverse approaches to defining rock glaciers, each shaped by the specific focus of the respective study. However, it is beyond the scope of this thesis to engage in a detailed discussion on the rock glacier genesis or propose a universally accepted definition. According to Barsch (1992), an adequate definition of rock glaciers should encompass three key aspects: the form, the material and the processes involved. These elements serve as a useful framework to discuss the most relevant characteristics of rock glaciers for this thesis. The following sections will briefly explore each of these aspects.

5.2. Form

Rock glaciers typically exhibit a distinct morphology. The IPA action group RGIK (2023) identifies three key characteristics that serve as the primary geomorphological indicators for recognizing rock glaciers in the landscape. According to the RGIK guidelines (2023), these features are:

- **Rock glacier front:** Generally characterized by a "*discernable* [quite sharp edge] *talus delimiting the terminus of a moving part of the rock glacier and usually displaying a convex morphology* [in plan view] *perpendicular to the main flow direction. For a rock glacier developing on a steep slope, the front may be difficult to recognize.*" (RGIK, 2023). The guidelines further distinguish

and specify various possible longitudinal profiles to account for the diversity of rock glacier forms.

- **Lateral margins:** These exhibit a "*discernible lateral continuation of the front, but may also be absent, particularly in the upper part of the landform.*" The RGIK guidelines (2023) distinguish between three types of margins: talus-margins, levees, and shear-margins, with combinations of these types also possible.

- **Ridge-and-furrow topography:** This feature originates from "*pronounced convex-downslope or longitudinal-surface undulations associated with current or former compressive flow*" (RGIK, 2023). It should not be confused with transversal cracks and scarps linked to destabilization.

The morphology of the rock glacier front and the lateral margins are considered mandatory criteria for identifying landforms as rock glaciers, while ridge-and-furrow topography is classified as an optional criterion in the RGIK guidelines (2023).

5.3. Material and structure

As mentioned above a rock glacier consists of unconsolidated material supersaturated with interstitial ice and ice lenses (Barsch, 1996). This debris can originate from various sources, including talus slopes with long-lasting rockfall activity, glacial debris (till), debris flows, debris-laden snow avalanches, episodic rock avalanches, or even anthropogenic activities (Barsch, 1992; Haeberli et al., 2006). Continuous debris input from adjacent rock walls is essential for the sustained development of a rock glacier. Common rock types found in rock glaciers include granite, gneiss, sandstone, and limestone (Haeberli et al., 2006).

Most rock glaciers exhibit a characteristic structure, with coarse, blocky debris forming the uppermost layer, known as the active layer. Typically a few meters thick, this layer acts as the interface between the ice-rich permafrost and the atmosphere (Cicoira, 2020; Haeberli, 1985). It plays a crucial role in regulating the energy balance of rock glaciers, controlling conductive, advective, and convective heat fluxes (Cicoira, 2020; Delaloye & Lambiel, 2005; Hanson & Hoelzle, 2004; Wicky & Hauck, 2017).

Beneath the active layer lies the ice-rich core, also referred to as the permafrost body by Haeberli (1985). This layer typically ranges from 10 to 25 meters in thickness and

consists of finer clasts, lithic fragments, and various types of ground ice, which may be polygenetic (Cicoira, 2020; Haeberli, 1985; Haeberli et al., 2006; Haeberli & Vonder Mühll, 1996). The volumetric ice content within the permafrost body is estimated to range between 40% and 70% in alpine rock glaciers (Arenson et al., 2002; Cicoira, 2020; Haeberli et al., 2006; Hausmann et al., 2007, 2012; Kääb & Reichmuth, 2005). However, accurately determining ice content is challenging due to its heterogeneity and limited data availability.

A shear horizon typically underlies the ice-rich core. Although much thinner than the core, usually only a few meters thick, it is crucial for rock glacier creep, as it accounts for 60% to 90% of the total deformation (Arenson et al., 2002; Cicoira, 2020). Within this layer, both the volumetric ice content (ranging from 20% to 50%) and debris grain size tend to decrease (Arenson & Springman, 2005; Cicoira, 2020; Haeberli et al., 1988).

The following figure summarizes the most relevant characteristics and their evolution across the different layers of a rock glacier.

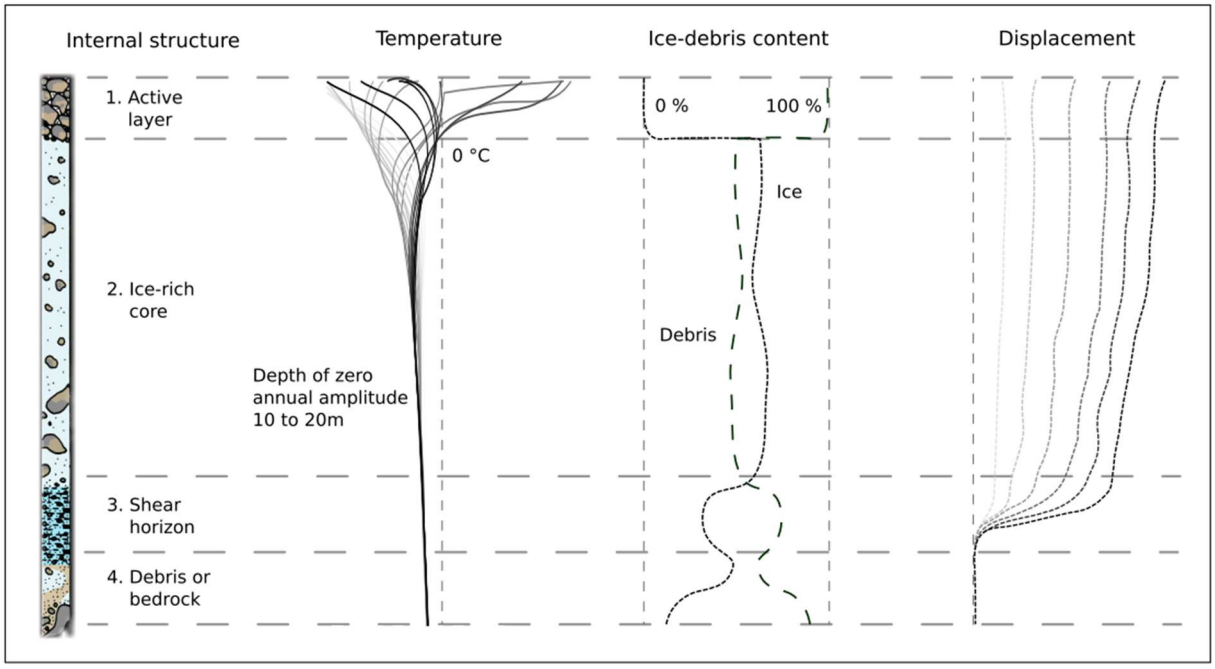

Figure 1Typical internal structure of a rock glacier based on borehole investigations (Figure from Cicoira, 2020).

5.4. Processes

The fundamental process underlying active rock glaciers is the creeping of permafrost downslope or downvalley, with typical velocities for alpine rock glaciers ranging from 0.1 to 2 m/year (Barsch, 1992, 1996; Delaloye et al., 2010, 2013; Haeberli, 1985; Haeberli et al., 2006). This creep is not evenly distributed vertically throughout the entire rock glacier but is strongly governed by deformation or shearing within the specific layers.

In the active layer, deformation primarily results from tilting, rolling, or sliding of boulders atop the permafrost table. However, its contribution to the overall surface velocity is typically low and considered negligible (Cicoira, 2020). In contrast, deformation within the ice-rich core is driven mainly by the creep of its ice component (Arenson et al., 2007), which is sensitive to temperature variations. Warmer ice exhibits greater ductility than colder ice, altering stress-strain relationships (Delaloye et al., 2013; Roer et al., 2008). Seasonal temperature fluctuations can penetrate the core with a time lag, causing temperature variations that influence its deformation behaviour. This layer is estimated to contribute 10–40% to the total rock glacier displacement (Arenson et al., 2002). The majority of the deformation, accounting for 60–90% of the total displacement, occurs within the shear horizon (Arenson et al., 2002). Borehole studies have identified the presence of unfrozen pore water in this layer, indicating a significant role of pore water on deformation behaviour (Buchli et al., 2018; Ikeda et al., 2008). Pore water pressure within the shear horizon strongly influence deformation rates by reducing effective stress, thereby weakening the ice-debris mixture and enhancing deformation (Cicoira, 2020; Ikeda et al., 2008; Moore, 2014).

The deformation behaviour in each layer is strongly influenced by the applied strain rate, as well as the specific characteristics and composition of the rock glacier. This results in substantial variability between different rock glaciers. Moreover, topographical factors significantly affect creep behaviour and should be carefully considered when analysing individual cases (Delaloye et al., 2010).

5.5. Current development

Over the past three decades, nearly all European alpine rock glaciers have experienced a significant acceleration in surface flow velocity. While there have been kinematic fluctuations during this period, with phases of faster and slower movement, the overall trend of acceleration is evident (Delaloye et al., 2010; Kellerer-Pirklbauer et al., 2024; Marcer et al., 2021; Roer et al., 2005). Figure 2 illustrates the relative change in rock glacier velocities of alpine rock glaciers compared to the reference period 2016–2018, clearly emphasizing this acceleration trend.

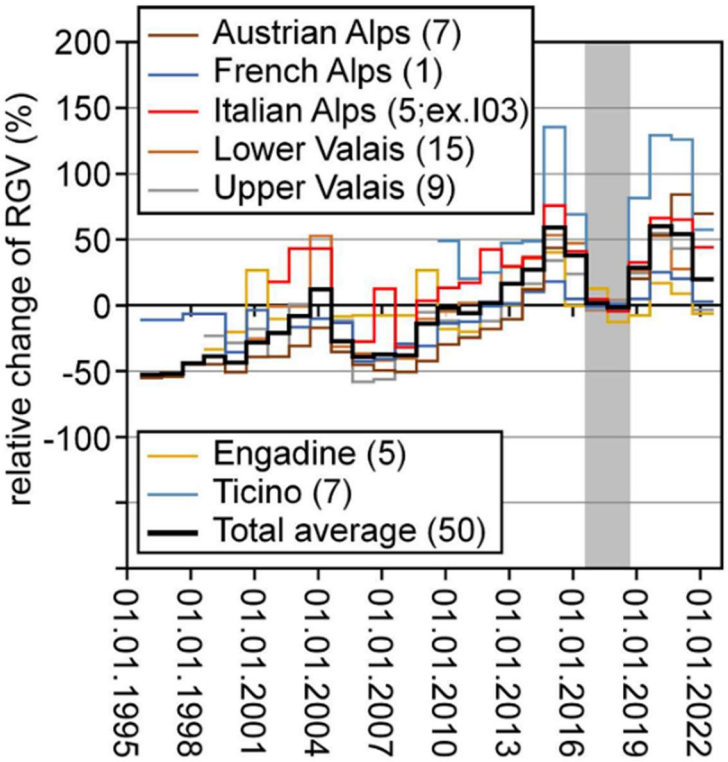

Figure 2 Regional and total averages of horizontal rock glacier velocity (RGV) relative to the reference period 2016-2018 (grey area) since 1995 (Figure from Kellerer-Pirklbauer et al., 2024).

While local factors must be considered when identifying the specific causes of acceleration at each location, a general link has been established between increased surface temperatures and higher surface flow velocities (Hartl et al., 2016; Kääb et al., 2007; Marcer et al., 2021). The precise interactions and underlying processes are complex and not yet fully understood, but two main dynamics have been proposed.

It is anticipated that an increase in surface temperature can cause significant changes in the mechanical properties of the rock glacier material, even at the depth of the shear horizon (Cicoira, 2020). Particularly under “warm” ground conditions, where perennially frozen material is close to 0°C, even a slight temperature rise can enhance

deformation in the shear horizon (Kääb et al., 2007). This is likely due to increased liquid pore water availability resulting from permafrost degradation (i.e. warming and thawing of permafrost). Higher pore water content raises pore pressure, which reduces the effective strength of the ice-debris mixture and promotes enhanced deformation (Cicoira, 2020; Davies et al., 2001; Ikeda et al., 2008; Moore, 2014). Nonetheless, the precise dynamics governing deformation within the shear horizon remain insufficiently understood, necessitating further research.

Another probable factor contributing to enhanced deformation and acceleration is the warming of permafrost in the ice-rich core. This leads to a change in the rheological properties of the ice, with warmer ice being more ductile than colder ice (Davies et al., 2001; Delaloye et al., 2013; Roer et al., 2008). The increased ductility and decreased internal strength of the ice itself leads to stronger deformation, which in turn contributes to overall increased rock glacier deformation. Additionally, it is plausible that thermal degradation increases the water content in the ice-rich core, further affecting the mechanical properties in this layer.

6. Destabilized Rock Glaciers – Typology & Definition

The concept of rock glacier destabilization has gained significant attention due to ongoing climatic changes that are increasingly influencing periglacial systems. Despite numerous studies focusing on destabilized rock glaciers, no universally accepted definition and classification system encompassing all observed types of destabilization currently exists. For instance, Schoeneich et al. (2015) propose a differentiation into five rock glacier reaction types associated to velocity increases. While this can serve as a useful starting point, it does not adequately account for topographical differences and falls short of categorizing and distinctly separating all observed forms of destabilization.

The following classification seeks to address these gaps by providing a clear framework to categorize all documented types of destabilized rock glaciers to date, with topography serving as the fundamental differentiator. This typology aims to capture the different destabilization processes observed in rock glaciers and emphasizes how these processes are influenced by various factors. By establishing the classification, it becomes clear what specific indicators to observe when assessing destabilization trends in the Turtmann Valley, making this a crucial step in the analytical process. Grounded in an extensive review of the existing literature on documented case studies, this typology further facilitates comparison and structured discussion of different cases. The proposed classification distinguishes the following types of (destabilized) rock glaciers:

6.1. Typology

6.1.1. Type 0: New "normal" alpine rock glaciers – Thermally induced degradation without destabilization

Type 0 represents the current state of most alpine rock glaciers, reflecting the impacts of ongoing climate change. Under present warming conditions, all alpine rock glaciers are increasingly affected by thermal degradation. Rising temperatures alter the mechanical and rheological properties of the ice-debris mixture, leading to increased surface creep velocities. The specific processes driving these changes are discussed in chapter *5.5*. Despite the acceleration, these rock glaciers generally retain their original morphology (mostly the form described in chapter 5.2) and do not exhibit significant structural changes. Therefore, increased creep velocities alone should not be mistaken for destabilization. Rather, it reflects the current reality, where creep rates are reaching new dimensions compared to older textbooks and studies. Type 0 serves as a baseline for understanding the thermal processes affecting alpine rock glaciers today, distinguishing these processes from the destabilization mechanisms that lead to more dramatic morphological changes. This type of rock glacier is independent of topography and can develop on any slope allowing rock glacier formation.

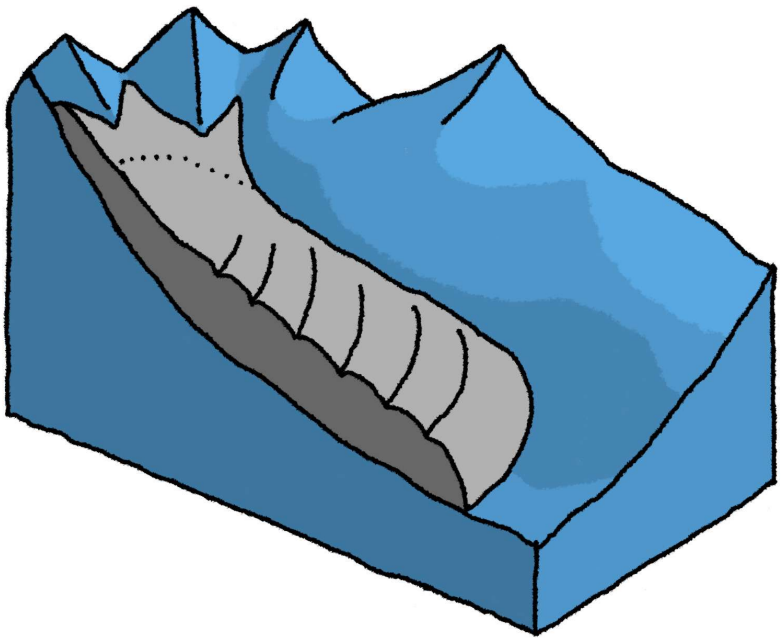

Figure 3 Schematic illustration of rock glacier type 0

6.1.2. Type 1: Destabilized rock glacier on a concave or uniform slope

The most observed form of destabilization occurs on rock glaciers situated on concave or nearly uniform slopes. These destabilized rock glaciers exhibit significant changes in kinematic behaviour, mostly characterized by localized acceleration in creep velocity, which can reach up to 2-5 meters per year. This kinematic shift is accompanied by the formation of transversal cracks and scars on the rock glacier surface (Delaloye & Morard, 2011; Hartl et al., 2016; Lambiel, 2011; Roer et al., 2008; Schoeneich et al., 2015). These cracks resemble crevasses on glaciers and are predominantly found in the middle and lower parts of the rock glacier. Due to their location on concave or linear slopes, no substantial evacuation of debris through secondary cascade processes occurs. Instead, the rock glacier tongue typically advances, overrunning its own blocks and leading to the formation of a rigid, blocky basal layer. This layer effectively traps sediment, thereby preventing the mobilization of large amounts of material further downslope (Kummert et al., 2017).

These characteristics are common to all destabilized rock glaciers of Type 1. For a more precise classification, these rock glaciers are further divided into two subtypes, as the overarching Type 1 category serves only as a general descriptor for those occurring on concave and linear slopes. The subtypes, distinguished by the presumed initiation mechanism of the destabilization process, are explained below.

- **Type 1a: Thermally and hydrologically induced**

  At rock glaciers of this type, the destabilization process can be induced by significant changes in the thermal and hydrological conditions. Permafrost warming increases ice ductility and enhances the presence of unfrozen pore water within the rock glacier (Delaloye et al., 2013; Ikeda et al., 2008; Lambiel, 2011). While these processes affect all alpine rock glaciers (see chapter 5.5), they are expected to occur here to such an extreme extent that they fundamentally alter the rheological behaviour. This leads to a severe increase in internal deformation and shearing, making the rock glacier more susceptible to destabilization. It is hypothesized that complete destabilization occurs after surpassing a critical threshold. In terms of dynamics and deformation processes, this type of destabilized rock glacier is often compared to rotational landslides in the literature (e.g. Buchli et al., 2018; Delaloye et al., 2010; Delaloye & Morard, 2011; Lambiel, 2011; Marcer et al., 2021; Roer et al., 2008).

Once the destabilization process has initiated, the ongoing dynamics and processes are expected to resemble those of rotational landslides, with rock glacier packages tilting along shear horizons in the lower part. Examples of this type of destabilized rock glaciers include those at Petit-Vélan (Delaloye & Morard, 2011), Tsaté-Moiry (Lambiel, 2011), and also Furggwanghorn (Buchli et al., 2018) and Gruob in the Turtmann valley (Roer et al., 2008), to name a few.

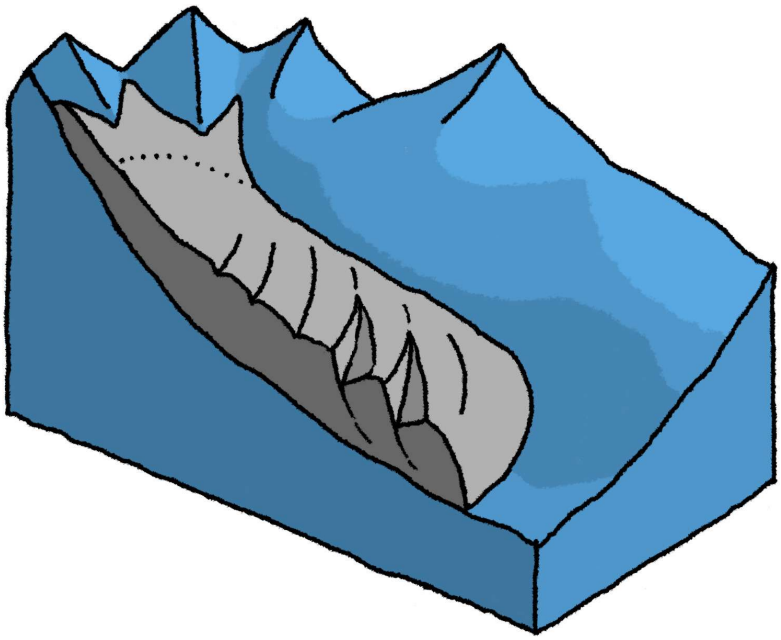

Figure 4 Schematic illustration of rock glacier type 1a

- **Type 1b: Mechanically induced destabilization**

  In addition to thermal and hydrological processes, external mechanical processes can also induce rock glacier destabilization. Specifically, this can involve mechanical overloading of the rock glacier through rockfall, landslides, or rock avalanches. The deposition of additional sediment on the rock glacier can cause strong deformation and initiate destabilization (Delaloye et al., 2013). While the precise dynamics of this process remain understudied, it can be hypothesized that sediment overloading alters internal stress distributions, thereby promoting destabilization. For example, Scotti et al. (2016) suggest that the destabilization of the Plator rock glacier in Italy may have been triggered by the overloading of rockfall deposits. If such deposits accumulate in the rooting zone of a rock glacier, a compression wave, also referred to as mechanical surge, can develop. This wave can then slowly propagate through the rock glacier, leading to destabilization over time (Delaloye et al., 2013).

  Other external mechanical processes capable of triggering rock glacier destabilization include advancing glaciers, which may disrupt pre-existing frozen sediments and destabilize the entire rock glacier (Reynard et al., 2003). Earthquakes are another potential mechanism; however, to date, no documented case has definitively linked an earthquake to the initiation of rock glacier destabilization.

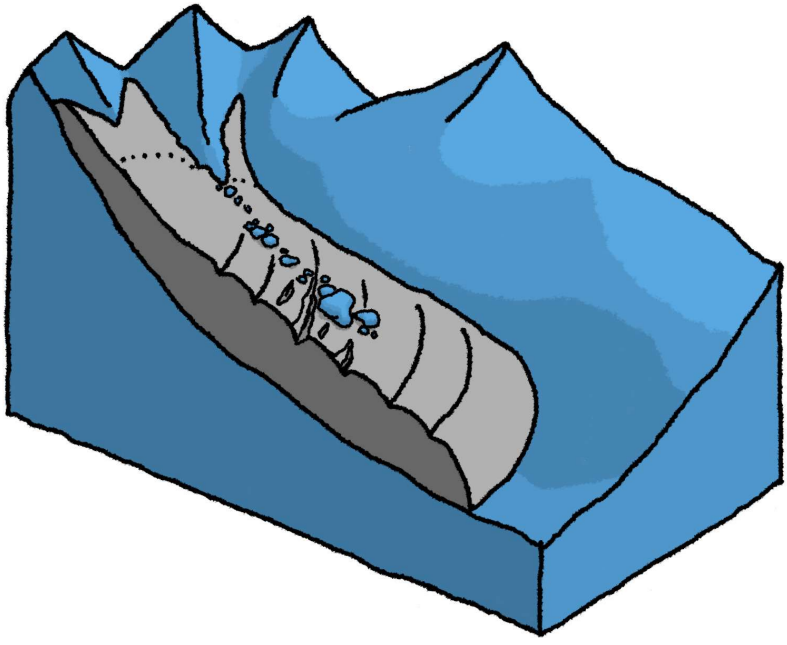

Figure 5 Schematic illustration of rock glacier type 1b

6.1.3. Type 2: Destabilized rock glacier on a convex slope with steep terminal section

Destabilized rock glaciers on convex slopes with steep terminal sections exhibit even greater kinematic changes compared to Type 1, with surface creep rates exceeding 5 meters per year (Delaloye et al., 2013; Kummert et al., 2017). In extreme cases, such as the Tsarmine rock glacier, these velocities can reach up to 22 meters per year (Vivero et al., 2022). These high creep velocities are reached because of the steep convex slopes, which favour the development of an extensive flow pattern (Delaloye et al., 2013). Additionally, such slopes often feature a distinct terrain knickpoint that transitions into an even steeper channel. The steep incline significantly increases gravitational forces, altering the shear stresses within the rock glacier. This typically results in substantial acceleration of creep velocity (Cicoira et al., 2021), leading to increased internal deformation of the rock glacier. If the deformation reaches a critical threshold, destabilization is expected to be initiated, causing the rock glacier to accelerate further. Part of this destabilization process involves the opening of surface cracks and crevasses due to tension stresses. These transversal cracks resemble those occurring on Type 1 destabilized rock glaciers.

Internal thermal and hydrological changes (as described in Type 1a for concave slopes) or external mechanical factors (Type 1b) may also contribute to the initiation of destabilization in Type 2. However, in this category, steep convex topography is the dominant factor that must be considered. It dictates the destabilization dynamics, serving as the primary driver of continued and often rapid acceleration. Once the rock glacier reaches the terrain knickpoint or the steep section of the convex slope, the steep inclination becomes the key influence in the destabilization process. Consequently, processes that may have played a role in triggering the initial destabilization become secondary, justifying a classification based solely on the characteristic topography of these destabilized rock glaciers.

Most destabilized rock glaciers of this type have their terminal sections situated in steep channels. Within these channels, they commonly experience significant erosion due to secondary cascade processes such as debris flows and rockfalls (Kummert et al., 2017). These processes often lead to retrogressive erosion, which can further exacerbate destabilization of the rock glacier. As a result, the actual advance of these rock glaciers is often less pronounced than their high creep rates would suggest. Due

to the potential for cascading hazards, this type of destabilized rock glacier is particularly relevant for natural hazard management and mitigation efforts.

In contrast to Type 1, Type 2 does not serve merely as an overarching classification requiring further subdivision into subtypes. Instead, Type 2 itself represents the typical case of destabilized rock glaciers on steep convex slopes. Examples include Dirru and Gugla in the Matter Valley (Delaloye et al., 2013; Kummert et al., 2017) as well as the Tsarmine rock glacier (Kummert et al., 2017; Vivero et al., 2022).

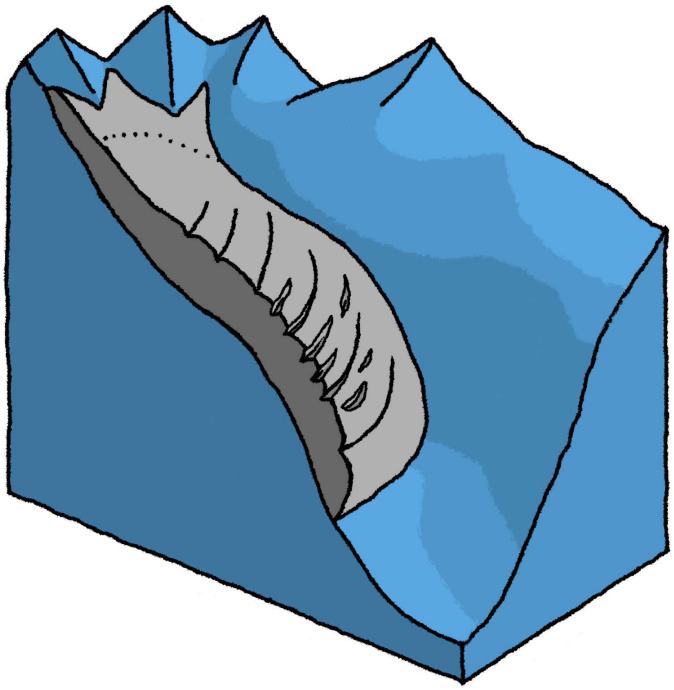

Figure 6 Schematic illustration of rock glacier type 2

However, there are follow-up categories for Type 2, which should be understood as developments of the general Type 2 destabilized rock glacier. These include the following types:

Type 2.1: Rupture of rock glacier into two parts

In this advanced stage of destabilization, a Type 2 rock glacier splits into two distinct sections: the upper section remains relatively intact, while the lower section undergoes significant destabilization. This rupture typically occurs at terrain knickpoints, where the rock glacier transitions into a steep slope. The process is driven by extreme creep acceleration in the lower section, with gravitational forces on the steep slope playing a central role in this rapid movement. The extensive flow pattern, characteristic of convex slopes and terrain knickpoints, further amplifies this effect. The eventual rupture between the two sections is often preceded by the development of prominent cracks and scarps, which serve as indicators of the ongoing destabilization. A documented example of this process is the Grosse Grabe rock glacier in the Matter Valley, where a rupture occurred at a terrain knickpoint transitioning from a gentle incline to a slope with an inclination of 30-35° (Delaloye et al., 2013).

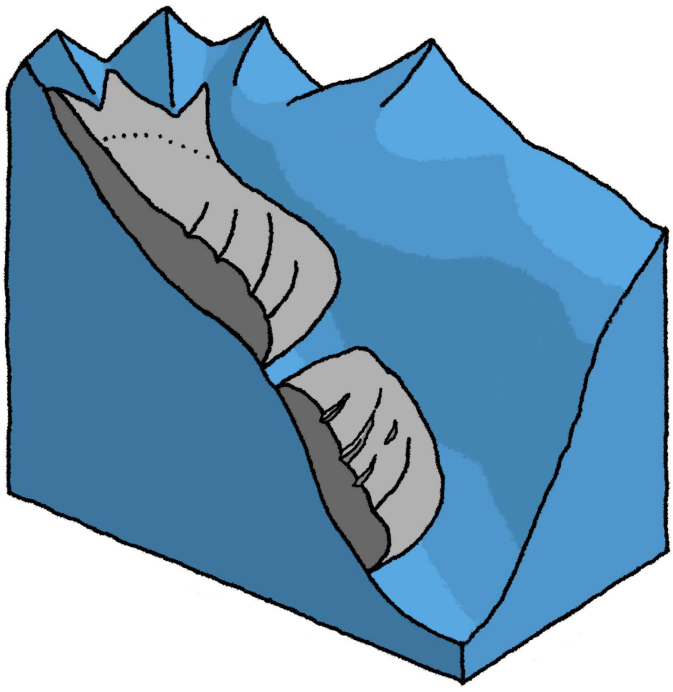

Figure 7 Schematic illustration of rock glacier type 2.1

Type 2.2: Partial failure of rock glacier front

Another extreme behaviour observed in type 2 rock glaciers is the partial failure of the front, where large sections of the rock glacier's front are eroded and transported by debris flows in a single event. Documented cases report failed volumes in the range of approximately 10,000 to 15,000 m³. These values are derived from three documented cases: the Hintergrat rock glacier and Similaungrube rock glacier in Italy (Kofler et al., 2021) as well as Lou rock glacier in France (Marcer et al., 2020). Such catastrophic failures are often linked to heavy rainfall events that exacerbate the instability of the rock glacier's surface, leading to large-scale erosion and sediment mobilization. It is assumed that prior destabilization significantly increases the likelihood of frontal failure, as pre-existing cracks and weakened structures make the front more susceptible to collapse under external stresses (Marcer et al., 2020).

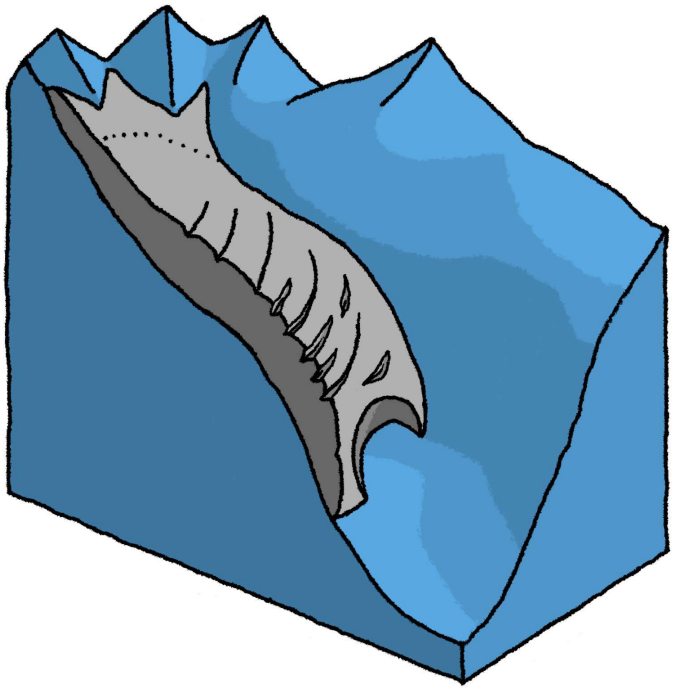

Figure 8 Schematic illustration of rock glacier type 2.2

Type 2.3: Complete failure and structural collapse of rock glacier

In the most extreme cases, Type 2 rock glaciers may undergo a complete structural collapse, according to Schoeneich et al. (2015) marking a potential final stage of rock glacier destabilization. This catastrophic event involves the rapid downward sliding of the entire rock glacier, often covering distances of several hundred meters within just a few days. During this process, the rock glacier disintegrates into multiple cohesive blocks, each moving independently with distinct dynamics. These collapses are typically accompanied by the mobilization of debris, including mudflows and hyperconcentrated flows, which further contribute to the destruction of the rock glacier and its surrounding environment. To date, only two instances of such complete rock glacier failure have been documented in the scientific literature: the Bérard rock glacier in France and the Las Tortolas rock glacier in Chile, both of which collapsed in 2006. In both cases, prior signs of destabilization, such as large cracks, were observed before the final failure event (Bodin et al., 2012, 2017).

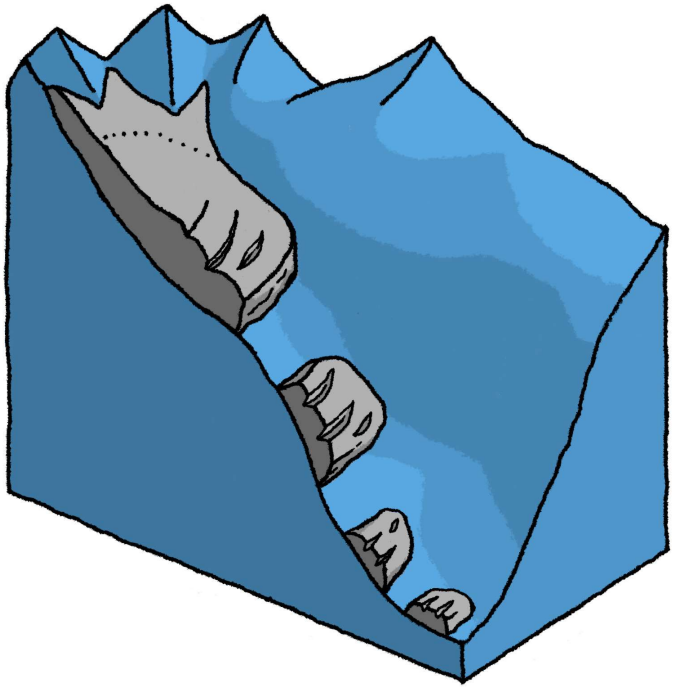

Figure 9 Schematic illustration of rock glacier type 2.3

6.2. Interactions between different types

In certain circumstances, a rock glacier may transition from one type to another. These transitions are not necessarily linear, as various factors such as thermal changes, topographical conditions, and external triggering events govern the evolution of rock glaciers. For example, a “normal” Type 0 rock glacier may become destabilized and evolve into one of the destabilized types depending on the triggering mechanism or the slope’s topography.

If a Type 0 rock glacier is situated on a concave slope and undergoes significant internal thermal and hydrological changes due to excessive degradation, it may transition to Type 1a once a critical threshold is exceeded, and destabilization occurs. Conversely, if an external mechanical disturbance, such as a rockfall, deposits a substantial amount of material onto a Type 0 rock glacier, the resulting mechanical surge can propagate through the rock glacier. Over time, this disturbance may alter internal stress distributions, potentially leading to destabilization and a transition into a Type 1b rock glacier.

A different scenario arises when a Type 0 rock glacier advances over a linear or concave slope but encounters a distinct terrain knickpoint transitioning into a steep channel. Upon reaching this knickpoint, the abrupt change in topography alters internal shear stresses, potentially initiating destabilization. Over time, this process can transform the rock glacier into a Type 2 destabilized rock glacier.

Similar transitions are plausible for Type 1a and 1b destabilized rock glaciers. If they advance and reach a steep convex slope or terrain knickpoint, they can rapidly transition into Type 2. At this stage, the steep topography and associated gravitational forces become the dominant influences, overriding the destabilization dynamics that previously governed their movement on concave or linear slopes. The Plator rock glacier in the Italian Alps serves as an example. Initially, it could be classified, albeit with some uncertainty, as a Type 1b rock glacier. In the summer of 2015, its front toe reached a knickpoint where the slope transitioned from a gentle incline to a much steeper gradient of 25–40°. Once the rock glacier crossed this knickpoint, its dynamics became primarily controlled by the steep topography, leading to significant acceleration and further destabilization (Bearzot et al., 2022; Scotti et al., 2016). This results in its reclassification as a Type 2 rock glacier. After passing the knickpoint, gravitational movements occurred at the front of the Plator rock glacier (Bearzot et al.,

2022). As a result, it became involved in cascade processes, another characteristic feature of Type 2 destabilized rock glaciers.

Type 2 destabilized rock glaciers can also progress to more advanced stages of destabilization. In extreme cases, a “normal” Type 2 rock glacier may evolve into Type 2.3, marked by a complete structural collapse. This progression depends on the severity of destabilization and external influences such as heavy rainfall or seismic events. However, not all destabilized rock glaciers follow this trajectory. Some may remain within their designated category, while others may bypass intermediate stages entirely, transitioning directly to more advanced forms of destabilization.

It is crucial to note that no fixed sequence of transitions exists for destabilized rock glaciers, as their development depends on a complex interplay of factors. Nonetheless, backward transitions are highly unlikely in most cases. For instance, a rock glacier that has experienced a rupture or complete collapse cannot revert to its original Type 0 form. While it is conceivable that remnants of a destabilized rock glacier could stabilize and evolve into “normal” rock glaciers over long timescales, this remains speculative due to a lack of scientific research. Documented cases exist where destabilization phases subside, and creep rates return to normal. However, these are not clear examples of backward transitions, as the characteristic morphology, including prominent surface cracks, persists long time after the high-velocity phase has ended (RGIK, 2023). Further research is needed to explore potential transformations, as understanding these pathways is vital for anticipating the future behaviour of destabilized rock glaciers in a changing climate.

6.3. Consequences for the definition of destabilized rock glaciers

Significant differences in topography, triggering factors, and kinematics can be observed between Type 1 and Type 2 destabilized rock glaciers. Moreover, various transitions between individual types can occur. However, these processes and interactions are highly complex and have, to date, been scarcely documented in scientific literature. Given these differences and the inherent complexity, establishing a uniform definition that encompasses all types of destabilized rock glaciers is challenging.

When comparing the characteristics of different types, only two features appear to be consistently present across all studied destabilized rock glaciers: a change in kinematic behaviour (mostly an acceleration of surface creep velocity) and the formation of surface cracks or scars. While Type 2 rock glaciers tend to exhibit higher creep velocities due to steep topography, the overall trend of kinematic abnormalities and acceleration is shared. These two characteristics (kinematic and morphological) thus provide a practical basis for a unified definition of destabilized rock glaciers. Although this approach simplifies the phenomenon and overlooks its full complexity, no additional criteria can be included without excluding certain types of destabilized rock glaciers, as they would not apply universally. Given the variety and uncertainty in triggering mechanisms, it is not practical to include all of them in detail within the definition. However, incorporating them in a general manner, aligned with the overarching fundamental dynamics, may provide a more comprehensive perspective.

Existing definitions of destabilized rock glaciers adopt similar approaches. For instance, the International Permafrost Association (IPA) Action Group Rock Glacier Inventories and Kinematics (RGIK, 2023) defines destabilized rock glaciers as exhibiting *"abnormally (i.e. no longer following the regional trend) large displacements, often associated with by the opening of large transversal cracks and/or scraps"*. This definition reflects the current state of the art, as RGIK comprises over 200 scientists from 29 countries, all specializing in permafrost research.

In most other studies on destabilized rock glaciers, significant acceleration relative to long-term regional trends and the development of surface cracks are the only criteria used to define destabilized rock glaciers. Examples of such studies include Bodin et al., 2017; Delaloye et al., 2010, 2013; Delaloye & Morard, 2011; Ghirlanda et al., 2016; Marcer et al., 2019; Roer et al., 2008; Scotti et al., 2016.

Based on the proposed classification of different destabilized rock glacier types and a review of the literature, the following definition of destabilized rock glaciers is suggested:

A destabilized rock glacier is characterized by notable kinematic anomalies, typically manifested as a significant and persistent acceleration of (local) surface creep velocity. This process is accompanied by the formation of surface disturbances (cracks or scarps), indicating a departure from typical long-term kinematic trends.

Such changes often signify advanced internal deformation driven by extreme thermal and hydrological conditions or the influence of external forces.

In this context, kinematic anomalies are understood as deviations from the long-term kinematic trends of individual rock glaciers that clearly exceed the magnitude and pattern of changes typically induced by regional climate trends.

It should be noted that this definition represents only the broadest framework for identifying destabilized rock glaciers. It serves as a general reference point, capturing the core features of the phenomenon without accounting for its underlying diversity. To better distinguish between specific destabilization processes and refine the definition, it is highly recommended to incorporate the proposed classification system, which differentiates between the various types of destabilized rock glaciers. This typology allows for a more precise understanding of their unique dynamics, contributing to a more detailed and context-sensitive characterization.

7. Study Area

7.1. General characteristics

The Turtmann Valley, located in the Valais Alps of Switzerland, covers an area of approximately 110 km². Elevations range from 620 m a.s.l. at the valley entrance near the village of Turtmann to over 4200 m a.s.l. at the Turtmann Glacier (Otto & Dikau, 2004). The valley extends roughly 15 km in a north-south orientation and features several hanging tributary valleys along the flanks of the main trough. The region experiences continental climatic conditions, with mean annual precipitation ranging from 600 to 900 mm at 2000 m a.s.l. (Tatenhove & Dikau, 1990). Periglacial landforms are well developed in the valley and include gelifluction lobes, ploughing boulders, and numerous rock glaciers in various states of activity (Otto & Dikau, 2004). More than 83 rock glaciers have been mapped between 2300 and 2900 m a.s.l., approximately one-third of which are classified as active (Nyenhuis et al., 2005). The valley's lithology is dominated by Palaeozoic gneisses and schists from the Penninic Siviez-Mischabel nappe (Gnägi & Labhart, 2017).

7.2. Conducted research

The Turtmann Valley has been the subject of numerous geomorphological and permafrost-related studies. One of the earliest systematic assessments of permafrost conditions in the valley was carried out by Tatenhove & Dikau (1990) More recent work by Roer et al. (2005) documents a general acceleration trend in surface creep across several active rock glaciers. In-depth studies have also been conducted on two destabilized rock glaciers in the valley, Furggwanghorn and Gruob, which are among the best-documented cases of rock glacier destabilization in the Alps (Buchli et al., 2013, 2018; Roer et al., 2008; Springman et al., 2013). Furthermore, two additional rock glaciers in the valley are part of the PERMOS (Swiss Permafrost Monitoring Network) program and are regularly monitored for ground surface temperature and surface displacement (PERMOS, 2024).

7.3. Rock glaciers of interest

Given the large number of rock glaciers in the Turtmann Valley, a targeted selection was made to enable a representative and comparative analysis. This study focuses on nine active rock glaciers located on the eastern slope of the valley, including the previously identified destabilized rock glaciers Furggwanghorn and Gruob. The selection aims to ensure a comprehensive overview by covering a broad range of characteristics such as elevation, aspect, topographic context, and size. In addition to these morphological and positional criteria, DEMs of Difference (DoDs) were calculated for all potential candidates as a preliminary screening tool to identify spatial patterns of vertical surface change. This allowed for the inclusion of rock glaciers exhibiting varying degrees of recent mass redistribution. The final selection thus reflects a diverse range of rock glacier behaviours and provides a diverse sample set suitable for evaluating destabilization trends in the valley. The methodology and results related to the DEM of Difference analyses are described in detail in the respective chapters.

The map in figure 10 shows the spatial distribution of the selected rock glaciers along with the naming convention used throughout this thesis. It should be noted that the rock glaciers referred to here as Hungerlihorli and Brändjispitz are listed as “Hut” and “Hut2”, respectively, in the PERMOS reports (2024).

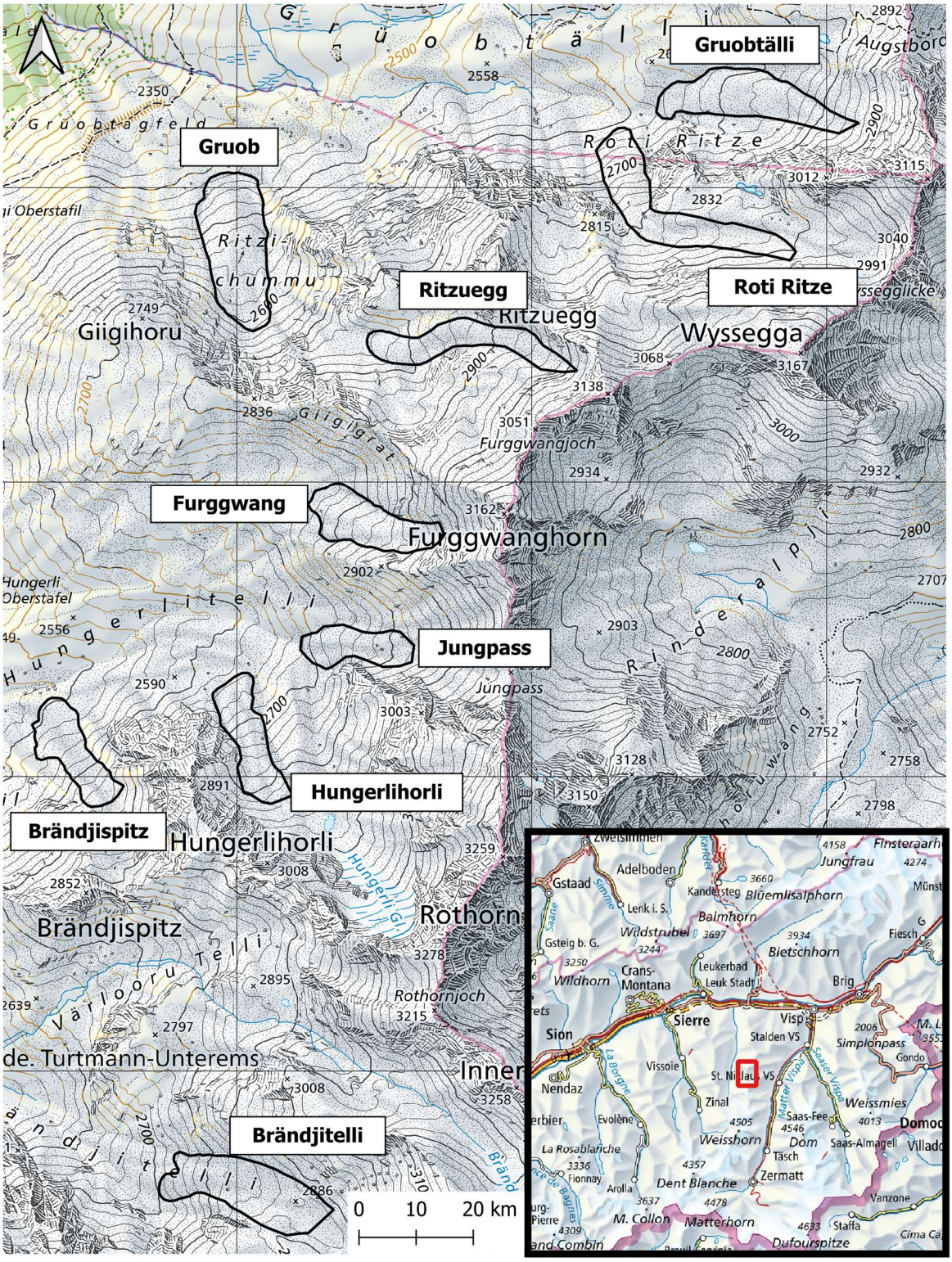

Figure 10 Map of the study area (Base layer: swisstopo, 2024)

8. Data and Methods

To address the research question and test the hypothesis outlined in chapter 4.2, multiple rock glaciers in the study area are be analysed. As discussed in the conceptual framework for defining and delineating destabilized rock glaciers (*chapter 6*), both the kinematic and morphological evolution over time must be considered to evaluate their destabilization state. A long observation period is essential to identify long-term trends and detect sustained kinematic anomalies. It also improves the ability to reconstruct morphological transformations and the development of surface disturbances. Given that rock glacier creep typically occurs at relatively low rates, usually in the range of a few centimetres to several metres per year, adequate spatial resolution is critical. Furthermore, the methodology must be capable of analysing and comparing nine different rock glaciers, which necessitates an efficient and scalable approach. In summary, the applied method must support the comparative analysis of multiple rock glaciers across an extended time span, while maintaining high temporal and spatial resolution.

In this context, digital photogrammetry techniques based on orthoimages provide a reliable approach for detecting geometric changes and surface creep in rock glaciers. These methods have been widely applied in previous studies and are well established for the long-term rock glacier observation (e.g. Eriksen et al., 2018; Kääb & Vollmer, 2000; Kaufmann & Ladstädter, 2002; Marcer et al., 2019, 2021; Roer et al., 2005; Scotti et al., 2016; Wangensteen et al., 2006). The following chapters describe the specific datasets, processing steps, and analytical methods used in this study.

8.1. Data

Switzerland has a long-standing tradition of systematic aerial image acquisition for national surveying purposes, initiated in the late 1920s for national surveying purposes (Bundesamt für Landestopografie swisstopo, 2024). This continuous data collection, maintained and developed by the Federal Office of Topography swisstopo, provides a high-quality geospatial foundation for long-term environmental monitoring. The availability of historical and recent image material makes it possible to analyse geomorphological processes over several decades, as pursued in this study.

8.1.1. Fundamental Principles of Orthophoto Generation

Orthophotos differ from conventional aerial photographs in that they have been geometrically rectified to eliminate distortions caused by terrain variations and perspective effects. Unlike raw aerial images, which are captured in central perspective, orthophotos represent an orthogonal projection of the Earth's surface, maintaining a consistent scale across the entire image. This correction is achieved through differential rectification, which relies on precise image orientation and a digital elevation model to account for topographic variations. A key principle in orthophoto generation is stereo photogrammetry, which utilizes overlapping images to extract three-dimensional elevation data. This technique ensures that distortions introduced by terrain relief are accurately removed, enabling the production of geometrically precise images (Kääb, 2005).

8.1.2. Processing Workflow for True Orthophoto Generation

In this study, true orthophotos are used, meaning that the elevation models used for orthorectification correspond to the time of aerial image acquisition. This approach ensures that terrain distortions are accurately corrected, and that image quality is maximized to allow highly accurate displacement measurements of destabilized rock glaciers. This approach is particularly critical in high-relief mountain environments, where terrain changes over time can introduce significant positional errors in standard orthophoto workflows. In this study, all processing steps, including the generation of elevation models and orthophotos, were carried out by the Federal Office of Topography swisstopo. The key processing steps are as follows:

1. Image acquisition and archival digitization

Aerial images are acquired using calibrated cameras with known interior and exterior orientation parameters. In Switzerland, the first aerial images were captured on glass plate negatives, which later transitioned to analogue black-and-white and colour film, and to fully digital imaging from 2005 onwards. Archival aerial photographs are preserved at swisstopo in Wabern, where they are stored alongside metadata detailing flight parameters, camera specifications, and image properties. Historical images are scanned using high-resolution photogrammetric scanners, enabling subsequent digital processing.

2. Georeferencing and image orientation

The initial georeferencing process assigns approximate spatial coordinates to each image. Traditionally, this involved manually identifying GCPs with known reference positions, but modern approaches automate this step using reference orthophotos and existing elevation data. To refine the spatial alignment of the images, a bundle block adjustment (BBA) is performed. This method minimizes distortions by adjusting the relative positions of multiple images using tie points (Heisig & Simmen, 2021).

3. DSM integration and true orthorectification

For each aerial image set, a digital surface model (DSM) is generated by correlating overlapping analogue frame images using stereo photogrammetric techniques. These DSMs represent the visible surface at the time of image acquisition. The models are integrated into the photogrammetric workflow to correct terrain-induced distortions and enable differential rectification. Based on this elevation information, the images are orthorectified by transforming them from their original perspective view into a true top-down projection. This process removes relief displacement and perspective effects, ensuring that all features appear in their correct spatial positions and that the resulting orthophotos meet the geometric accuracy required for displacement analysis.

From 2005 onwards, aerial imagery in Switzerland is acquired using digital line sensors that capture continuous image strips instead of individual analogue photographs. While the principle of stereo coverage remains unchanged, processing steps related to the digitization of film-based images such as scanning and geometric correction are no longer required.

8.1.3. Data sets

As the goal of this study is to reconstruct the long-term evolution of rock glacier behaviour in the study area with the highest possible temporal resolution, all available elevation models (DSM or DTM) and orthophotos (OP) are used from the earliest to the most recent acquisition. The table below provides an overview of the dataset.

Table 1 Overview of the dataset used in this study.

Year	Flight date	Products	Image type	Interval to previous
1968	18.10.1968	True OP b/w DSM	analogue frame images	-
1975	20.08.1975 + 06.10.1975	True OP b/w DSM	analogue frame images	7 years
1981	06.08.1981	True OP b/w DSM	analogue frame images	6 years
1987	16.08.1987	True OP b/w DSM	analogue frame images	6 years
1993	20.08.1993 + 01.09.1993	True OP b/w DSM	analogue frame images	6 years
1999	25.07.1999 + 01.09.1999	True OP colour DSM	analogue frame images	6 years
2005	17.08.2005	True OP colour DSM + DTM	analogue frame images	6 years
2011	15.09.2011	True OP colour DSM	digital strip	3 years
2014	27.08.2014 + 23.09.2014	True OP colour DSM	digital strip	3 years
2017	21.09.2017	True OP colour DSM	digital strip	3 years
2020	09.09.2020	True OP colour DSM	digital strip	3 years
2023	23.08.2023	True OP colour DSM + DTM	digital strip	3 years

The original image metadata include additional information such as interior and exterior orientation parameters, overlap ratios, flight line geometry, and scanning specifications for analogue photographs. A list of the individual images used for DSM reconstruction and orthophoto generation is available upon request.

In this study, a uniform pixel size of 0.25 m is used for all orthophotos, as it represents the best overall compromise across the available datasets. According to personal communication with Heisig (2024), the original ground resolution of the images varies depending on flight altitude, focal length, terrain elevation, and scan resolution. The chosen resolution of 0.25 m minimizes excessive stretching or unnecessary compression during orthorectification and is therefore considered an appropriate common target resolution.

The elevation models are used at a resolution of 1 m. In most cases, they are digital surface models (DSMs) derived from overlapping aerial images of the respective year

or, for more recent datasets, from digital image strips. The DTM from 2023 is a terrain model based on high-precision LiDAR data in which vegetation and other surface features have been removed.

8.1.4. Accuracy assessment

The processing workflow proposed by Heisig & Simmen (2021) provides high-quality data and is particularly well suited for historical image material. The use of time-specific elevation models further increases the geometric accuracy of the resulting orthophotos. However, qualitative assessments reveal slight horizontal shifts between images from different years, even in areas assumed to be stable. These positional offsets tend to increase with the age of the imagery. Although the deviations are generally small, improving positional accuracy through post-processing remains essential, as the reliability of the kinematic analyses of rock glaciers strongly depends on accurate image alignment.

The quality of the elevation models is assessed through surface model differencing, in which digital surface models (DSMs) from two different time steps are subtracted. In areas without mass movements, significant erosion, anthropogenic influence, vegetation change, or glacier melt, no change in surface elevation is expected. Accordingly, the resulting surface difference model should display values close to zero in these stable zones. In this study, the data quality proves to be very high, with only minor deviations observed, primarily in the older datasets.

8.1.5. Co-Registration approaches

As discussed before, post-processing is required to further improve data quality, in particular the positional accuracy of the historical datasets. A suitable approach for this purpose is image co-registration, which allows positional correction of historical orthophotos and elevation models by aligning them with a reference dataset. In this study, the 2023 data are used as a reference, as they are expected to have the highest geometric precision due to the use of modern acquisition techniques and processing workflows.

Various co-registration methods have been tested in the context of this study. The elevation models are not further adjusted, as sub-pixel positional accuracy is not required for their use in this analysis. In contrast, the accuracy of the orthophotos plays

a crucial role in the kinematic evaluation of surface displacements and is therefore subject to refinement.

One tested method is manual co-registration. In this approach, control points are manually identified in the target image and matched with corresponding features in the reference image within a georeferenced coordinate system. Stable and clearly identifiable features, such as building corners or prominent rocks, are selected as tie points. A geometric transformation is then computed based on the matched control points, and the target image is resampled accordingly. While this method is conceptually straightforward, it is time-consuming depends heavily on the operator's judgment and experience. It was therefore not considered suitable for the purposes of this study.

Another widely used method is the DEM-based co-registration approach developed by Nuth & Kääb (2011). This technique identifies horizontal misalignments between two DEMs by analysing elevation differences over stable terrain and their systematic relationship to slope and aspect. Systematic elevation differences are analysed as a function of aspect and fitted with a sinusoidal model, from which the direction and magnitude of the horizontal shift vector are derived. The target DEM is then iteratively shifted until these systematic deviations are minimised. In this study, the method was tested to assess whether the derived shift vector could be transferred to the associated orthophotos. However, a direct co-registration of the orthophotos was considered more appropriate than an indirect adjustment via the DEMs. Consequently, the method was not implemented.

A method where this direct correction of the orthoimages is achieved, is presented by Scheffler et al. (2017). AROSICS (Automated and Robust Open-Source Image Co-Registration Software) employs a phase correlation-based method for subpixel-accurate image registration. The Fourier shift theorem is applied within a moving window to determine offsets between the target and reference images. The method is robust to spectral and temporal changes, atmospheric conditions, and sensor differences. It includes automatic validation and filtering of mismatches and applies either a global affine transformation or a local displacement field for geometric correction.

In this study, this method is applied using the QGIS plugin *Coregistration* (Version 24.12), which provides a graphical interface to the AROSICS framework. All available

historical orthophotos are co-registered to the 2023 reference image. To maximise spectral correspondence during the matching process, RGB orthophotos are aligned using the RGB version of the reference image, while black-and-white images are matched against a greyscale version of the reference.

8.1.6. Co-registration effectiveness

To evaluate the effectiveness of the image-to-image co-registration performed with AROSICS, the root mean square error (RMSE) is used as a quantitative indicator of geometric alignment accuracy. RMSE is a widely established metric for assessing spatial deviation between corresponding datasets and is commonly applied in remote sensing and photogrammetric quality control (e.g. Abdullah et al., 2024; Agüera-Vega et al., 2017; Bagheri & Sadeghian, 2013; GÜNGÖR et al., 2022; Hashim et al., 2013; Korumaz & Yildiz, 2021; Scheffler et al., 2017; Tsai & Lin, 2017). In this context, RMSE expresses the average magnitude of positional discrepancies between a reference image and the target image and is therefore particularly suitable for assessing whether the co-registration has improved the geometric consistency of multi-temporal orthophotos.

The RMSE is calculated based on a set of manually identified check points representing stable and clearly identifiable features, such as large rocks. These points are first digitised in the reference orthophoto from 2023 and then visually matched in the original, uncorrected image as well as in the co-registered image. For each of these two comparisons, the Euclidean distances between the corresponding point pairs are computed, and the RMSE is derived as the square root of the mean squared deviations. All coordinates are in the Swiss LV95 system (EPSG:2056), and RMSE values are thus given in metres:

$$\mathrm{RMSE} = \sqrt{\frac{1}{n}\sum_{i=1}^{n}\left[\left(X_i^{ref} - X_i^{target}\right)^2 + \left(Y_i^{ref} - Y_i^{target}\right)^2\right]}$$

$\boldsymbol{X_i^{ref}, Y_i^{ref}}$ *X and Y coordinates of control point i in the reference image (2023)*

$\boldsymbol{X_i^{target}, Y_i^{target}}$ *X and Y coordinates of the same control point i in the target image (either before or after co-registration)*

Table 2 RMSE values before and after co-registration for each year and percentage change in geometric accuracy.

Year	RMSE before (m)	RMSE after (m)	Change in %
1968	1.611	0.641	60.2
1975	1.172	0.637	45.6
1981	0.872	0.523	40
1987	0.634	0.386	39.1
1993	0.588	0.321	45.4
1999	0.592	0.420	29
2005	0.381	0.284	25.4
2011	0.224	0.189	15.6
2014	0.207	0.203	1.9
2017	0.210	0.216	-2.86
2020	0.197	0.192	2.5

The RMSE values calculated for each acquisition year are summarised in Table 2. They show a clear reduction in positional error after co-registration for most image sets. The improvement is particularly pronounced for older image material, with reductions of over 60 % in 1968 and around 40 % between 1975 and 1993. These results reflect the strong effect of systematic correction on early analogue datasets, which were acquired with less advanced techniques and generally exhibit lower initial geometric precision.

From the early 2000s onwards, the relative improvements become smaller, which corresponds to the already higher quality of more recent orthophoto products. In 2014 and 2020 the correction effect is marginal, while for 2017 a slight deterioration is observed (–2.9 %). This may be attributed to weak image contrast, subtle structural differences between the reference and target images. At this level of precision, the manual identification of corresponding features becomes increasingly difficult, especially when the RMSE values approach or fall below the nominal ground sampling distance of 0.25 m. Although care was taken to select stable and clearly distinguishable features, small inaccuracies in point placement cannot be ruled out and may influence the results. The values presented here should therefore be interpreted as reliable approximations of positional accuracy, rather than exact measures.

Overall, the final RMSE values after correction range between 0.2 m and 0.65 m, which is well within the range reported in the literature for co-registered orthophotos based on aerial imagery with stable ground control (e.g. Abdullah et al., 2024; Tsai & Lin,

2017). Despite minor variation across acquisition years, the resulting positional accuracy can be considered sufficient for the intended displacement analysis. The co-registration approach using AROSICS is thus shown to be effective in enhancing geometric consistency across the orthophoto time series, providing a reliable basis for the spatiotemporal analysis of destabilised rock glaciers.

8.2. Kinematics – Horizontal displacement analysis with CIAS

As a central component of the destabilization assessment, the kinematic behaviour of the investigated rock glaciers is analysed over the entire observation period. Horizontal surface displacements are reconstructed for all time intervals to detect changes in creep dynamics. These displacements are derived through automated image correlation using the Correlation Image Analysis Software CIAS (Heid & Kääb, 2012; Kääb & Vollmer, 2000; Vollmer, 1999). CIAS applies a normalized cross-correlation algorithm to compare grayscale orthoimages from two time steps and identifies local displacements based on matching grayscale patterns (Kääb, 2005).

8.2.1. General principle CIAS

The CIAS algorithm selects a reference block in the orthoimage of the earlier time step, whose centre coordinates are known due to georeferencing. Within the orthoimage of the later time step, CIAS then searches for the best-matching block within a predefined search area around the same location. All potential blocks of the same size are systematically compared to the reference block using a normalized cross-correlation function.

Figure 11 illustrates this procedure. A reference block is extracted from orthoimage time 1 and compared to all possible test blocks within the search area of orthoimage time 2. For each candidate position, a correlation coefficient is calculated based on the similarity of grey value patterns. The position with the highest correlation indicates the most probable displacement of that terrain patch. The corresponding shift vector represents the local horizontal displacement between the two time steps.

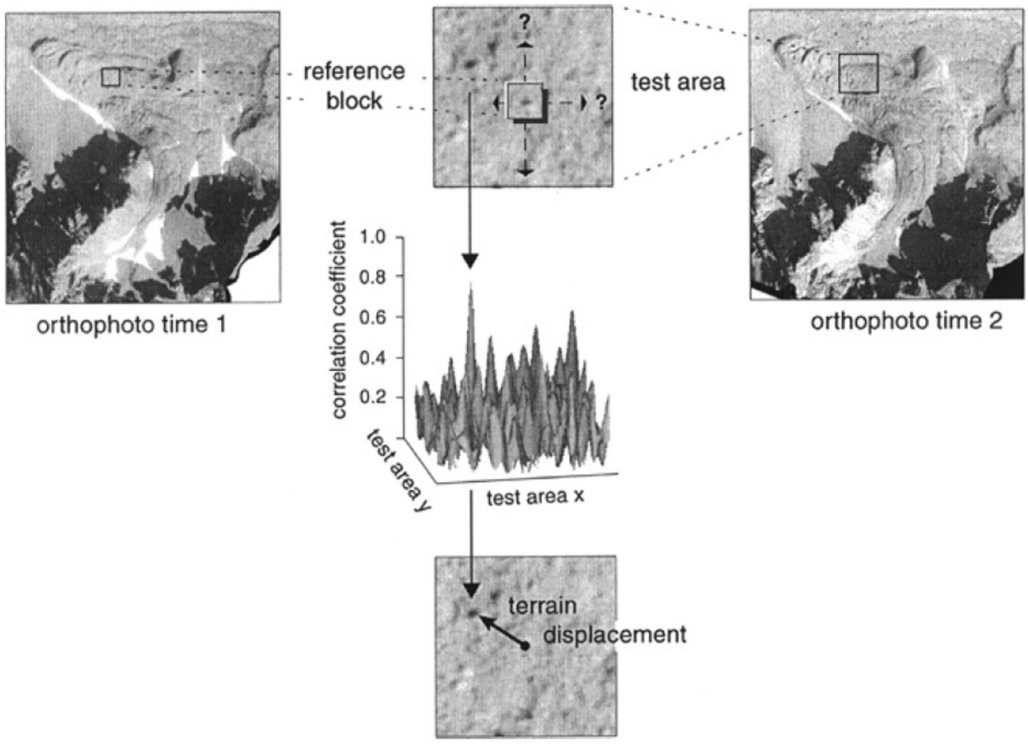

Figure 11 Schematic illustration of the CIAS matching procedure. A reference block from orthoimage time 1 is searched within a defined test area in orthoimage time 2. The displacement vector is derived from the position with the highest correlation coefficient (Figure from Kääb & Vollmer (2000)).

The similarity between the blocks is quantified using this double cross-correlation (Kääb, 2005; Kääb & Vollmer, 2000; Vollmer, 1999) :

$$\phi(i,k)= \frac{\sum_j \sum_l s((i+j, k+l) - (\frac{T_{test}}{N_{test}})) * m((j,l) - (\frac{T_{ref}}{N_{ref}}))}{\sqrt{\sum_j \sum_l s^2((i+j, k+l) - (\frac{T_{test}}{N_{test}})) * \sum_j \sum_l m^2((j,l) - (\frac{T_{ref}}{N_{ref}}))}}$$

Table 3 Parameters of the cross-correlation formula. (From Durisch (2023) based on Vollmer (1999))

Parameter	Explanation	Reference / test block
ϕ	Double cross-correlation function	
(i, k)	Coordinates	Test block
(j, l)	Coordinates	Reference block
s	Spatial grey-value function	Test block
s(i, k)	Grey value at the location (i, k)	Test block
m	Spatial grey-value function	Reference block
m(j, l)	Grey value at the location (j, l)	Reference block
T_{test}	Sum of grey values	Test block
T_{ref}	Sum of grey values	Reference block
N_{test}	Number of pixels	Test block
N_{ref}	Number of pixels	Reference block

The test block with the highest φ-value is assumed to represent the same terrain patch, now displaced in the later image. The horizontal shift between the centres of the reference and test blocks constitutes the displacement vector at that location. This process is repeated over a grid of predefined points to generate spatially distributed velocity fields.

Normalization ensures that the metric is insensitive to uniform changes in brightness or illumination differences between image pairs, making the correlation robust under varying radiometric conditions (Kääb, 2005; Kääb & Vollmer, 2000).

8.2.2. CIAS Parameters

To ensure consistent and reliable results across different sites and time intervals, careful selection of the reference block size, search area size, and grid spacing is essential. These parameters directly influence the accuracy, stability, and computational efficiency of the analysis.

In this study, the positions of the reference blocks are predefined and provided to CIAS via their centre coordinates. A grid spacing of 10 m is chosen to generate high-resolution velocity fields that allow the identification of local anomalies. A key advantage of this approach is that the same reference points are used across all time steps, enabling direct comparisons between different periods. However, this method may include reference blocks with insufficient optical contrast, which can lead to unreliable correlation results.

The size of the reference block is a critical parameter and must be adapted to the surface texture and spatial resolution. Blocks that are too small often result in ambiguous correlation maxima, while excessively large blocks significantly increase computing time (Kääb, 2005). The optimal block size should encompass the largest rocks in the study area to maximize contrast and pattern uniqueness. Since the largest rocks measure approximately 5–6 m in diameter and the predefined grid points do not necessarily coincide with their centres, a slightly larger reference block is required. To determine a suitable block size, several options were tested. Ultimately, a size of 10 m (equivalent to 40 pixels) proved to be the best compromise between achieving clearly defined correlation maxima and maintaining acceptable computation times.

The size of the search area must be large enough to accommodate the expected maximum displacement. If too small, the actual displacement may lie outside the search window; if too large, computation time increases significantly (Kääb, 2005). A common rule of thumb is:

Search area size ≈ 2 × (maximum velocity × average time interval between orthophoto)

Based on comparisons with previous studies in the region (e.g Buchli et al., 2013; Delaloye et al., 2010; Gärtner-Roer & Nyenhuis, 2009; PERMOS, 2019; Roer et al., 2005) and prior manual measurements on the orthoimages, a maximum creep velocity of around 5 m/year is assumed. Given an average image interval of five years, a search area of 50 m (200 pixels) is recommended. While this setting yields reliable results for most rock glaciers, it requires substantial computational resources. Additional tests revealed that a reduced search area of 30 m (120 pixels) produces consistent and generally reliable results with acceptable processing times for most rock glaciers and periods. This configuration is therefore applied as a first step across all sites. However, in some cases, the actual displacement exceeds this range during specific periods. For these instances, larger search areas are evaluated. A test area of 60 m (240 pixels) proves most effective and is applied accordingly where the smaller search window is insufficient.

In this study, CIAS is applied to all consecutive, previously co-registered orthoimages to calculate horizontal displacement for each respective period. For recent years, where orthoimages are available at 3-year intervals, CIAS is applied both for the 3-year periods and for combined 6-year intervals. This ensures consistency with the temporal resolution of earlier data. All input orthoimages must be provided as single-band grayscale GeoTIFF files with identical spatial resolution (0.25 m in this study).

8.2.3. Displacement accuracy and handling of matching errors

In addition to parameter selection, factors such as snow cover, shadow, and clouds can significantly affect the displacement results from CIAS, as they change the surface appearance between two images. This may lead to mismatches between reference and test blocks, resulting in erroneous displacement vectors. Kääb & Vollmer (2000) generally estimate the error of horizontal displacements derived through CIAS to be around 10-15%.

A common approach to identify and remove such mismatches is strict filtering based on the maximum correlation coefficient, with low values indicating unreliable matches (Kääb & Vollmer, 2000; Redpath et al., 2013; Wangensteen et al., 2006). However, this approach is not suitable in the context of this study, as it also targets destabilized rock glaciers. In such cases, surface transformations between time steps can be so pronounced that CIAS fails to identify the correct matching block even in the absence of snow or cloud cover. This results in low correlation coefficients and clearly erroneous vectors. Yet such mismatches may contain valuable information about surface instability and should not be excluded without careful consideration.

To make full use of the diagnostic potential of CIAS while ensuring reliable results for quantitative analysis, the following stepwise procedure is applied for all rock glaciers and time intervals:

1. Initial Screening: All displacement vectors are first visualized. Outliers that clearly deviate in length or direction are examined to determine whether they result from snow, shadow, or cloud cover. If such external influences are present, the vectors are classified as normal mismatches. If not, the affected area is inspected for morphological change between the two orthoimages. Where structural alterations are visible, the vector is retained and flagged as a possible indicator of destabilization. This approach allows valuable information to be extracted from mismatches before directly filtering them out.

2. Filtering: Once the initial interpretation is complete, all mismatches regardless of their origin are removed to avoid biasing the calculation of quantitative metrics (e.g. mean creep velocity). This is done in two steps:

> **Automatic filtering** based on expected vector length and direction. These thresholds are derived from manual displacement estimates and are deliberately conservative to prevent the exclusion of valid vectors.
>
> **Manual filtering** to address remaining mismatches. All vectors clearly associated with snow, shadow, cloud cover, or previously identified structural changes are removed. Remaining conspicuous vectors in visually stable areas are manually assessed through side-by-side comparison of the orthoimages. If their plausibility remains uncertain, the correlation coefficient is used as a final criterion, and vectors with values below 0.4 are excluded.

Throughout this process, a cautious and conservative filtering strategy is adopted to avoid removing potentially meaningful data. Special care is taken to prevent preconceptions about expected displacement fields from influencing the evaluation.

Figure 12 illustrates the effect of this filtering approach using the example of Gruobtälli rock glacier during the period 1993–1999. In the raw CIAS output, several vectors are visibly affected by snow patches and would bias the results if left unfiltered. After the filtering procedure, only reliable vectors remain, providing a robust foundation for subsequent kinematic analyses relevant to the assessment of destabilization. These include the calculation of average creep velocities, the detection of acceleration phases, the comparison of maximum displacement values, and the derivation of spatial patterns. The concrete procedures and rationale for each of these analyses are described in the corresponding result sections, where they are introduced in direct connection with the observed data. Together, these evaluations provide a comprehensive overview of rock glacier kinematics in the study area. Based on this, each rock glacier can be assessed for kinematic anomalies, which, in combination with the morphological analysis, form the foundation for evaluating signs of destabilization.

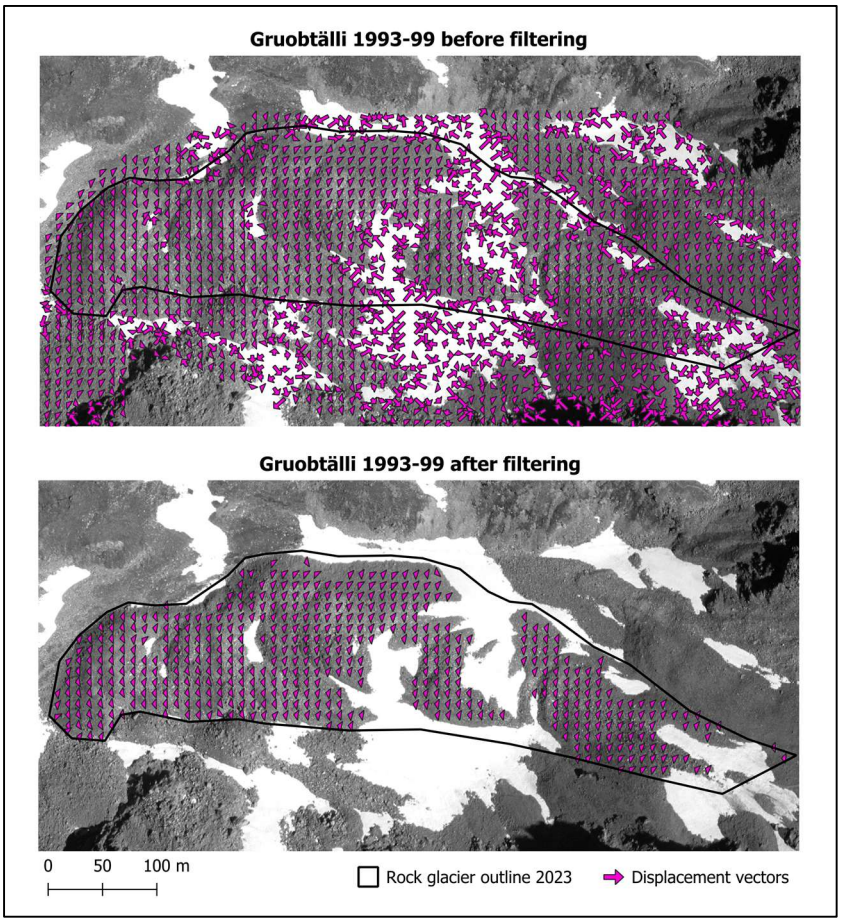

Figure 12 Example of the effect of filtering on CIAS-derived displacement values.

8.3. Morphological analysis and vertical change

In addition to kinematic behaviour, the development of morphological surface changes represents a second key indicator in the assessment of destabilization trends. First indications of such morphological transformations may already appear in the CIAS results, where significant surface restructuring leads to correlation mismatches. However, these qualitative observations are not sufficient for systematic analysis. Therefore, two dedicated and complementary approaches are implemented in this study to assess morphological change in a more targeted and reproducible way.

8.3.1. DEM of Difference – Vertical change

As a first step, elevation data are used to identify and quantify vertical surface changes over time. By subtracting digital elevation models from different time steps, changes in surface height can be detected. In high alpine settings such as the study area, such differences are often influenced by varying snow cover, changes in glacier extent, or geomorphic processes. When applied to rock glaciers, this method allows for the detection of mass redistribution patterns, which may point to surface instability.

Since kinematic analysis using CIAS only captures horizontal displacement, the incorporation of vertical change offers an additional dimension to the understanding of rock glacier evolution. In this study, the goal is not to perform a continuous time-series analysis of elevation change, but rather to obtain a general overview of vertical surface development. For this purpose, a DEM of Difference (DoD) is created for the period between 1968 and 2023. Intermediate periods are not considered.

Because high-precision alignment is not required for this general analysis, the elevation models are not further co-registered. DSMs derived from analogue frame images (1968) and digital aerial image strips (2023) are available for both time steps. Additionally, a high-resolution digital terrain model (DTM) based on airborne LiDAR is available for 2023. While using DSMs from both years would be preferable in terms of methodological consistency, tests reveal that the 1968 DSM and the 2023 DTM yield the most reliable DoD. In the high alpine context of the study area, vegetation is sparse and anthropogenic structures are absent, such that the DSMs closely approximate the terrain surface. Especially on rock glaciers, the DSM and DTM can be considered largely equivalent. Tests with both the 2023 DSM and DTM show that shadow artefacts appear in the DoD when using the photogrammetrically derived 2023 DSM. These

artefacts are absent when using the LiDAR-based 2023 DTM. In areas unaffected by shadows, elevation differences between both variants are minimal. Therefore, the 2023 DTM is used for DoD computation, ensuring a consistent and artefact-scarce vertical change analysis between 1968 and 2023.

8.3.2. Systematic classification of surface disturbance evolution

The DEM of Difference (DoD) analysis provides a spatial overview of where significant vertical changes have occurred over the entire study period. However, vertical change alone does not allow for a detailed assessment of how the surface morphology of individual rock glaciers has evolved over time. In particular, it does not reveal the timing, nature, or development of surface disturbances, which are a key characteristic of destabilized rock glaciers, as outlined in the theoretical framework.

To address this, a systematic analysis of surface morphology is conducted based on the approach developed by (Marcer et al., 2019). In the context of a study on rock glacier destabilization in the French Alps, they proposed a decision-tree method to classify the destabilization stage of rock glaciers based on the temporal evolution of surface disturbances. This approach requires the availability of multiple high-resolution orthoimages covering different time periods, which is fulfilled in this study. The method enables a consistent and structured interpretation of surface changes through time and supports the identification of destabilization patterns at the object scale.

The decision tree builds upon the identification and temporal development of specific morphological surface features:

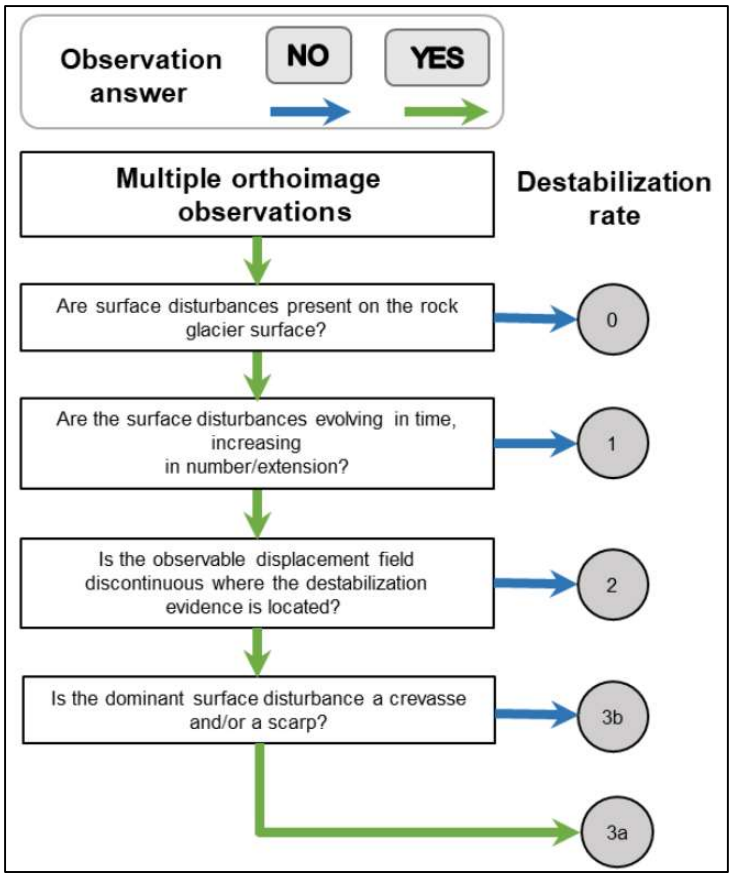

Figure 13 Decision tree for assessing rock glacier destabilization based on the evolution of surface disturbances, as proposed by Marcer et al. (2019).

Based on the answers to the decision tree, each rock glacier is assigned to a destabilization class. The classes defined by (Marcer et al., 2019) are as follows:

- **Class 0 Non-observable destabilization** – active rock glacier considered as stable
- **Class 1 Unlikely destabilization** – surface disturbances exist but do not evolve over time
- **Class 2 Suspected destabilization** - surface disturbances evolve in time, but the deformation field remains continuous
- **Class 3a Potential destabilization** - advanced destabilization with dominant scarps or crevasses and a discontinuous displacement pattern
- **Class 3b Potential destabilization** - advanced destabilization with dominant shallow surface features such as cracks

To ensure consistency in the interpretation, the following definitions of surface disturbance types from Marcer et al. (2019) are adopted:

- **Cracks**: Shallow, linear incisions in the surface, either individually or grouped in clusters, typically affecting only the active layer of the rock glacier
- **Crevasses**: Deep transverse incisions, typically cutting through the frozen body of the glacier, often up to several metres wide and deep
- **Scarps**: Steep morphological steps several metres high, transversally cutting the entire rock glacier, marking the presence of deep shear planes that separate sectors of different creep

This classification approach is applied to all investigated rock glaciers in the study area. For each object, the temporal evolution of surface disturbances is assessed using the full set of available data. The analysis is primarily based on the interpretation of orthoimages. However, hillshades derived from the DSMs are used as a valuable complement, particularly in areas with low optical contrast or partial snow cover. Starting with the earliest data from 1968, each available year is systematically examined for the presence of surface disturbances. If such features are identified, their temporal development is analysed by assessing whether they increase in number or spatial extent.

This evaluation is supported by kinematic data from the CIAS analysis, which is used to determine whether the displacement field remains continuous in the affected areas. In a final step, the type and configuration of the observed disturbances are interpreted, and each rock glacier is assigned to a destabilization class according to the decision tree proposed by Marcer et al. (2019). If surface disturbances are present, the year in which this activity begins is documented. It is also recorded if, from a certain point onwards, no further development is observed, and the existing features remain unchanged. This classification forms a central element of the overall destabilization assessment and is evaluated in conjunction with the vertical change analysis and the kinematic evaluation.

8.4. Integrated assessment of destabilization

After the described kinematic analysis and the morphological assessment, all investigated rock glaciers are individually evaluated with respect to the presence of kinematic anomalies and the development of surface disturbances. The final step in the destabilization assessment is to combine these two aspects of the analysis in order to derive a comprehensive classification of destabilization trends in the study area.

This integrative evaluation considers whether individual rock glaciers exhibit anomalies in both dimensions, in only one, or in neither. Particular attention is given to the temporal relationship between the onset of kinematic anomalies and the emergence or evolution of surface disturbances. The goal is not only to identify potentially destabilized objects but also to investigate whether morphological change follows or coincides with dynamic acceleration, thus revealing process-based relationships.

The specific procedures and classifications resulting from this integrative assessment are not described here in detail, as they are closely linked to the individual data characteristics and temporal patterns of each rock glacier. They are therefore presented directly within the results and discussion sections, where they are developed in combination with the observed evidence. This approach ensures that the final classification is based on a consistent evaluation of all available evidence.

9. Results

9.1. Kinematics

As outlined in the theoretical and methodological chapters, rock glacier kinematics represent a key indicator for detecting destabilization. In this study, the displacement patterns are presented in various formats, each allowing the analysis of different aspects of kinematic anomalies and acceleration phenomena.

9.1.1. Displacement vectors

The CIAS-based procedure is applied to all selected rock glaciers in the study area. After the calculation of horizontal displacement and the removal of mismatches, the resulting vectors are displayed for each time interval and each rock glacier. These vectors represent the horizontal surface displacement between two image acquisition dates and thus make the creep of rock glaciers directly visible.

Figures 14 and 15 illustrate the displacement vectors for the Jungpass and Brändjispitz rock glaciers, respectively, and serve as representative examples of the applied visualisation method. Equivalent figures for all other investigated rock glaciers are included in the appendix. Although high-resolution orthoimages are available at three-year intervals between 2011 and 2023, a uniform six-year interval is applied throughout the entire study period to ensure comparability in terms of absolute displacement. For Brändjispitz rock glacier, no reliable displacement data could be obtained for the period 1968–1975 due to insufficient image quality in 1968. Consequently, this interval is not included in the visualisations.

Each displacement vector set is displayed on the orthoimage from the more recent year of the respective interval (e.g. 1981 for the period 1975–1981). Vectors are grouped into classes according to length and colour-coded accordingly. The rock glacier outlines shown in all figures correspond to the margins determined for 2023 and are used as a reference for all periods. However, it must be noted that the actual extent of the rock glaciers may have differed substantially in earlier years, as several rock glaciers advanced significantly over the study period. For instance, Gruob advanced by approximately 78 m between 1968 and 2023, Furggwang by about 57 m, Brändjispitz locally by 33 m, and the remaining glaciers by approximately 10 m.

Jungpass rock glacier:

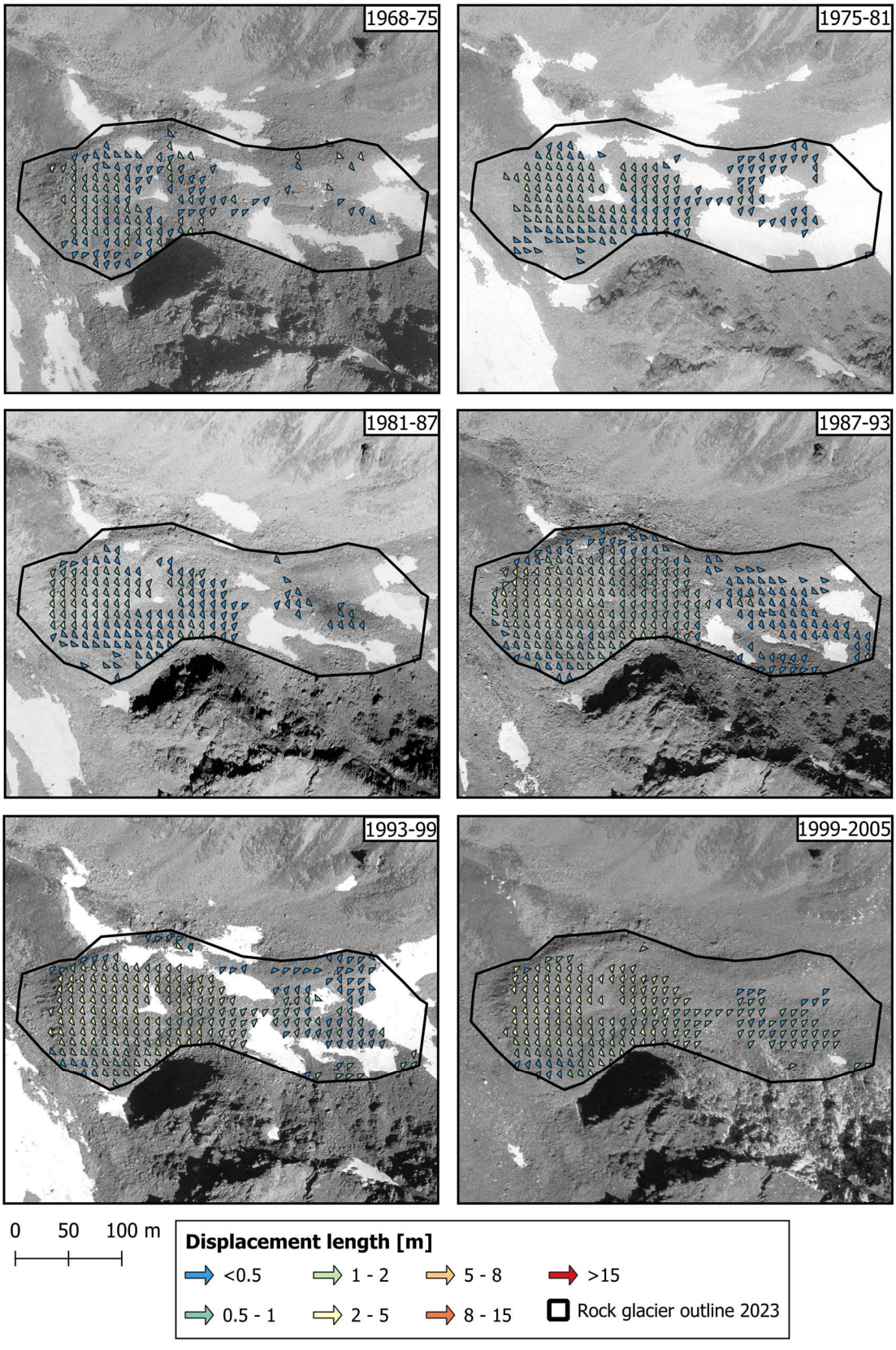

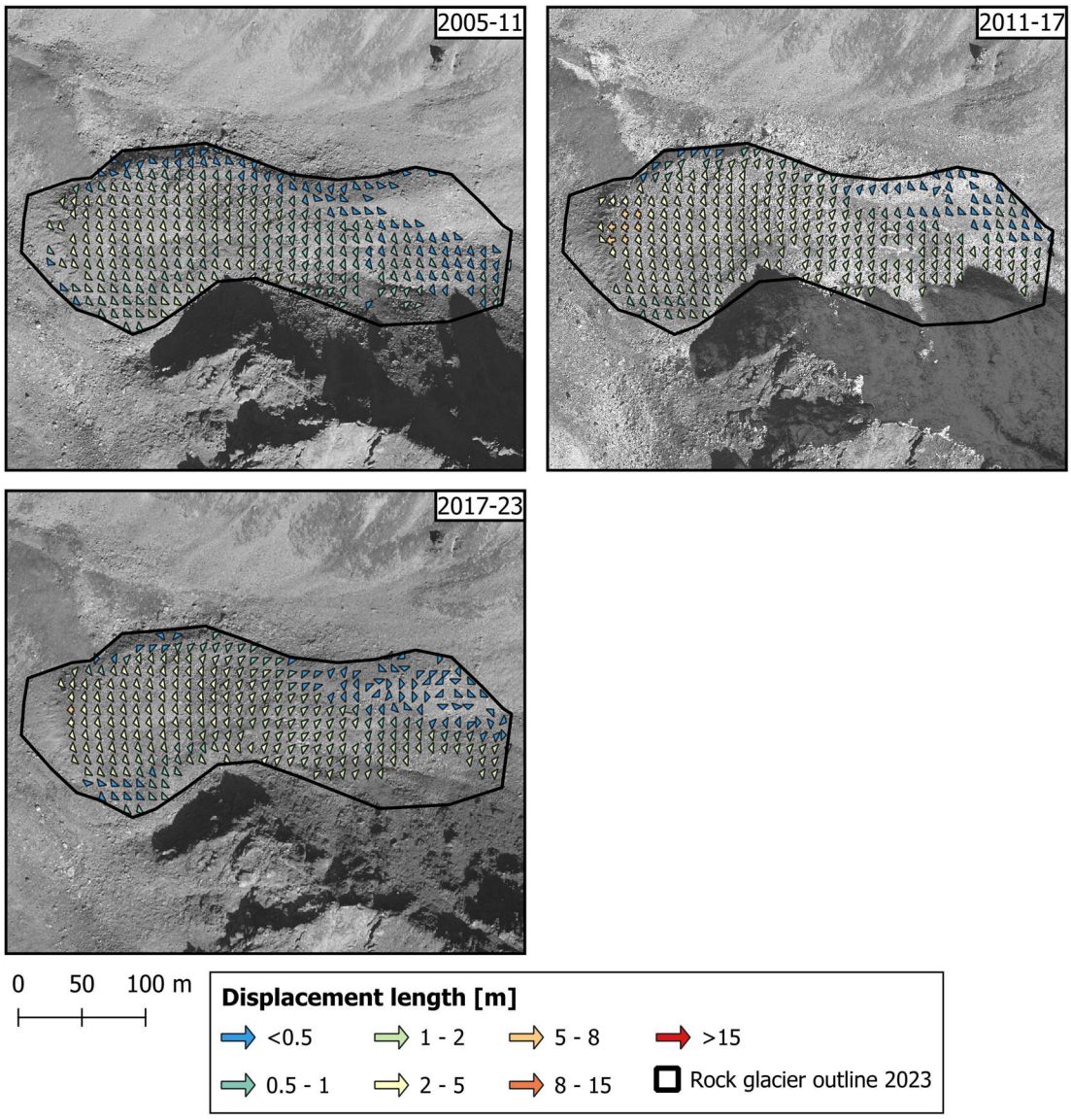

Figure 14 Displacement vectors for Jungpass rock glacier from 1968-2023.

Brändjispitz rock glacier:

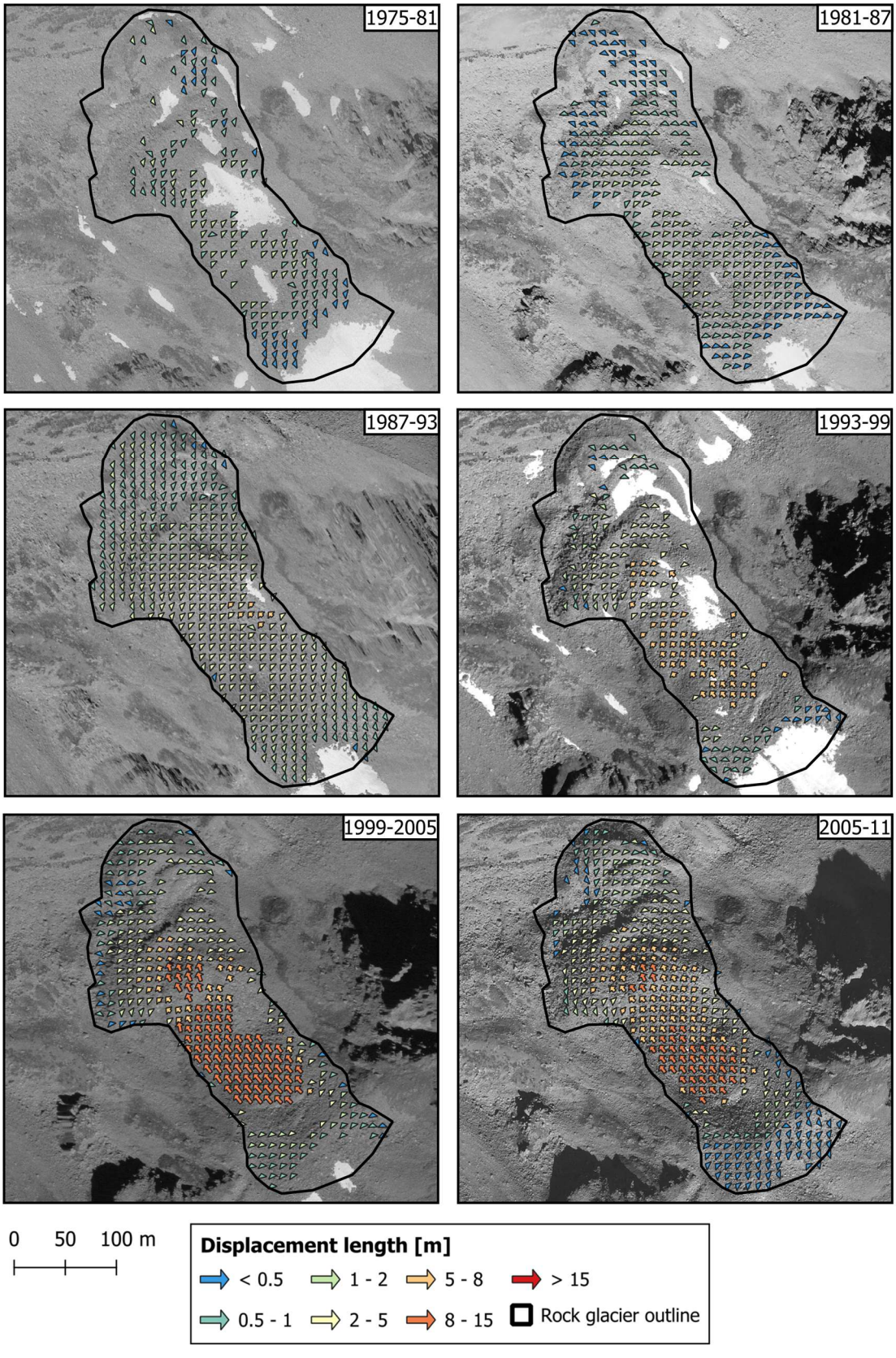

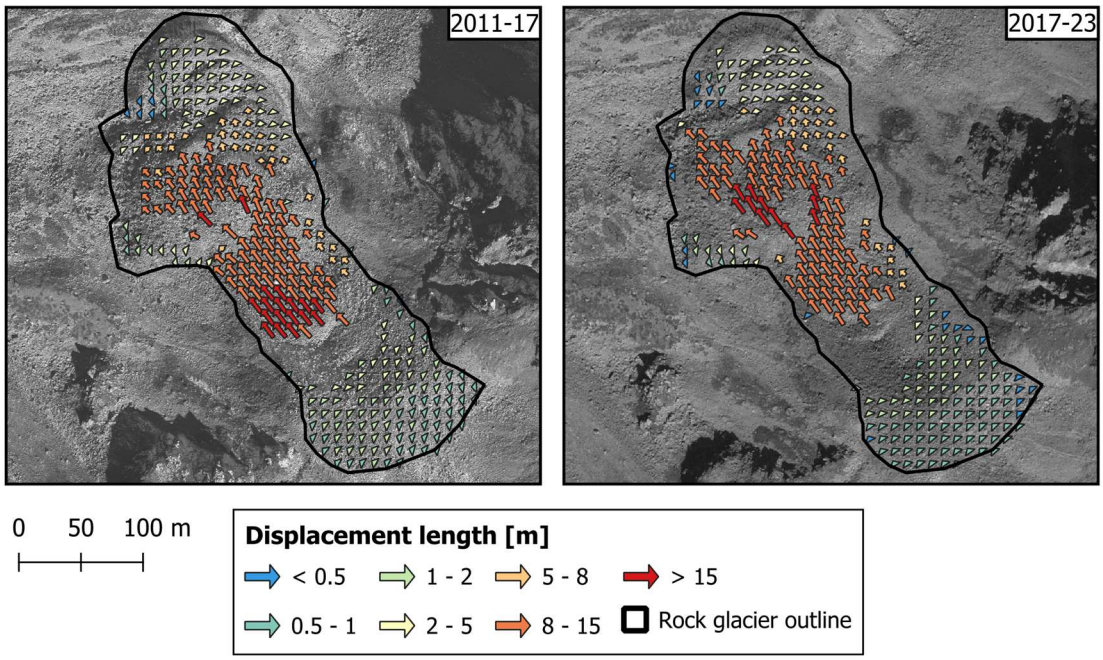

Figure 15 Displacement vectors for Brändjispitz rock glacier from 1975-2023

Figure 14 illustrates the evolution of horizontal surface displacement at the Jungpass rock glacier over successive six-year periods (with a seven-year interval for 1968–1975) from 1968 to 2023. A comparison of the individual time steps reveals moderate fluctuations in displacement magnitudes over the study period, but no abrupt changes are evident. During the first three intervals up to 1987, all displacement vectors remain below 2 m, indicating low creep rates. From 1987 to 2011, displacement gradually increases, with some areas reaching up to 5 m per period. The highest values, up to 8 m, are observed in isolated areas during the most recent periods starting in 2011. However, the majority of vector lengths remain between 2 and 5 m.

Throughout the study period, the velocity field of the rock glacier appears spatially consistent. Higher displacement rates are concentrated at the frontal zone, while the rooting zone and upper sections remain largely inactive, typically showing displacements of less than 0.5 m per six-year period. Overall, the data indicate a slow but steady acceleration of the rock glacier, without evidence of a spatial shift in the activity pattern.

An examination of the underlying orthoimages shows that earlier images (especially prior to 1999) frequently contain snow-covered areas, whereas they are largely absent in more recent datasets. Since CIAS cannot produce reliable displacement results in snow-covered zones, these areas are excluded from the analysis, resulting in a lower

density of displacement vectors in earlier periods. In addition, lower image quality and greater positional offsets in older image pairs contribute to more frequent filtering of erroneous values. Shadows also affect the results for 2011 and 2017, where large shaded areas produced no valid displacement vectors. Importantly, all areas lacking displacement data can be plausibly attributed to snow cover, shadows, low contrast, or image quality issues. Accordingly, the CIAS analysis for Jungpass rock glacier does not indicate the presence of significant morphological transformations during the study period.

Figure 15 shows the displacement vectors derived from CIAS for the Brändjispitz rock glacier. As previously noted, no meaningful results could be obtained for the first study period (1968–1975) due to low optical contrast, and the analysis therefore begins with the period 1975–1981. Displacement rates remain below 2 m until 1987, comparable to those observed at the Jungpass rock glacier. Between 1987 and 1999, creep velocities gradually increase, followed by a marked acceleration in the central part of the rock glacier. From 2011 onwards, displacement vectors in this area exceed 15 m over six years, indicating a phase of rapid and localized deformation. Particularly striking is the change in the spatial pattern of displacement. While the creep field was relatively uniform until around 1993, the onset of localized acceleration in the central part of the rock glacier disrupts this pattern.

Snow-covered areas continue to result in missing displacement vectors in some periods, as with other sites. However, unlike Jungpass, there are additional zones on Brändjispitz where displacement vectors are absent, despite the absence of snow cover, shadow, or low optical contrast. These areas become prominent from the 1993–1999 period onward and appear both upslope and downslope of the central acceleration zone. Detailed analysis and comparison of the corresponding orthoimages reveal that the cause lies in drastic surface changes between the image pairs. The emergence of cracks and other surface disturbances prevents CIAS from matching test blocks to their reference counterparts. In such cases, the absence of reliable vectors in CIAS output can itself be interpreted as an indicator of significant surface transformation, an aspect that is further explored in the morphological analysis.

Jungpass and Brändjispitz represent two contrasting cases within the study. Whereas Jungpass shows a steady and spatially consistent creep pattern over time, Brändjispitz exhibits pronounced acceleration and a spatially heterogeneous velocity field. These

visualizations provide important insights into the displacement dynamics of individual rock glaciers. However, to enable a systematic comparison across all studied sites, further quantitative analyses are required. These are presented in the following sections.

9.1.2. Mean annual surface creep

The displacement data derived from CIAS are converted into mean annual surface creep rates to allow a direct comparison of the temporal creep behaviour across all studied rock glaciers. Figure 16 illustrates the development of these rates over time, with individual glaciers shown in distinct colours and the overall mean displayed to highlight general trends. It offers a concise overview of temporal developments and facilitates an immediate comparison between individual rock glaciers.

To ensure maximum temporal resolution, displacement data from all available time intervals are used. Although the periods vary in length, this is unproblematic as the values are normalised to annual rates. The x-axis reflects the actual duration of each period, preventing visual distortion.

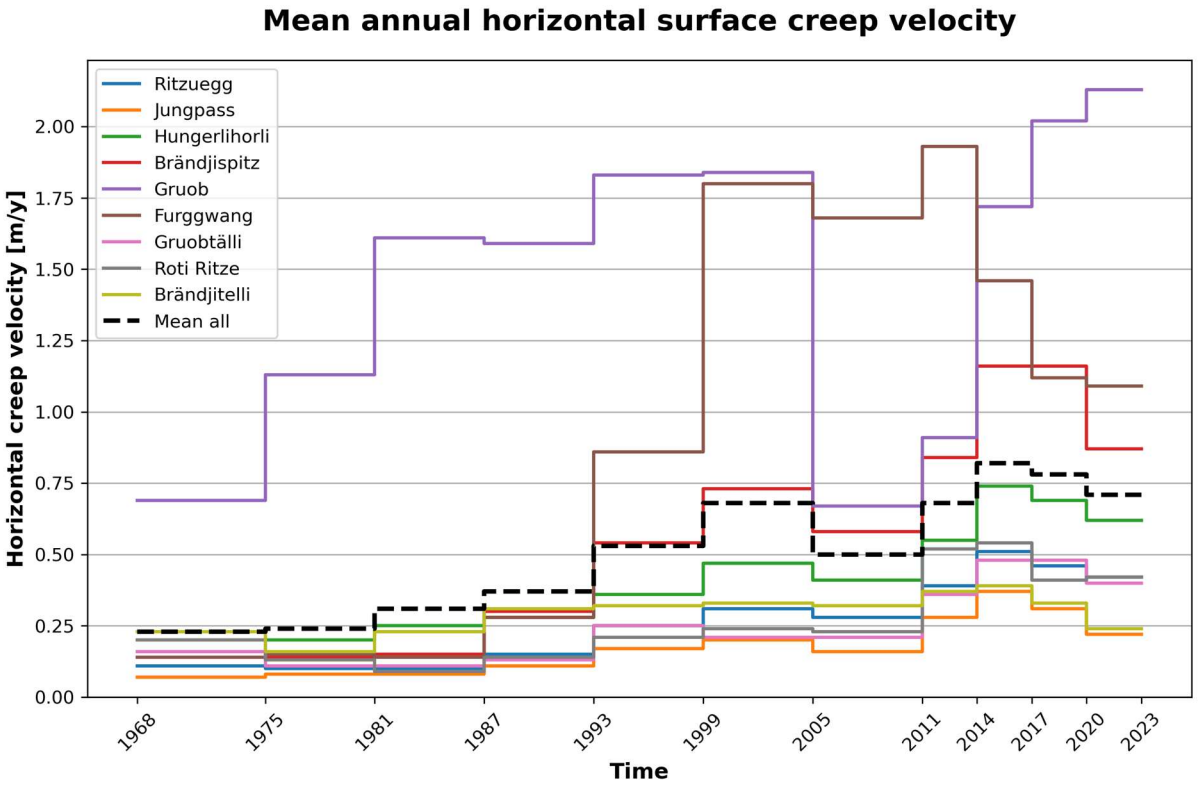

Figure 16 Mean annual horizontal surface creep velocity of all studied rock glaciers from 1968 to 2023.

The temporal evolution of mean annual horizontal surface creep velocities reveals both overarching trends and pronounced differences among the investigated rock glaciers (Figure 16). While several rock glaciers exhibit persistently low velocities, others display distinct acceleration phases and considerable temporal variability.

A majority of the rock glaciers including Ritzuegg, Jungpass, Brändjitelli, Gruobtälli and Roti Ritze relatively low and stable mean creep velocities during the early observation periods. From around the 1990s, a slight acceleration becomes apparent, though velocities remain below 0.33 m/y until the early 2000s. Following a temporary decline, all of these glaciers show a general increase in velocity after 2005–2011, with varying intensity. Roti Ritze, for instance, displays a notably stronger increase between 2011 and 2014 compared to the others in this group. Brändjitelli deviates slightly from the general trend by reaching a mean velocity of 0.31 m/y as early as 1987–1993 and maintaining a stable trajectory for several decades, with only moderate acceleration in recent years. From around 2017 until the end of the observation period, a declining trend in horizontal creep velocities is observed across this group.

Brändjispitz also shows low and stable velocities during the early observation periods but undergoes a marked acceleration beginning in 1987 to 1993. After a temporary slowdown during 2005 to 2011, which corresponds with the general regional trend, the rock glacier resumes its acceleration and reaches a peak mean velocity of 1.16 m/y in the period 2014 to 2020. Although a decline follows, recent values remain clearly higher than those observed for the majority group. Hungerlihorli follows a broadly similar pattern, although at a lower overall velocity. It begins to accelerate moderately as early as 1975 to 1981, experiences a minor decline in 2005 to 2011, and reaches its maximum value of 0.74 m/y between 2014 and 2017.

Gruob and Furggwang rock glaciers exhibit distinctly higher creep velocities than the other investigated rock glaciers. Already in the first observation period from 1968 to 1975 the mean creep velocity of Gruob rock glacier is at least three times higher than that of the others. From this elevated baseline the velocity continues to rise with only minor fluctuations, reaching 1.84 m/y in the period from 1999 to 2005. A pronounced drop follows in 2005 to 2011, after which the creep rate increases again and reaches a maximum of 2.13 m/y in the most recent period from 2020 to 2023. Furggwang rock glacier on the other hand does not initially deviate from the general pattern observed across the study area. However, after 1993 it shows a marked acceleration. Although a

moderate decline is observed between 2005 and 2011, the creep rate peaks at 1.93 m/y during 2011 to 2014 and subsequently decreases only slightly, remaining at a high level. Despite their distinctly higher velocities and divergent long-term trajectories, Gruob and Furggwang rock glaciers show certain temporal fluctuations that resemble broader patterns observed across the study area.

Regional trend

On a regional scale, the data reveal a consistent temporal pattern across most rock glaciers. During the early observation periods, creep velocities are relatively uniform and low. From the late 1980s onward, a general acceleration is observed, continuing through the following decades. This trend is briefly interrupted between 2005 and 2011, when most rock glaciers show a temporary decrease in velocity. Subsequently, velocities increase again, reaching a peak around 2014 to 2017. In the most recent periods, a declining tendency is apparent.

9.1.3. Distribution of annual surface creep

Figure 16 provides a clear initial overview of the general trend in creep velocities for each rock glacier throughout the study period. However, mean values do not reflect the full range of displacements and obscure spatial variability within individual rock glaciers. In particular, no conclusions can be drawn about the homogeneity of the displacement field or the magnitude of maximum and minimum values. These aspects are essential for identifying kinematic anomalies, which often affect only parts of a rock glacier and may not be reflected in mean annual rates. Therefore, the spatial distribution of horizontal surface displacement is analysed in more detail in the following section.

To account for this spatial variability, boxplots are created for each rock glacier and each observation period. These plots are based on the filtered displacement vector lengths, converted into annual values to enable comparison between periods of different duration. The black dashed line indicates the mean annual creep velocity across all studied rock glaciers, corresponding to the average shown in Figure 16 and serving as a reference. However, it is important to note that the central line in each box represents the median, not the mean, and direct comparisons with the overall average should be interpreted with caution.

Additionally, the number of displacement vectors included per year is indicated in the plot. A higher number of valid vectors improves the representativeness of the actual creep behaviour across the extent of each rock glacier and enhances the reliability of the derived statistics. Variations in the number of included vectors are primarily caused by factors such as snow cover, shadow, image quality, and surface disturbances, all of which influence the performance of CIAS. However, the number of vectors cannot be directly compared between different rock glaciers, as it is also a function of their respective sizes. Since the grid spacing is uniformly set to 10 metres, larger glaciers naturally yield more vectors.

Ritzuegg, Jungpass, Gruobtälli rock glaciers

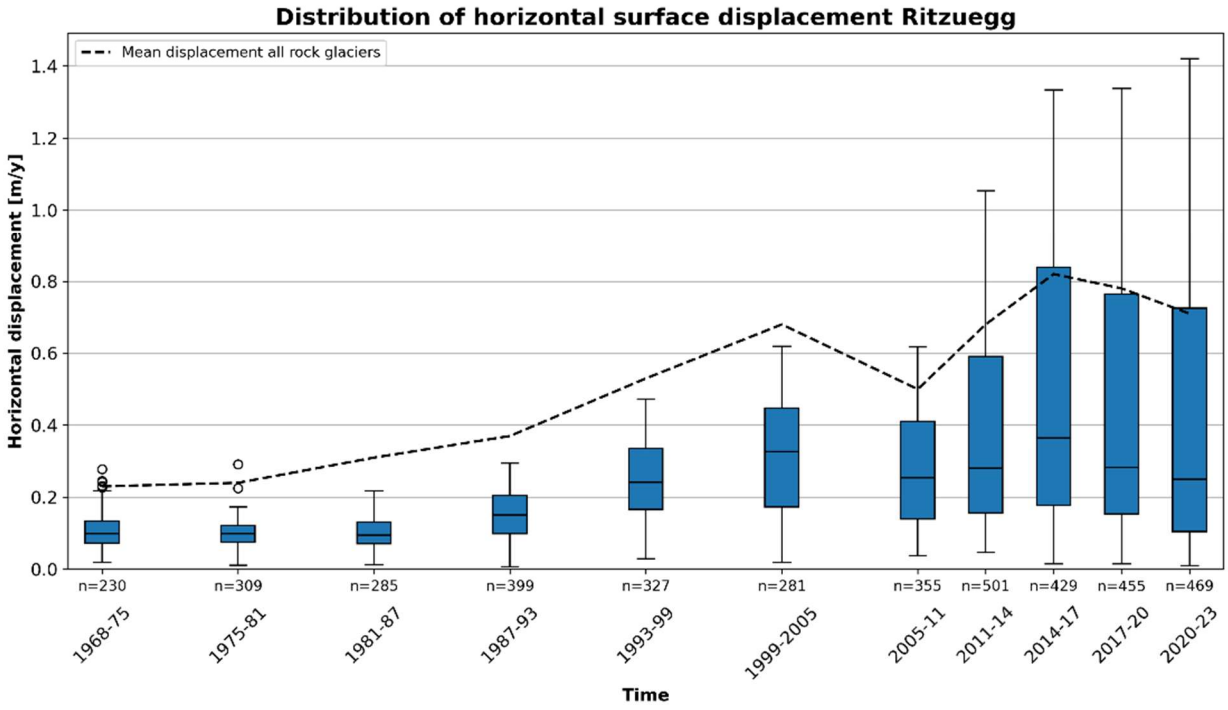

Figure 17 Distribution of the horizontal surface displacement values for Ritzuegg rock glacier from 1968-2023.

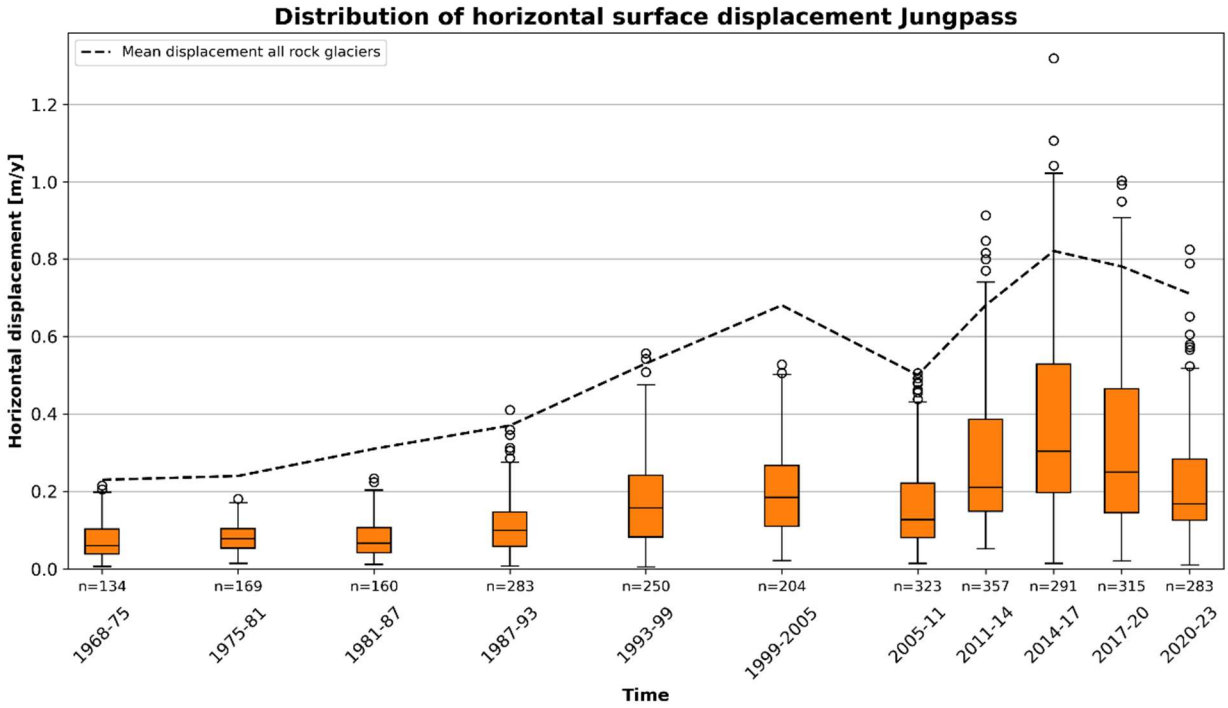

Figure 18 Distribution of the horizontal surface displacement values for Jungpass rock glacier from 1968-2023.

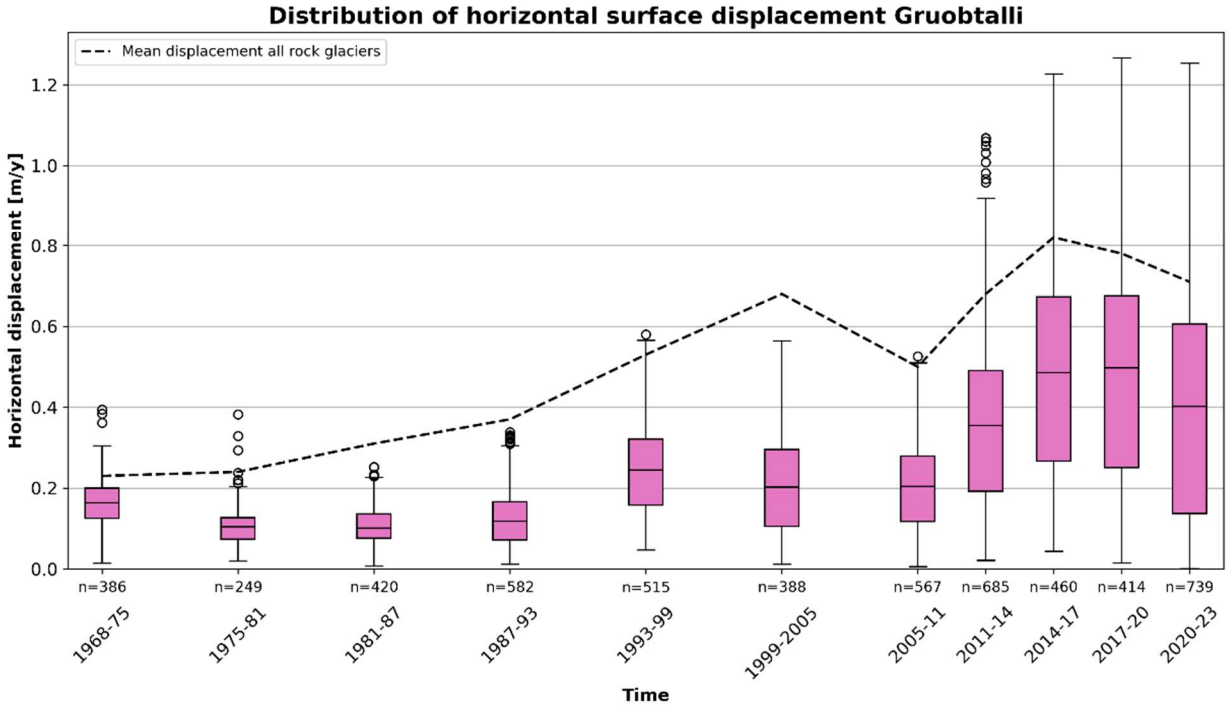

Figure 19 Distribution of the horizontal surface displacement values for Gruobtälli rock glacier from 1968-2023.

The distribution of horizontal surface displacement values for the Ritzuegg, Jungpass, and Gruobtälli rock glaciers (Figures 17-19) reveals key aspects of their temporal and spatial dynamics. In the early observation periods (1968–75 to 1981–87) displacement values remain low with maximum annual rates below 0.4 m/y. The data are closely clustered, as indicated by narrow interquartile ranges and short whiskers, suggesting

a spatially homogeneous velocity field with little internal variation and no indication of localised acceleration.

From the mid-1980s onward both the median displacement and the overall spread of values gradually increase. The widening of the boxes and elongation of the whiskers indicate increasing spatial variability, likely reflecting the emergence of locally accelerated zones that do not extend across the entire landform alongside areas with negligible displacement. This trend becomes particularly pronounced from 1993–99 with a marked rise in maximum values from 2014–17 onwards, peaking at around 1.4 m/y.

Despite this increase in internal variability and maximum displacement the overall behaviour of Ritzuegg, Jungpass, and Gruobtälli remains moderate when compared to the more strongly accelerating rock glaciers in the study. The number of valid displacement vectors fluctuates throughout the study period, with higher counts in recent years due to improved image quality and reduced snow cover. Nonetheless, all periods contain a sufficient number of observations to ensure reliable statistical interpretation.

Brändjitelli rock glacier

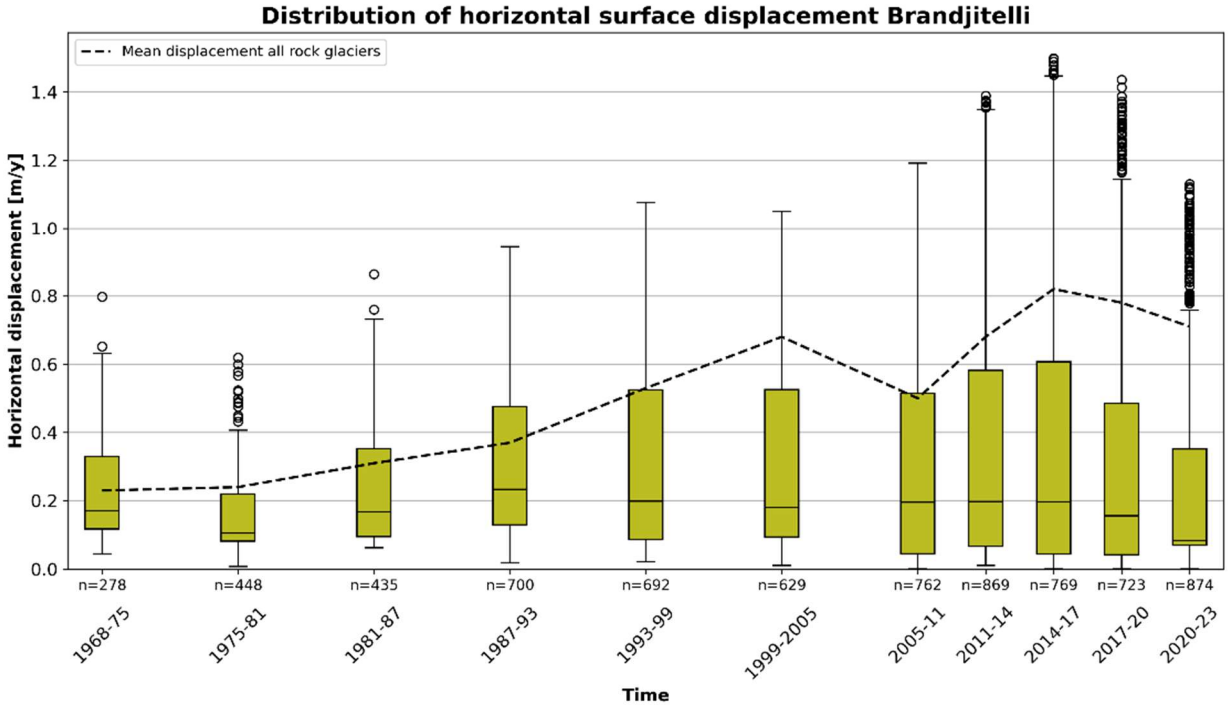

Figure 20 Distribution of the horizontal surface displacement values for Brändjitelli rock glacier from 1968-2023.

The Brändjitelli rock glacier (Figure 20) displays a relatively stable development over the entire observation period. In contrast to many others, no clear acceleration trend is evident and creep rates remain remarkably constant throughout the decades. The interquartile range increases slightly from the mid-1980s onward similarly to the previously discussed rock glaciers, suggesting some localized variation with maximum creep rates of 1.5m/y in 2014-17. However, the majority of values remain within a narrow range around 0.2 m/y. In the most recent periods, the number of very slow or nearly immobile points increases. This could reflect either actual deceleration in some sectors or improved data coverage due to reduced snow cover. Still, the general behavior remains stable, and the rock glacier continues to creep at a moderate and persistent rate.

Roti Ritze rock glacier

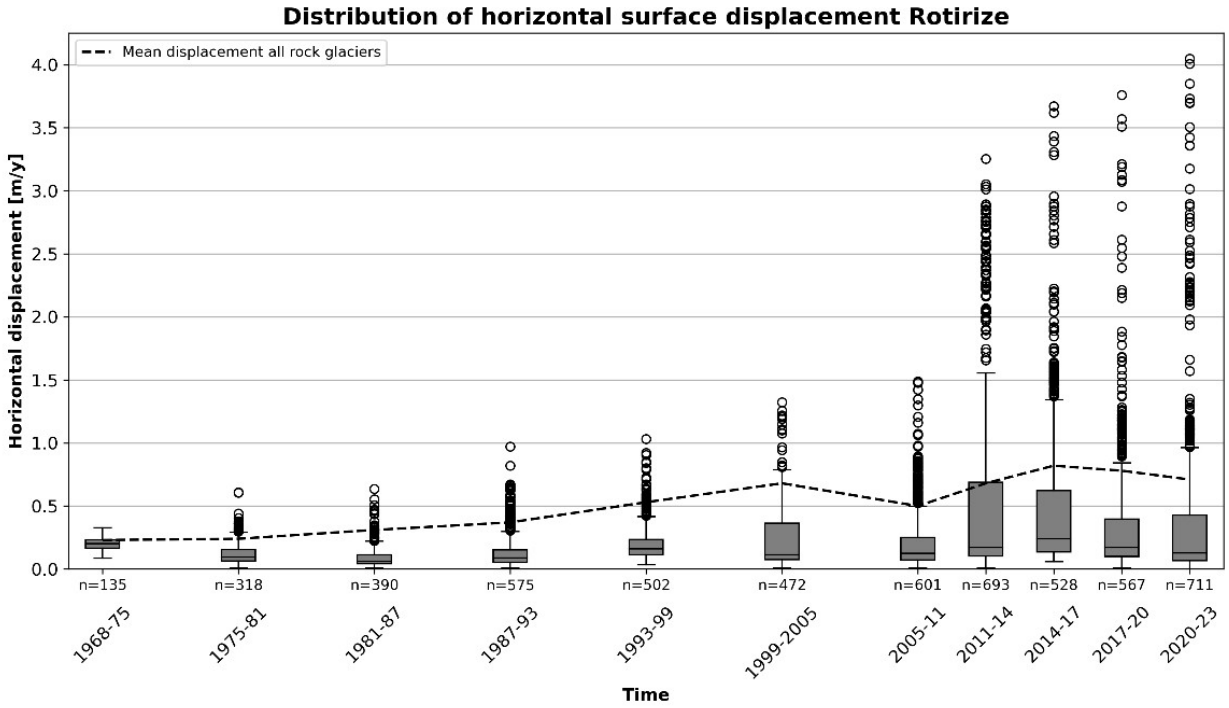

Figure 21 Distribution of the horizontal surface displacement values for Roti Ritze rock glacier from 1968-2023.

The Roti Ritze rock glacier (Figure 21) displays a distribution of creep velocities that is broadly similar to those of Ritzuegg, Jungpass, and Gruobtälli in terms of box size and whisker range. However, what distinguishes it is the exceptionally high number and magnitude of outliers, particularly from the 2011–2014 period onward, with maximum values exceeding 3 m/y. Although the median velocity slightly declines after 2014–2017, the outlier values continue to increase, reaching up to 4.05 m/y in the most recent observation period.

Given the frequency and consistency of these outliers across several periods, it is unlikely that they result from measurement errors. Instead, the data suggest that specific sectors of the rock glacier are undergoing pronounced localized acceleration, while the majority of the glacier continues to follow the regional trend with median velocities around or below 0.2 m/y. This coexistence of fast- and slow-moving areas indicates considerable kinematic heterogeneity and sets Roti Ritze apart from the more uniformly creeping rock glaciers discussed previously.

Hungerlihorli and Brändjispitz rock glacier

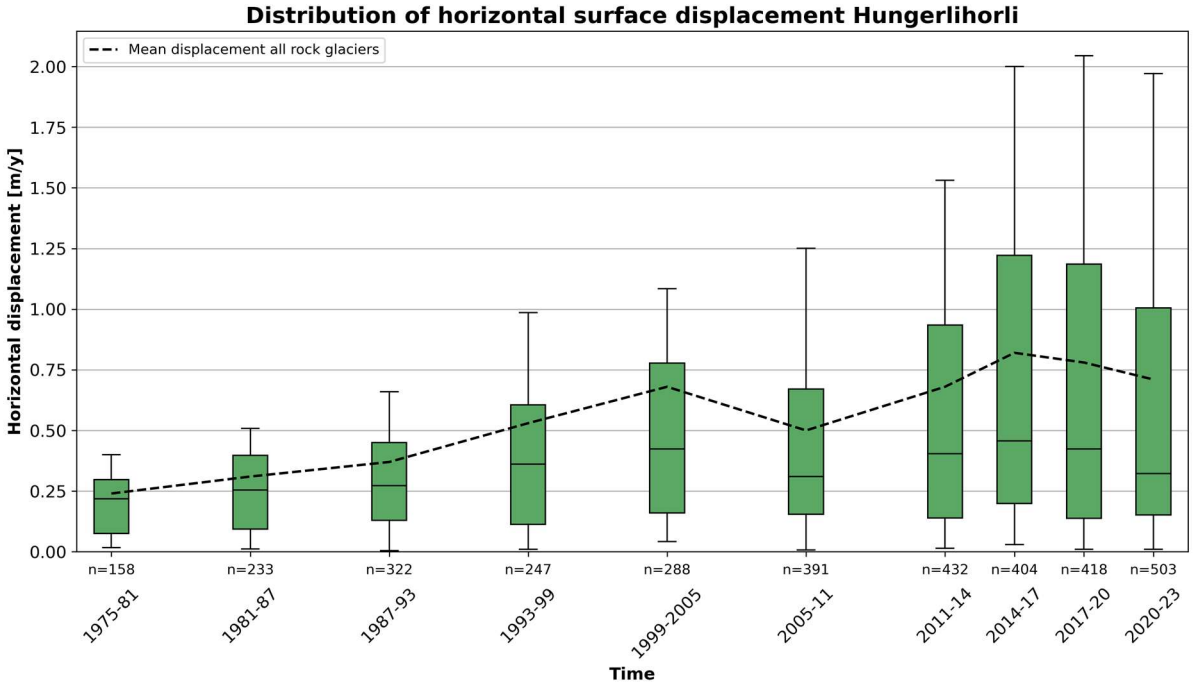

Figure 22 Distribution of the horizontal surface displacement values for Hungerlihorli rock glacier from 1975-2023.

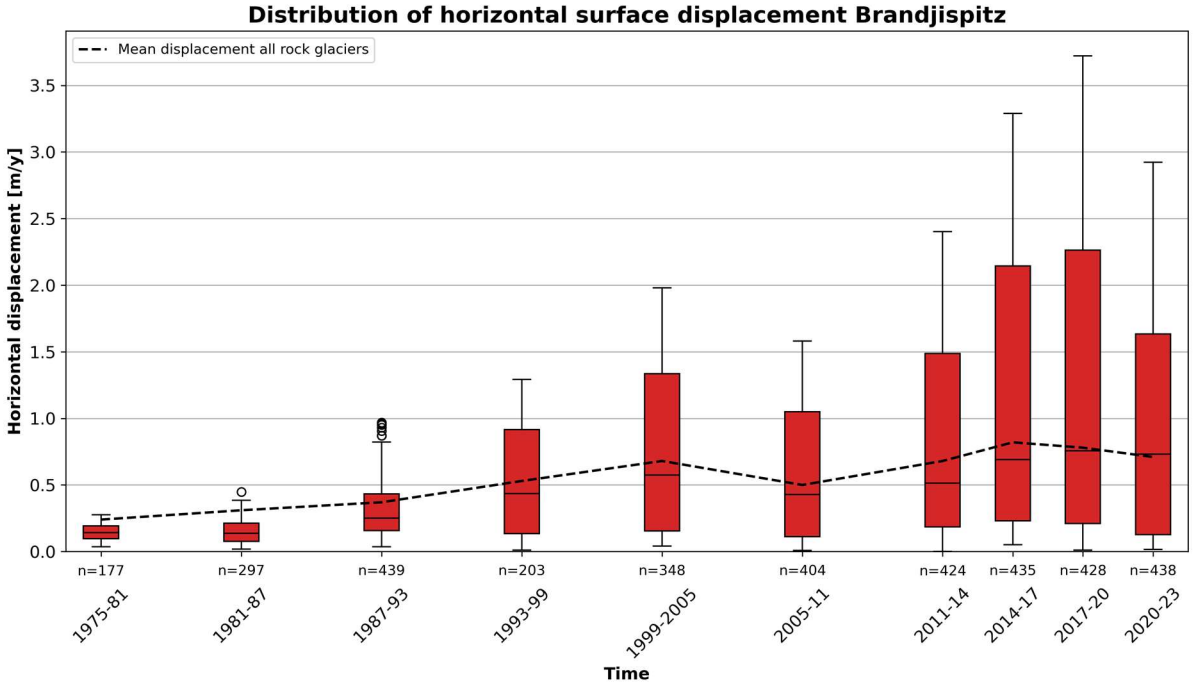

Figure 23 Distribution of the horizontal surface displacement values for Brändjitelli rock glacier from 1968-2023.

Brändjispitz and Hungerlihorli (Figures 22-23) display a pattern very similar to previously discussed rock glaciers such as Ritzuegg, Jungpass, and Gruobtälli. In both cases, the boxplots and whiskers evolve in comparable ways, indicating a generally coherent kinematic behaviour over time. However, the absolute displacement values are remarkably higher. This is particularly evident at Brändjispitz, where maximum

velocities reach 3.72 m/year in the 2017–20 period, making it one of the most active rock glaciers in the dataset. Hungerlihorli rock glacier experiences maximum displacement values of 2.04m/y in the same period.

In both cases, the displacement distributions also include a notable proportion of very low values, with some vectors indicating minimal or no movement. This suggests a high degree of internal variability, with faster-moving zones occurring alongside slower or near-stationary areas. The spatially heterogeneous creep behaviour observed here is consistent with the patterns already apparent from the displacement vector plot from Brändjispitz shown in Figure 15.

Furggwang rock glacier

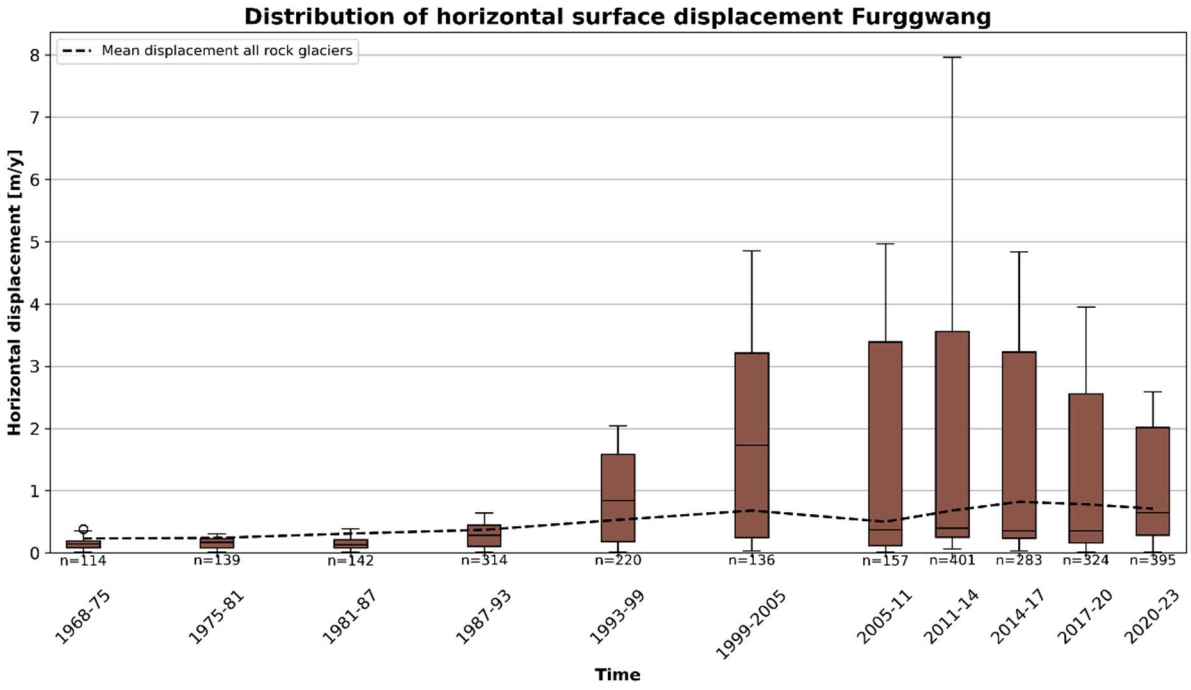

Figure 24 Distribution of the horizontal surface displacement values for Furggwang rock glacier from 1968-2023.

The overall development of Furggwang rock glacier (Figure 24) is initially comparable to other sites such as Ritzuegg, Jungpass, and Gruobtälli. In the early observation periods, creep rates are similarly low, and the narrow interquartile ranges and short whiskers indicate a relatively uniform displacement pattern. Maximum values are likewise consistent with those of the aforementioned glaciers, reaching approximately 0.4 m/year.

From 1993–99 onwards, however, Furggwang exhibits a marked increase in displacement that exceeds the trends observed at the other sites. This culminates in

the 2011–14 period, where individual values reach up to 7.97 m/year, while the median remains below 0.5 m/year. This pronounced divergence between central and extreme values, coupled with a widening interquartile range, points to an increasingly heterogeneous velocity field with some zones undergoing extreme acceleration while large parts of the rock glacier remain relatively slow-moving.

It should be noted that several periods are based on a limited number of displacement vectors. In the earlier years, this is primarily due to persistent snow cover, while in periods such as 1999–2005 and 2005–11, extensive surface changes reduced the performance of the CIAS algorithm. As a result, particularly the mean and maximum velocities should be interpreted with caution, as they may not fully capture the complex kinematic behaviour of the glacier.

Gruob rock glacier

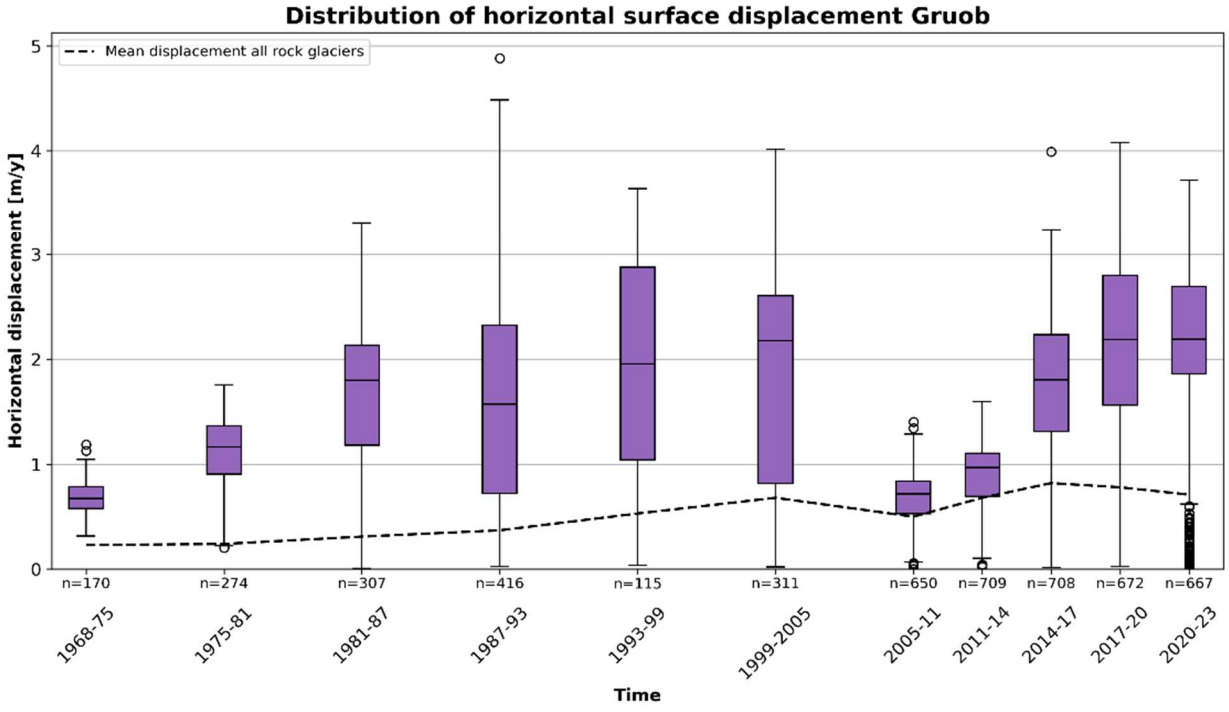

Figure 25 Distribution of the horizontal surface displacement values for Gruob rock glacier from 1968-2023.

Gruob rock glacier (Figure 25) differs significantly from the rest of the dataset. From the earliest periods, it exhibits pronounced spatial variability in creep behaviour, as evidenced by wide interquartile ranges and long whiskers. Already in 1987–1993, displacement values range from near zero to approximately 4.5 m/year, with a maximum outlier of 4.88 m/year. This indicates a heterogeneous velocity field long before similar dynamics emerge at other sites.

This pattern persists until 2005-11, where a substantial narrowing of both the interquartile range and the whiskers occurs for two periods. This stands in contrast to the general trend observed at other rock glaciers, where variability tends to increase over time. In the case of Gruob, this may point to a temporary homogenisation of surface movement, which coincides with a marked reduction in overall creep velocities during this time. From 2014–2017 onward, however, creep rates increase again. The most recent period is characterised by a relatively small interquartile range and short whiskers, while the median remains high. This indicates a more uniform but still rapid creep behaviour across the rock glacier surface.

It is important to note that the 1993–1999 period is based on a limited number of displacement vectors (n = 115), which is low given the rock glacier's size. The values from this period should therefore be interpreted with caution, as they likely underestimate the actual displacement due to CIAS limitations in areas affected by significant surface transformation.

Summary displacement distribution

Most rock glaciers in the dataset, such as Ritzuegg, Jungpass, Gruobtälli, and Brändjitelli, exhibit a consistent temporal pattern: initially low and spatially uniform displacement rates, followed by a gradual increase in both magnitude and spatial variability from the mid-1980s onwards. This is reflected in the widening of boxplots and whiskers, suggesting the emergence of localised acceleration zones. However, the overall magnitude of change remains moderate, with maximum velocities around 1.5 m/year and no evidence of widespread kinematic transformation across the rock glaciers.

In contrast, several rock glaciers deviate from this general pattern. Furggwang exhibits extreme inhomogeneity, with peak velocities exceeding 8 m/year in 2011–14, while the median remains low. Roti Ritze is marked by a high number of large outliers across multiple periods, indicating persistent local acceleration. Brändjispitz and Hungerlihorli are characterized by high overall velocities and a wide internal spread with maximum displacements reaching approximately 3.7 and 2m/year, respectively. Gruob is exceptional in that it shows high variability already in the 1980s, followed by a rare temporary homogenisation in the 2000s. These cases highlight that while a

general trend exists, some rock glaciers exhibit pronounced kinematic anomalies driven by highly localised acceleration.

9.1.4. Change in annual surface creep

The previous chapter highlighted the individual evolution of the investigated rock glaciers, revealing heterogeneous creep behaviour and the presence of acceleration phases. Since acceleration is a key indicator of destabilization, it is specifically addressed in this section. To appropriately contextualize the observed developments, regional trends must be considered. A comparative visualization of changes in annual surface creep across all rock glaciers enables this contextualization most effectively.

Figure 26 displays the percentage change in mean annual horizontal surface creep velocity relative to the previous period for each rock glacier. Each bar represents one rock glacier for a specific time interval, while the black bar shows the average change across all rock glaciers for that period. Positive values indicate acceleration compared to the previous period, negative values indicate deceleration. To ensure comparability between periods, the 6-year intervals used for the visualization of the displacement vectors are applied here as well.

To capture shorter-term variability, the same plot is also generated for the available 3-year intervals (Figure 27). While this higher temporal resolution allows for the identification of short-term kinematic changes, the percentage values should not be directly compared to those from the 6-year intervals, as the time base for change is halved.

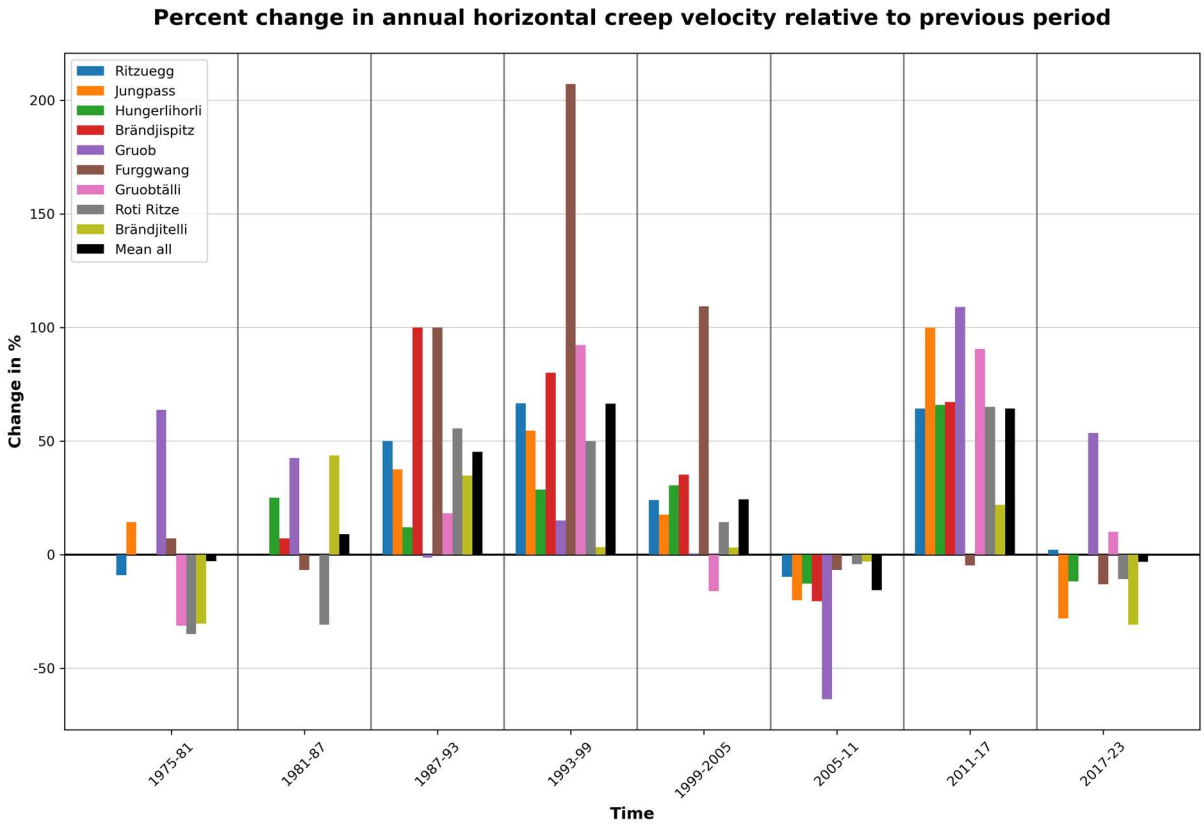

Figure 26 Relative change in annual horizontal creep velocity relative to previous period for all studied rock glaciers.

Most rock glaciers follow a shared regional pattern in their relative velocity changes. After a generally rather stable phase, a marked acceleration begins in 1987-93 and initiates a prolonged trend of increasing creep velocities that continues until 2005–2011. This phase is followed by a regional deceleration, affecting all investigated rock glaciers. A subsequent acceleration occurs thereafter, before velocities decline again in the period 2017–2023 at most sites. Despite this overarching pattern, several rock glaciers display distinct individual trajectories that clearly deviate from the regional trend.

Gruob rock glacier deviates markedly from the regional pattern in several periods. It exhibits a strong acceleration already in the 1975–1981 period, well before similar trends become apparent at most other sites. While many rock glaciers begin to accelerate in the early 1990s, Gruob maintains relatively stable velocities between 1987–1993 and 1999–2005, with only minor changes below 16%. In 2005–2011, Gruob follows the general regional trend and decelerates. However, the magnitude of this decrease is substantially higher than average, with a relative change of –64% compared to a mean deceleration of –16% across all rock glaciers. In the final period from 2017–2023, Gruob again diverges from the general pattern. While most rock glaciers

decelerate, Gruob accelerates by 54%, indicating a renewed increase in creep velocity contrary to the regional trend.

Furggwang rock glacier initially follows the regional trend but enters a phase of pronounced acceleration after the 1981–1987 period. While all rock glaciers show increasing creep velocities during this time, the magnitude of change at Furggwang exceeds that of all other sites clearly. It records three consecutive periods of exceptionally high acceleration: 100% between 1987–1993, 207% between 1993–1999, and 109% between 1999–2005. This results in a severalfold increase in creep velocity within less than two decades—an unusually intense and sustained anomaly that sets Furggwang apart from all other rock glaciers in the dataset.

Similar to Furggwang, Brändjispitz rock glacier shows a marked acceleration in the period 1987–1993, with a velocity increase of 100%. This value clearly exceeds those of most other sites except Furggwang, with the next highest change being less than half as large. In the subsequent periods, the development of Brändjispitz aligns more closely with the general regional trend.

Gruobtälli generally follows the regional trends but shows a notable deviation in the 1999–2005 period, where it decelerates by 16% compared to 1993–1999, while all other rock glaciers continue to accelerate. A similar deviation is observed in the most recent period from 2017 to 2023, during which Gruobtälli accelerates by 10%, whereas the majority of rock glaciers exhibit a deceleration.

Ritzuegg, Hungerlihorli, Roti Ritze, and Brändjitelli rock glaciers closely follow the regional trends and do not exhibit notable deviations in any observation period. They neither reach extreme values that markedly differ from other sites nor show opposing trends relative to the majority of the rock glaciers. Their development consistently reflects the general pattern of acceleration and deceleration phases observed across the study area.

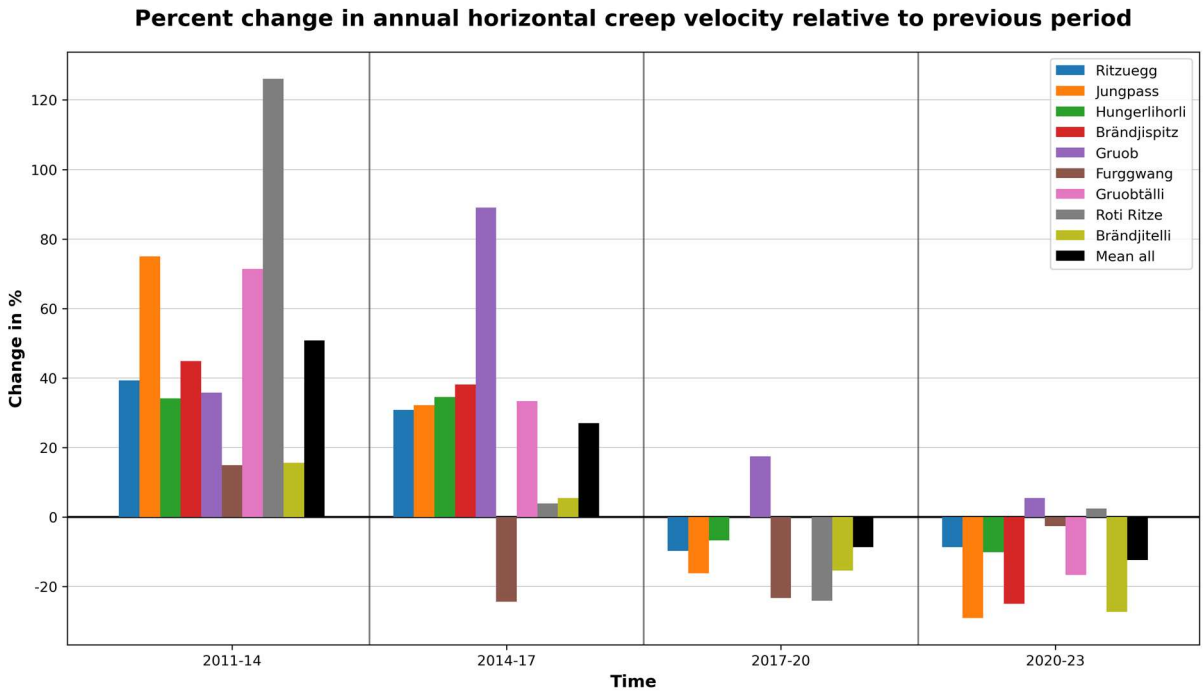

Figure 27 Relative change in annual horizontal creep velocity relative to previous period for all studied rock glaciers with 3-year intervals.

The examination of Figure 27, which displays the 3-year intervals, reveals interesting differences compared to the 6-year interval results shown in Figure 26. While the higher temporal resolution confirms the general regional trends, several noteworthy deviations become apparent.

In particular, the acceleration of Roti Ritze rock glacier during the 2011–2014 period stands out. This acceleration is not visible in the 6-year analysis, where it is neutralized by the low change rates recorded in 2014–2017. In the 3-year dataset, Roti Ritze exhibits a 126% increase in mean creep velocity within just three years, representing a remarkable and exceptional acceleration. This value is considerably higher than those observed at the other sites during the same period and far exceeds the previous maximum acceleration of Roti Ritze, which was +56% during 1987–1993.

Another notable deviation concerns Jungpass and Ritzuegg rock glaciers. In the 3-year interval analysis, both show a deceleration during the periods 2017–2020 and 2020–2023. These observations align with the general regional trend of declining creep rates and contradict the slight acceleration suggested by the 6-year interval data.

9.1.5. Summary Kinematics and potential destabilization

As outlined in the theoretical background, destabilized rock glaciers are typically characterized by kinematic anomalies, meaning a deviation from the overarching, long-term regional trend. In this chapter, the kinematics of the studied rock glaciers are summarized and evaluated for such anomalies.

Mean creep velocity

In the proposed typology of destabilized rock glaciers, typical local horizontal creep rates are reported to reach 2–5 m/y for Type 1 destabilized rock glaciers and to often exceed 5 m/y for Type 2. However, these values primarily refer to localized displacement and are not directly applicable to the mean creep velocity of an entire rock glacier. Additionally, it is not meaningful to apply fixed thresholds to mean creep velocities for distinguishing kinematically anomalous behaviour from regionally consistent development over the whole study period, as regional trends themselves evolve over time.

Regarding mean creep, Gruob and Furggwang clearly show anomalies and deviate strongly from regional patterns. Brändjispitz rock glacier generally follows the regional trend but exhibits significantly elevated mean creep velocities in recent periods.

Creep heterogeneity and maximum displacement

The distribution of displacement values provides further insights into the spatial variability of creep and the occurrence of maximum displacement rates. As discussed in the theoretical part, spatially heterogeneous creep with localized areas of enhanced velocity is a characteristic of destabilized rock glaciers. As previously noted, local horizontal creep rates in known cases of destabilized rock glaciers typically range from approximately 2 m/y to more than 5 m/y, depending on the type of destabilization. Among the studied rock glaciers, Gruob, Furggwang, Roti Ritze, Brändjispitz, and Hungerlihorli exceed these values and are all characterized by heterogeneous creep behaviour.

Creep acceleration and deceleration deviating from regional trends

The rock glacier acceleration is a key feature of destabilized rock glaciers. To better differentiate remarkable changes from regional climate-driven trends affecting all rock glaciers, relative changes in creep velocity are analysed. Applying a fixed threshold to distinguish anomalous behaviour across all periods is not appropriate, as it would not adequately capture period-to-period variability related to overarching climate trends. Rock glaciers that clearly deviate from regional trends across several periods are Gruob and Furggwang. Brändjispitz and Roti Ritze also exhibit notable deviations in at least one observation period.

Overall assessment kinematics and destabilization

Furggwang, Gruob and Brändjispitz rock glaciers stand out in all kinematical analyses. These rock glaciers exhibit significant acceleration, high creep velocities and inhomogeneous creep with fast-moving and slow-moving areas coexisting. Roti Ritze, despite not being striking in terms of mean creep, shows considerable acceleration and inhomogeneous creep in recent periods with high-velocity zones. These glaciers exhibit kinematic anomalies that deviate from regional trends in terms of temporal and spatial evolution of the creep behaviour.

Hungerlihorli presents a more borderline case. It shows slightly elevated mean creep velocities and its maximum displacement values reach 2m/y. However, it does not substantially deviate from regional trends, as no notable anomalies are detected in the analysis of creep rate changes.

Ritzuegg, Jungpass, Brändjispitz, and Gruobtälli exhibit acceleration but largely follow regional trends. These rock glaciers display relatively homogeneous creep behaviour with more gradual shifts in their creep patterns. While their acceleration is noticeable, it remains within the expected range for the region without the pronounced anomalies seen in the more dynamic rock glaciers.

9.2. Morphological evolution

Aside from kinematic anomalies, the occurrence of surface disturbances such as cracks, scarps, and crevasses is identified in the typology as a defining feature of destabilized rock glaciers. All study sites are therefore analysed according to the procedure introduced in the methodology.

9.2.1. Vertical change

The first step in identifying areas of enhanced morphological activity is the analysis of vertical changes using the DEM of Difference (DoD). The same DoD was also used in the preliminary study to support the selection of the study sites.

Spatial analysis

Figure 28 shows the DoD over the entire study period from 1968 to 2023. The outlines of the investigated rock glaciers correspond to their extent in 2023. Blue colours indicate areas where surface elevation has increased since 1968, whereas red colours denote elevation loss. Yellow shades represent areas with little or no change. It must be noted that differences in snow cover between the two elevation models introduce artefacts: while the 2023 DTM shows almost no snow cover, the 1968 DSM is locally elevated due to snow accumulation. Consequently, some apparent elevation changes are attributable to seasonal snow rather than actual surface deformation. This particularly affects certain sectors of Ritzuegg and the southwestern part of Hungerlihorli rock glacier.

While the DoD captures a range of geomorphic processes across the region, including glacier retreat and rock avalanches, the following discussion focuses exclusively on the rock glaciers of interest. Overall, all rock glaciers show some degree of mass gain in their frontal parts due to advance, but considerable differences in surface change patterns are observed between sites.

Gruobtälli and Ritzuegg rock glaciers display typical ridge-and-furrow topography, with relatively homogeneous mass redistribution across the landform. Excluding an area of strong elevation loss at the eastern end of Ritzuegg (attributable to snow artefacts), no concentrated zones of mass loss or gain are apparent, suggesting stable

internal deformation without localized anomalies. Jungpass rock glacier similarly shows only very limited mass relocation throughout the study period.

Brändjitelli rock glacier also exhibits pronounced ridge-and-furrow topography, especially in the lower parts. In the upper, eastern section, however, the mass redistribution is more spatially extensive, with broader zones of gain and loss rather than a distinct ridge-and-furrow pattern.

Hungerlihorli rock glacier shows classic ridge-and-furrow structures in its frontal part. In the upper (southern) sectors, however, the DoD reveals irregular and small-scale patterns of mass gain and loss without systematic alignment, suggesting localised and spatially disorganized surface dynamics. The larger mass loss values observed in the southwestern section are attributed primarily to differences in snow cover and are not further considered.

Brändjispitz and Roti Ritze rock glaciers both show localized zones of significant elevation change. Each exhibits a confined area of mass loss, adjacent to slightly larger zones of mass gain. In Brändjispitz the frontal parts additionally show ridge-and-furrow features and initial indications of surface disturbance opening, such as incipient cracks in the zones of highest loss.

Gruob and Furggwang rock glaciers clearly exhibit the most substantial mass redistribution among the study sites. Both show general mass loss in their upper sections combined with massive accumulation in their lower parts, indicating pronounced downslope advance of the whole rock glacier. While Furggwang's mass loss is somewhat more spatially concentrated, Gruob exhibits a broader pattern of redistribution affecting almost the whole rock glacier. At both sites, clear morphological evidence of surface disturbance formation, such as crack opening, is visible in the areas of greatest elevation loss.

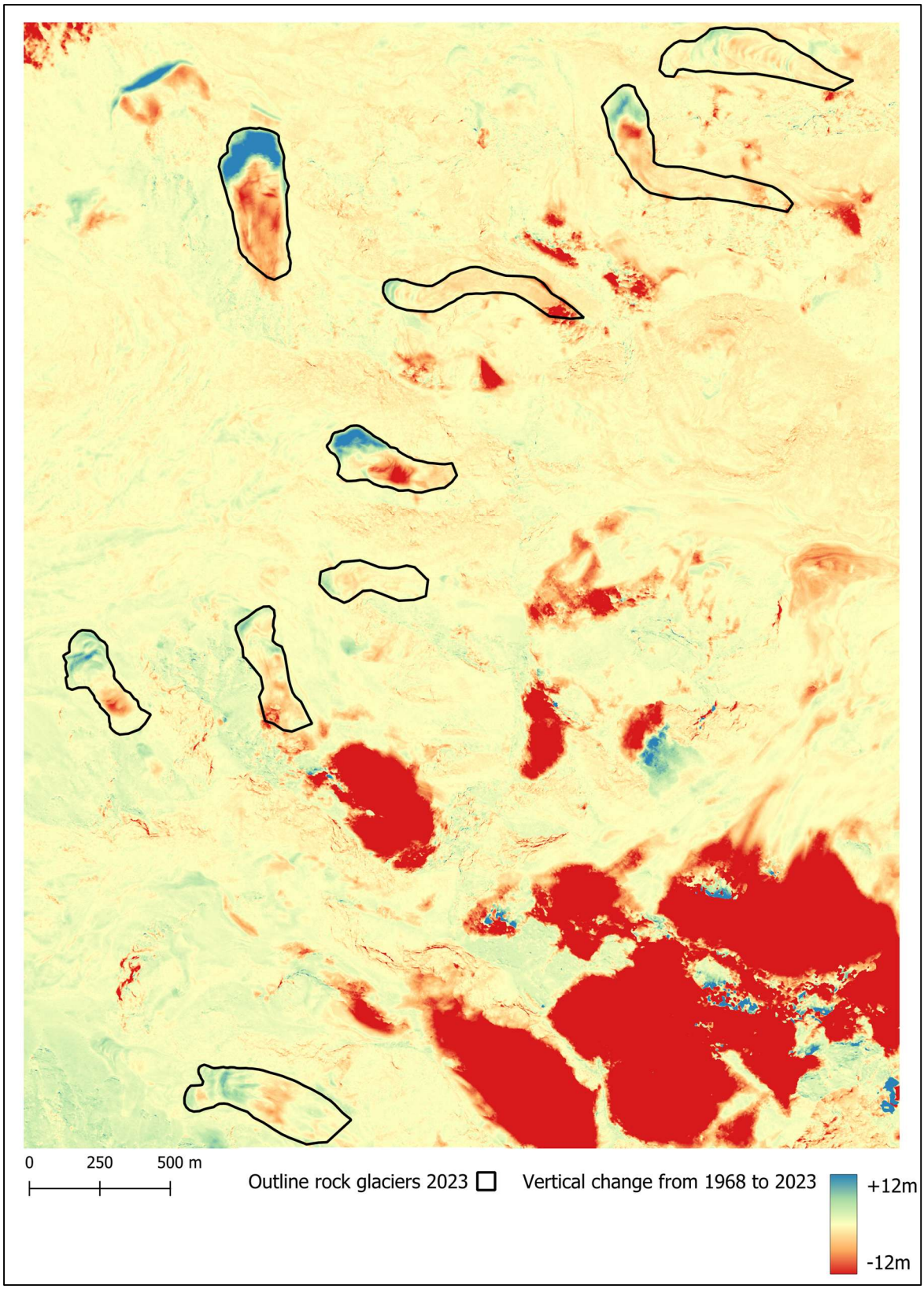

Figure 28 DEM of Difference for the whole study area from 1968-2023.

Quantitative vertical change

Following the analysis of the spatial patterns of mass relocation at the study sites (Figure 28), the elevation changes derived from the DEM of Difference are quantified using violin plots (Figure 29). These plots display the median, minimum, and maximum values as well as the overall distribution of elevation changes. The width of the violin at a given vertical change value reflects the relative frequency of that value within the dataset, providing insights into the dominant elevation change patterns across each rock glacier.

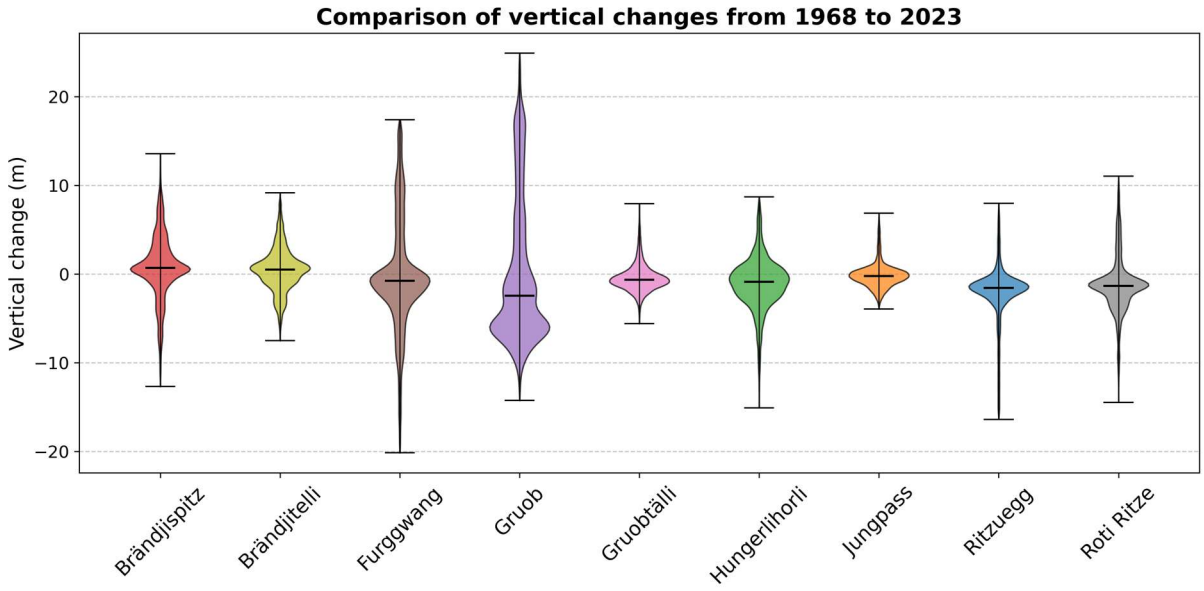

Figure 29 Value distribution of the vertical elevation changes from 1968-2023 displayed for all rock glaciers.

The distribution of long-term elevation changes from 1968 to 2023 reveals both consistent patterns and marked site-specific deviations among the investigated rock glaciers (Figure 29).

Gruobtälli and Jungpass rock glaciers exhibit closely comparable distributions, with median values near 0 m and elevation change limits generally constrained between –6 m and +8 m. The majority of values cluster tightly around zero, suggesting that large parts of these rock glaciers have remained relatively unchanged in terms of surface elevation. Ritzuegg shows a very similar overall distribution shape, with a close bulk of values also centred near zero and comparable maximum values. While a few values extend to significantly lower elevations, reaching minima beyond –15 m, these outliers originate from the zone strongly influenced by changes in snow cover rather than actual surface lowering of the rock glacier itself. When excluding those snow-affected areas, the minimum values are consistent with those observed for Gruobtälli and

Jungpass, which supports grouping Ritzuegg with this relatively stable subset of rock glaciers.

Hungerlihorli and Brändjitelli rock glaciers generally exhibit a similar distribution of vertical change values, with median and maximum values falling within the same range as the previously discussed sites. At Hungerlihorli, the minimum values are again likely influenced by snow cover and are therefore not considered fully representative of actual surface changes. However, the main body of the violin is slightly broader and rounder compared to the other rock glaciers, suggesting a slightly more heterogeneous distribution of surface changes across the rock glacier area or a larger portion of the surface affected by mass relocation.

Brändjispitz and Roti Ritze rock glaciers show similar patterns. In both cases, the majority of values and the median are close to 0 m, but the overall range exceeds ±10 m. At Brändjispitz in particular, maximum values reach approximately +14 m, indicating that some zones have experienced significant localized elevation gain.

The most pronounced deviations are observed at Furggwang and Gruob. These rock glaciers exhibit the widest elevation change ranges by far, with Furggwang reaching a minimum of −20 m and Gruob a maximum of +25 m. In the case of Gruob the distribution is notably shifted downward, with most values clustering around −5 m rather than centring around zero. This pattern indicates that nearly the entire rock glacier surface has experienced net surface lowering, with very few areas showing no change.

Summary vertical change

The combination of spatial and quantitative analysis of vertical changes from 1968 to 2023 reveals generally consistent patterns. Gruobtälli, Jungpass, and Ritzuegg rock glacier show limited surface change with spatial patterns dominated by rock glacier-typical ridge and furrow structures and no concentrated zones of mass loss or gain. This visual impression is confirmed by the quantitative data, which show violin plots centred around zero with no extreme values, indicating that large parts of these rock glaciers remained largely unaffected.

Brändjitelli shows a slightly higher distribution of the change values in Figure 29 than the rock glaciers mentioned above. This is consistent with the observations from the

spatial visualization of the change through the DoD, where a more extensive but still moderate pattern of mass relocation could be identified. However, the magnitude of this relocation is rather low and occurs alongside regular ridge and furrow structures, as reflected by minimum and maximum change values that are comparable to those of the rock glaciers showing limited activity.

Hungerlihorli shows a more heterogeneous surface pattern with irregular small-scale zones of elevation gain and loss, particularly in its upper parts. This spatial variability is reflected in the slightly broader distribution of values in the violin plot and indicates a somewhat more complex surface evolution.

Brändjispitz and Roti Ritze are characterised by spatially confined areas of elevation change, with small zones of pronounced loss and gain. This pattern is consistent with the violin plots, which show limited but distinct extremes and point to localized but marked surface processes.

Furggwang and Gruob show the most pronounced changes both spatially and quantitatively. Furggwang is characterised by intense mass loss in its upper part and strong accumulation in the lower part, which is reflected in the extreme minimum and maximum values in the violin plot. Gruob exhibits widespread surface lowering across almost the entire rock glacier. This pattern is consistent with the violin plot, where the majority of values lie below zero. These results confirm that Furggwang and Gruob underwent the most extensive and dynamic surface changes during the study period.

9.2.2. Rock glacier surface disturbance evolution

All study sites are systematically assessed for the development of surface disturbances following the decision tree introduced in the methodology chapter. Based on this analysis, each rock glacier is rated with regard to morphological indicators of potential destabilization. In addition to the destabilization rating, the temporal characteristics of the detected surface disturbances are summarised in Table 4. The Start of disturbances column indicates the last year in which no surface disturbances are visible, meaning that disturbances must have developed during the following observation period. This approach is chosen because the exact timing of the initial occurrence within the subsequent interval cannot be determined. The end of the active phase refers to the year after which no new surface disturbances form on the rock glacier.

Table 4 Rock glacier surface disturbance rating based on the decision tree by Macer et al. (2019)

Rock glacier	Rating	Start of disturbances	End of active phase
Ritzuegg	0 non-observable destabilization	-	-
Jungpass	0 non-observable destabilization	-	-
Gruobtälli	0 non-observable destabilization	-	-
Brändjitelli	0 non-observable destabilization	-	-
Hungerlihorli	3b potential destabilization	After 2005	2020
Brändjispitz	3a potential destabilization	After 1993	Active
Gruob	3a potential destabilization	After 1981	1999
Furggwang	3a potential destabilization	After 1993	2020
Roti Ritze	3a potential destabilization	After 2011	Active

The analysis reveals that the studied rock glaciers fall into two main groups. Four rock glaciers are rated as showing no observable destabilization, meaning that surface disturbances are either absent or too minor to be detected. In contrast, five rock glaciers exhibit distinct surface disturbances that evolve in intensity over time and are associated with a discontinuous displacement field, leading to a rating of potential destabilization according to the decision tree.

Brändjispitz, Gruob, Furggwang, and Roti Ritze initially show the typical morphology of a "normal" rock glacier (compare chapter 5.2). Over the study period, deep crevasses, scarps, and cracks develop across all four sites, fundamentally altering their surface morphology. At the locations of these disturbances, a clearly discontinuous displacement field emerges (compare chapter 9.1.1 and appendix), fulfilling another key criterion of the decision tree.

There is a temporal offset in the onset of these features between the sites, with first disturbances occurring after 1981 at Gruob, after 1993 at Furggwang and Brändjispitz, and after 2011 at Roti Ritze, where deep crevasses begin to form at the rock glacier front. In all cases, the morphological changes are accompanied by increasing spatial heterogeneity in the creep behaviour. For Gruob and Furggwang, the phase of active disturbance formation appears to end around 1999 and 2020, respectively. Although their surfaces remain dominated by existing disturbance features, no new notable

cracks evolve, and displacement becomes more homogeneous. This results in morphological destabilization phases of approximately 18 years for Gruob and 27 years for Furggwang. In contrast, Brändjispitz and Roti Ritze are still active and continue to develop new surface disturbances.

At Hungerlihorli, surface disturbances develop between 2005 and 2020 but remain shallow and spatially confined to a small area in the central part of the rock glacier. At the location of the cracks, the displacement field shows minor discontinuities. Based on these observations, the rock glacier is classified as 3b potentially destabilized with shallow surface disturbances.

While on Brändjispitz, Gruob and Furggwang rock glacier big areas of the rock glacier are affected by surface disturbances, at Hungerlihorli and Roti Ritze only some parts display cracks and crevasses.

9.2.3. Summary morphology

In the analysis of vertical surface change, Furggwang, Gruob, Brändjispitz, and Roti Ritze stand out, either through extreme overall mass relocation or through spatially confined zones of very high elevation change. All four are additionally classified as potentially destabilized rock glaciers with deep surface disturbances based on the systematic assessment using the decision tree.

Hungerlihorli shows slightly heterogeneous mass relocation beyond typical ridge–furrow structures but lacks pronounced local elevation changes. It is classified as potentially destabilized with only shallow surface disturbances in the decision tree. Both its vertical change pattern and morphological characteristics deviate moderately from the typical rock glacier behaviour, but not as distinctly as in the four cases mentioned above.

Ritzuegg, Jungpass and Gruobtälli rock glaciers are rated with non-observable destabilization in the surbace disturbance evolution analysis and don’t show any irregular vertical changes. Brändjitelli shows slightly greater mass relocation in the vertical change analysis but does not display any surface disturbances and is likewise classified with non-observable destabilization. It can therefore also be grouped with the stable rock glaciers.

9.3. Integrated assessment of destabilization

The ultimate step is to combine the findings on the rock glacier kinematics and morphology from the previous chapters. Furggwang, Gruob, Brändjispitz and Roti Ritze rock glaciers show both kinematic anomalies and are rated as potentially destabilized rock glaciers based on the surface morphology. Ritzuegg, Jungpass, Gruobtälli and Brändjitelli rock glaciers don't remarkably deviate from regional trends and don't fancy morphological destabilization through surface disturbances. Hungerlihorli rock glacier represents a borderline case in both kinematics and morphology with slightly deviating from regional kinematical trends and showing unusual morphological features, but both to moderate extent.

While most rock glaciers either fulfil both criteria for destabilization or neither, a final assessment based solely on this binary distinction would be overly simplistic. Instead, the temporal dimension must also be considered to evaluate whether the observed kinematic and morphological changes are linked and form part of a coherent destabilization phase.

Figure 30 synthesizes the core findings of this study by visualising the temporal occurrence of three key indicators: acceleration of creep velocities in response to climate trends (green), kinematic anomalies (orange), and the onset of morphological surface disturbances such as cracks and scarps (blue). This integrated timeline allows for a direct comparison of the timing, intensity, and duration of these anomalies and forms the basis for the final destabilization assessment.

The plot reveals that while most rock glaciers underwent climate-driven acceleration at some point during the study period, only a subset displays overlapping kinematic and morphological anomalies, which are critical indicators for destabilization.

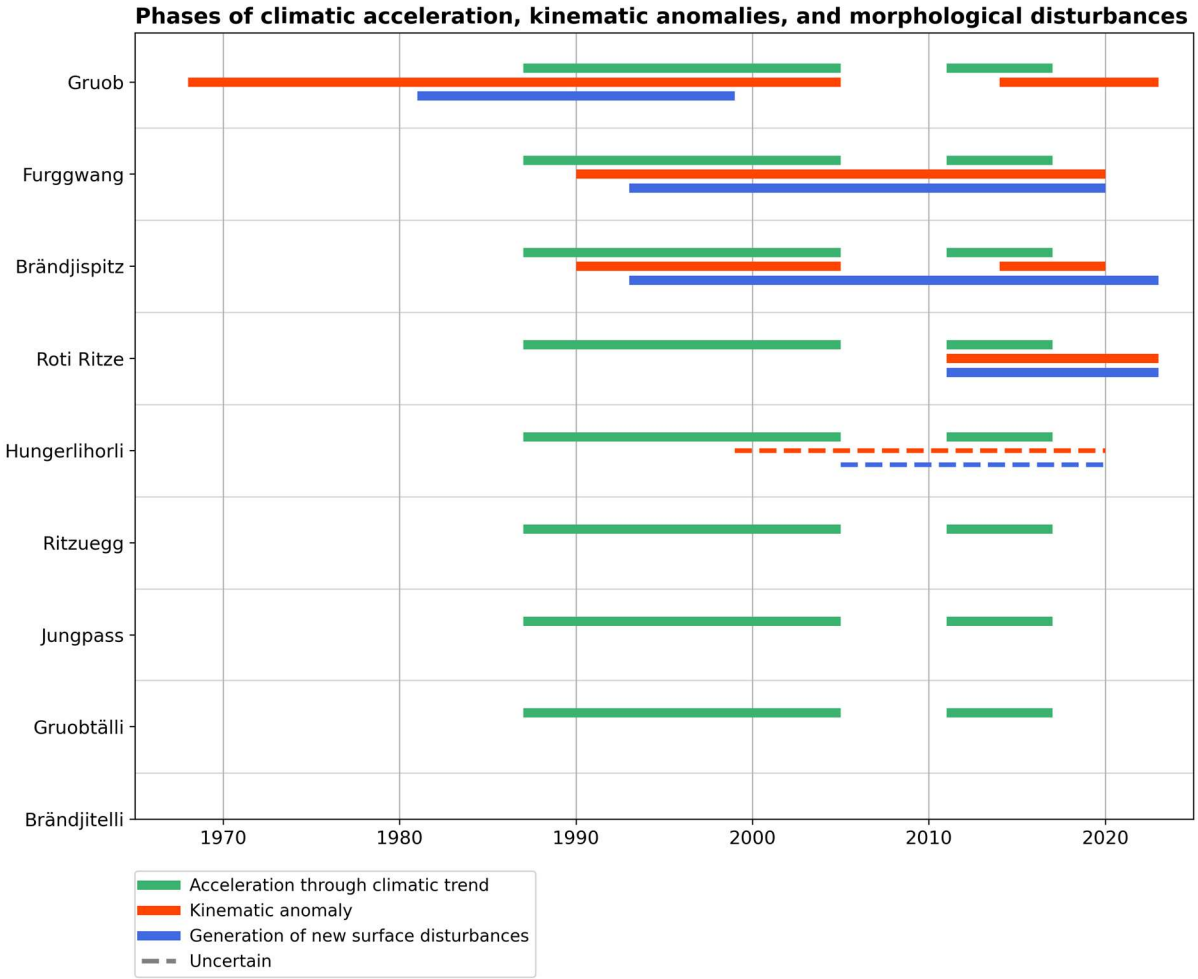

Figure 30 Summary with phases of climatic acceleration, kinematic anomalies and morphological disturbances from 1968-2023 for all studied rock glaciers.

9.3.1. Rock glaciers with clear indication of destabilization

Gruob, Furggwang, and Brändjispitz rock glaciers show the clearest and most sustained signatures of destabilization. At Gruob, the kinematic anomaly begins already in the late 1960s and thus precedes both the onset of climate-related acceleration and the emergence of surface disturbances. The latter begin shortly after 1981 and persist until 1999, corresponding well with both elevated and heterogeneous creep rates and widespread surface lowering across the rock glacier. At Furggwang and Brändjispitz rock glaciers the kinematic anomaly begins around 1990 and is followed by the development of surface disturbances from 1993 onward. At Brändjispitz, the kinematic anomaly is not continuous. It is interrupted between 2005 and 2011, during which the rock glacier largely follows the regional trend. In contrast, Furggwang maintains a clear deviation during this time. While both kinematic and morphological activity at Furggwang appear to cease after 2020, Brändjispitz continues to show active

surface transformation, with new crevasses still forming in recent years. The simultaneous presence of high and spatially concentrated displacement rates and deep crevasses indicates an ongoing phase of surface transformation. The consistent overlap of kinematic anomalies and fundamental morphological changes at all three sites confirms their classification as destabilized rock glaciers.

Roti Ritze shows a slightly different pattern compared to the three rock glaciers described above. Both the kinematic anomaly and the development of morphological disturbances begin simultaneously around 2011. At this time, strongly accelerating creep develops in localized areas, accompanied by the formation of deep crevasses and a discontinuous displacement field. This coincides with a renewed phase of climate-related acceleration. Since then, both the kinematic anomaly and the morphological activity have continued to intensify, with creep rates further increasing and new surface disturbances still forming in the most recent period. Although the temporal pattern differs slightly from the other destabilized rock glaciers through the simultaneous onset of kinematic and morphological change, the distinctiveness of both phenomena justifies its rating as a rock glacier with clear evidence for partial destabilization.

9.3.2. Ambiguous indication of destabilization

Hungerlihorli follows the typical sequence of an initial kinematic anomaly followed by the emergence of surface disturbances. The subtle anomaly begins around 1999 and is expressed through slightly elevated and spatially variable creep behaviour, ending around 2020. Surface disturbances develop between 2005 and 2020 but remain shallow and are restricted to a small area in the central part of the rock glacier. Both anomaly types are subtle, which makes classification unclear, as the rock glacier exhibits some features of destabilized systems but does not strongly deviate from regional trends.

9.3.3. No indication of destabilization

In contrast, Brändjitelli, Gruobtälli, Jungpass, and Ritzuegg display only climatic acceleration phases with no kinematic or morphological anomalies. Their velocity development follows regional trends, their surface morphology remains intact, and no surface disturbances evolve over the study period. These sites are therefore classified as stable, non-destabilized rock glaciers.

9.3.4. Spatial distribution of destabilized rock glaciers

Figure 31 provides a spatial overview of the destabilization classification assigned to each investigated rock glacier.

The visualized typology shows that rock glaciers with clear evidence of destabilization in specific periods are distributed across the study area without apparent spatial clustering. Likewise, the rock glaciers without any indication of destabilization do not concentrate in a particular subregion.

All rock glaciers without indications of destabilization are located on west-facing slopes. Furggwang rock glacier also shares this orientation, despite exhibiting clear signs of destabilization. In contrast, Brändjispitz, Gruob, and Hungerlihorli are situated on northwest-facing slopes. Roti Ritze rock glacier displays a distinct bend, with a change in slope orientation and creep direction from east–west to southeast–northwest. The kinematically and morphologically active zone is located within the northwest-facing segment. These observations suggest a potential relationship between slope orientation and destabilization, as all non-destabilized rock glaciers are situated on west-facing slopes, whereas three of the four rock glaciers with clear destabilization features deviate from this orientation.

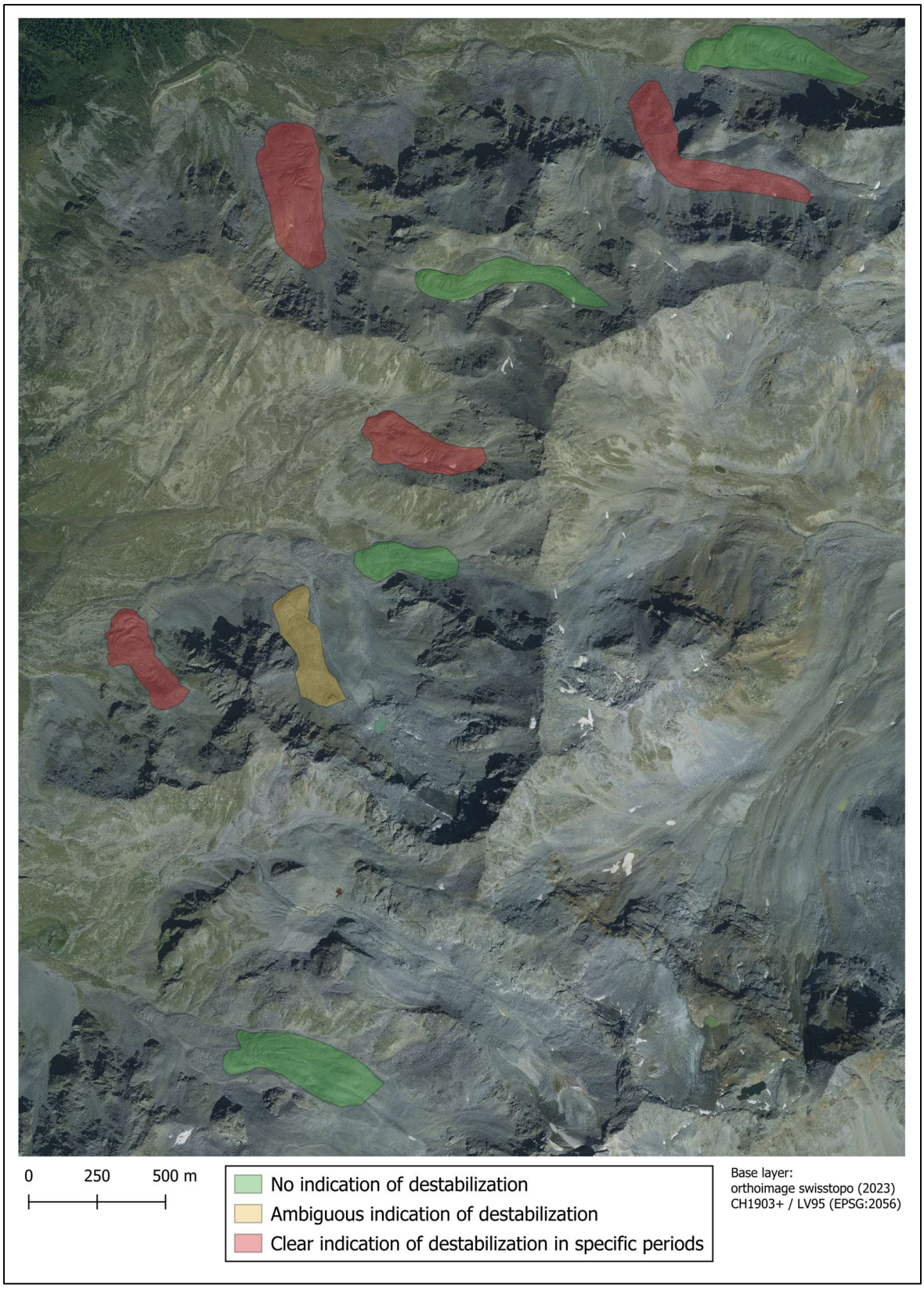

Figure 31Orthophoto of the study area showing the studied rock glaciers coloured according to destabilization indications.

10. Discussion

10.1. Typological assignment of investigated rock glaciers

This section applies the typology of destabilized rock glaciers developed in the theoretical framework to the individual sites studied in the Turtmann Valley. Each rock glacier is assigned to one of the defined types based on its topographic context and morphological configuration. This typological classification forms the basis for interpreting the observed creep behaviour and surface evolution in light of conceptual process understanding.

Ritzuegg, Jungpass, Gruobtälli, and Brändjitelli can all be assigned to Type 0. These rock glaciers exhibit temporal accelerations in creep velocity, yet they show no signs of destabilization. Their kinematic evolution clearly follows the regional trend and is most likely driven by thermally induced changes in the rheological properties of the ice-debris mixture, as described in the typology. Morphologically, they have retained their structural integrity throughout the study period and do not display surface cracks or other indicators of internal deformation. The observed kinematic changes can therefore be interpreted as part of the "new normal" of alpine permafrost environments under climate warming, in line with the concept of Type 0.

By contrast, Furggwang and Gruob show clear signs of destabilization. At Furggwang, ground-penetrating radar data presented by Buchli et al. (2018) confirm a concave to linear bedrock geometry, providing a robust basis for the typological classification. The rock glacier has undergone persistent surface deformation over the entire study period, and no external mechanical processes are known that could have triggered destabilization. Instead, the destabilization appears to be internally driven and strongly influenced by complex subsurface processes. Buchli et al. (2013, 2018) emphasize the role of hydrological dynamics, including unfrozen water and pressure fluctuations, in shaping the glacier's internal structure and promoting instability through shear horizon. These findings support the present interpretation of Furggwang as a thermally and hydrologically destabilized rock glacier. Roer et al. (2008) further describe Furggwang as destabilized and exhibiting landslide-like behaviour, which is fully consistent with the characteristics of Type 1a rock glaciers defined in the applied typology. The classification of Gruob is less straightforward. Although the surface morphology appears slightly convex today, it was clearly linear at the beginning of the observation period. Moreover, the topographic context, especially

the terrain immediately adjacent to the rock glacier, suggests a linear to slightly concave slope geometry. As the typology is based on the geometry of the underlying slope rather than the surface morphology this supports a classification as Type 1a. Roer et al. (2008) also identify Gruob as a destabilized rock glacier with landslide-like deformation patterns, in agreement with the findings of this study. No external mechanical processes have been recorded here either. Taken together, the evidence points to a thermally and hydrologically induced destabilization, justifying its assignment to Type 1a, albeit with a certain degree of uncertainty due to the ambiguous slope geometry.

Brändjispitz and Roti Ritze also exhibit signs of destabilization, though within a different morphological context. Both are situated on convex slopes and creep across a distinct terrain knickpoint. The upper part of Brändjispitz lies within a characteristic cirque, suggesting that the rock glacier advances over the corresponding cirque lip. Surface disturbances and the highest displacement rates are documented just below this knickpoint, where the slope steepens markedly. A similar pattern is observed at Roti Ritze, which transitions into a steeper section after a pronounced bend. Again, the highest displacement vectors and initial cracking coincide with this steeper segment.

Given their position on convex slopes with steep terminal sections, both rock glaciers meet the topographic and morphological criteria of Type 2. No rupture into distinct parts or complete frontal collapse has yet occurred, which would justify classification into one of the more advanced follow-up types within the Type 2 category. Accordingly, both are assigned to the classical form of Type 2, where the convex slope geometry is seen as the dominant factor driving destabilization.

The case of Hungerlihorli remains inconclusive, as it is unclear whether the rock glacier is destabilized. Therefore, a classification is proposed for both plausible interpretations. If considered stable, it would be assigned to Type 0, although it appears to be more strongly affected by climate-induced changes in ice rheology and internal hydrology than the other Type 0 examples in this study. In this case, the observed surface changes would reflect an increased sensitivity to warming rather than the onset of destabilization. If, however, the surface disturbances are interpreted as early signs of destabilization, a classification as Type 2 would be plausible. The rock glacier appears to creep across a minor topographic step, which has been visible since the beginning of the study period. This step is likely associated with a cirque rim,

similar to the situation at Brändjispitz, but its expression is less distinct due to the influence of additional morphological factors in the surrounding terrain. Consequently, the classification remains tentative and subject to considerable uncertainty.

The table below summarizes the assigned typological classifications.

Table 5 The studied rock glaciers assigned to the destabilization types of the established typology.

Rock glacier	**Destabilization type**
Ritzuegg	Type 0
Jungpass	Type 0
Gruobtälli	Type 0
Brändjitelli	Type 0
Hungerlihorli	Type 0 or 2
Brändjispitz	Type 2
Gruob	Type 1a
Furggwang	Type 1a
Roti Ritze	Type 2

10.2. Evaluation of the typology

The following section reflects on the practical application and conceptual robustness of the typology used, which forms the analytical foundation for subsequent interpretations throughout this chapter. The application of the typology to the rock glaciers in the Turtmann Valley reveals both the practical value and the limitations of the proposed classification system. While the typological categories provide a helpful framework for interpreting destabilization tendencies based on topographic context, several challenges emerged during their concrete implementation.

A key methodological difficulty lies in determining the geometry of the subsurface rock glacier bed. Since surface topography does not necessarily reflect the shape of the underlying slope, the assignment to a typological category often requires indirect inference. In this study, bed geometry was estimated based on long-term surface profiles and the morphological configuration of the surrounding terrain such as the presence of cirques or other characteristic landforms indicative of a specific slope geometry. In most cases, this approach allowed for a plausible interpretation.

However, uncertainties remain, particularly in cases such as Gruob, where the surface morphology has changed considerably over time, or Hungerlihorli, where no clearly defined large-scale morphological feature is present that would allow for an unambiguous assessment of the slope geometry. These examples highlight that the classification of individual rock glaciers inevitably involves interpretative judgement and cannot be fully resolved based on surface data alone.

A further complication arises when comparing the observed creep behaviour with the velocity patterns suggested by the conceptual typology. In the present dataset, some Type 1 rock glaciers (e.g. Furggwang and Gruob) exhibit higher creep velocities than the two Type 2 glaciers (Brändjispitz and Roti Ritze), although the latter are theoretically associated with more rapid displacement due to their steep and convex slope settings. This discrepancy highlights that creep velocity is not governed by topography alone and suggests that including fixed velocity thresholds as defining criteria may oversimplify the complex interplay of contributing factors. While slope geometry remains the primary differentiating factor within the framework, other influences such as internal ice content, hydrological conditions, or potential feedbacks between surface morphology and deformation likely contribute to the observed kinematic variability. However, such internal factors were not examined in this study and remain speculative.

Despite these limitations, the typology proves useful for structuring the analysis and organizing the interpretation of observable patterns. It enables a first-order differentiation of destabilization tendencies based on morphological and topographic features and provides a conceptual framework for linking these features to known destabilization modes. As demonstrated in this study, the classification supports the identification of plausible destabilization trajectories and their spatial context. Nevertheless, the typology should be applied with caution and ideally be supported by complementary geophysical methods to better constrain subsurface structure and slope geometry.

10.3. Temporal and spatial destabilization patterns in the study area

10.3.1. Temporal patterns

The temporal evolution of destabilization across the studied rock glaciers reveals recurring patterns in the sequence and interaction of climatic influences, kinematic anomalies, and morphological surface changes. While each rock glacier exhibits a unique development path, several overarching tendencies can be identified, which may point to common mechanisms or thresholds involved in the destabilization process.

One of the most striking observations is the consistent sequence in which signs of destabilization unfold: across several sites, particularly Gruob, Furggwang, and Brändjispitz, an initial kinematic anomaly in the form of localized acceleration occurs before the onset of visible morphological changes. In all three cases, surface disturbances later emerge in exactly those sectors where creep acceleration had previously been strongest. This pattern suggests a causal relationship, where increased internal deformation, potentially driven by changes in thermal or hydrological conditions, leads to a redistribution of stress and, ultimately, surface failure. This interpretation aligns with the conceptual model described in the theoretical framework, although internal processes were not directly analysed in this study.

The timing of these kinematic anomalies in relation to regional acceleration trends further adds nuance to the interpretation. In both Furggwang and Brändjispitz, the onset of localized acceleration and subsequent surface cracking occurs with a delay of roughly one observation period after the beginning of climatically driven regional acceleration. This temporal offset might indicate that climatic forcing initiates a gradual internal transformation, which eventually exceeds a critical threshold, thereby triggering a more pronounced and localized destabilization response that evolves independently of the broader regional trend.

A particularly early case is Gruob, which already exhibits anomalously high creep rates and a marked acceleration in the late 1960s, well before regional climate-induced trends became apparent. This could suggest that internal conditions in Gruob reached a threshold independent of external climate forcing, or that local factors accelerated its response. Interestingly, a second phase of kinematic anomaly has emerged at Gruob since around 2014. Given the long delay between the initial acceleration in the 1960s and the first surface disturbances, it is conceivable that the current phase again

represents a precursor to renewed morphological destabilization, which may become evident in the near future. The apparent phased development with multiple peaks of acceleration over time points to a possible episodic nature of destabilization, rather than a continuous process.

This idea of multi-phase destabilization also finds support in the evolution of Brändjispitz. Here, the initial kinematic anomaly ceased around 2005, yet the formation of new surface disturbances continued. Since overall creep rates remained high but no longer deviated from the regional trend, the anomaly may simply no longer register as such, despite a high level of activity. A renewed period of exceptionally high displacement rates follows shortly after the next climate-driven regional acceleration, which could indicate that external forcing reactivated a previously established destabilization dynamic.

Roti Ritze represents a contrasting case, where multiple destabilization indicators emerge simultaneously. Around 2011, the site exhibits a marked increase in displacement rates that exceeds the regional trend, coinciding with the immediate appearance of new surface disturbances. Maximum displacement values continue to rise until the end of the study period, and the surface cracks become increasingly pronounced. This suggests that Roti Ritze may currently be in the early stages of a major destabilization phase, in which internal processes, surface deformation, and slope geometry (particularly the bend and terrain step) interact more directly and abruptly than in other cases.

In contrast, the situation at Furggwang appears to reflect a potential end of a destabilization phase. After nearly 30 years of kinematic anomalies and the progressive development of surface disturbances, both indicators show a marked reduction after 2020. Whether this represents a genuine stabilization or merely a temporary decrease in activity remains unclear and will require continued observation in the coming years.

The case of Hungerlihorli remains uncertain. On the one hand, the rock glacier exhibits moderate deviations from the regional trend, both in terms of creep velocity and the appearance of shallow surface disturbances. As observed at other sites, the kinematic anomaly precedes the morphological changes, which could indicate the early onset of destabilization. This sequence would fit the broader pattern in which climate-induced acceleration initiates internal changes that eventually lead to destabilization processes continuing independently. On the other hand, both kinematic activity and surface

deformation visibly decline after 2020. This weakening suggests that the process may not have progressed beyond an initial response to climatic forcing. While the glacier may have been more sensitive than others to recent climatic changes, the absence of persistent anomalies or structural transformation implies that no fundamental shift in process dynamics has occurred. Consequently, while a short-lived destabilization phase cannot be ruled out, the available evidence more strongly supports the interpretation that Hungerlihorli has remained within the range of intensified but still typical rock glacier behaviour under current climatic conditions.

10.3.2. Spatial patterns

In addition to the temporal dynamics, the spatial expression of destabilization varies both between individual rock glaciers and across the study area. On the individual level, a marked contrast exists in the extent of destabilization. At Gruob and Furggwang, almost the entire rock glacier body is affected by both kinematic anomalies and surface restructuring. This widespread transformation indicates a fundamental reorganization of internal processes, possibly involving large-scale deformation and deep-reaching destabilization dynamics. In contrast, Brändjispitz and Roti Ritze show morphologically active zones that remain spatially limited, although these areas have expanded over time. Whether this more localized destabilization reflects differences in topography, the current stage of development, or other internal controls remains unclear.

At the scale of the entire study area, no spatial clustering of destabilized or stable rock glaciers is apparent. Sites with and without signs of destabilization are evenly distributed across the valley. However, a tentative pattern emerges when considering aspect and creep direction: all rock glaciers without signs of destabilization are oriented roughly east–west, whereas most clearly destabilized ones - Brändjispitz, Gruob, and the active sector of Roti Ritze—have a predominant orientation of southeast–northwest. In the case of Roti Ritze, the destabilized zone is located precisely in the part of the glacier where the orientation shifts from east–west to southeast–northwest. This may point to a radiation-related control, in which differences in solar input influence internal thermal or hydrological conditions. However, this observation remains speculative and is based on a small number of cases. It should therefore be considered only as a tentative hypothesis with limited

explanatory power, which would require targeted investigation and larger sample sizes to verify.

An exploratory analysis of elevation yields mixed results. The lowest frontal positions are found at Gruob (ca. 2410 m), Brändjispitz (ca. 2490 m), and Roti Ritze (ca. 2610 m), all of which lie below the front of the lowest undisturbed glacier, Gruobtälli (ca. 2620 m). This may suggest a greater vulnerability of low-lying rock glaciers, or at least of their lower sections, to internal process changes and destabilization. However, this trend is not consistent across all sites. Furggwang, which shows clear signs of destabilization, lies considerably higher at around 2750 m, well above stable glaciers such as Jungpass (2670 m) and Brändjitelli (2700 m). A similar picture emerges when comparing the upper boundaries. Gruob (ca. 2620 m) and Brändjispitz (ca. 2660 m) lie at relatively low elevations, while Furggwang (ca. 2950 m) and Roti Ritze (ca. 2900 m) extend into higher elevation zones, exceeding the upper margins of undisturbed rock glaciers such as Gruobtälli (ca. 2850 m), Jungpass (ca. 2820 m), and Brändjitelli (ca. 2870 m). These observations suggest that elevation may influence destabilization, especially at the lower margins. However, the pattern is inconsistent, and no clear threshold can be identified. The findings remain exploratory and would require a more systematic analysis to assess the role of elevation reliably.

10.3.3. Summary of temporal and spatial patterns

The temporal analysis reveals a recurring sequence in the evolution of destabilization. Localized kinematic anomalies typically precede the development of surface disturbances, often with a delay following the onset of climate-driven regional acceleration. This suggests that destabilization may be externally initiated but only progresses once internal thresholds are exceeded. In several cases, destabilization occurs in multiple, temporally distinct phases, pointing to a non-linear and potentially episodic process shaped by the interaction of external forcing and internal system dynamics.

The spatial expression of destabilization varies in both extent and distribution. While some rock glaciers show widespread surface change, others exhibit more localized activity, often confined to specific zones. No clear spatial clustering is observed across the study area. However, tentative patterns in aspect and elevation suggest that northeast-facing orientations and lower-lying glacier sections may be more susceptible

to destabilization. These trends remain inconsistent and are based on a very limited number of cases. As such, they should be viewed as exploratory and require further investigation through larger and more systematic spatial analyses.

Together, these temporal and spatial insights offer a basis for identifying broader destabilization patterns and provide a comparative framework for evaluating rock glacier dynamics in other regions.

10.4. Comparison with destabilization cases studies from other alpine regions

This section explores how the broader findings of this study align with existing research on destabilized rock glaciers in other regions of the Alps. It does not aim to compare each individual site with equivalent examples in the literature, as many of the diagnostic characteristics have already been considered during the typological classification in chapter 10.1. The typology applied in this study is itself derived from an extensive review of the scientific literature and integrates the defining features of the most frequently documented types of destabilization. As such, assigning a rock glacier to a particular type implicitly places it in relation to a wider set of comparable cases.

Nevertheless, typological classification does not capture all aspects of rock glacier behaviour, especially those related to temporal dynamics, the episodic nature of destabilization, or potential thresholds in internal system evolution. This chapter therefore focuses on comparing the overarching patterns observed in the Turtmann Valley, particularly the sequence and timing of kinematic and morphological changes, with selected case studies from other regions. The aim is to assess whether the observed destabilization trajectories align with broader patterns reported in the literature or reflect locally specific dynamics.

Given the limited number of well-documented cases and the considerable variability in data quality and observation duration across studies, the following comparisons should be understood as tentative. They serve to contextualize the findings of this study and to identify potential directions for future research, rather than to draw definitive conclusions about the general behaviour of destabilized rock glaciers.

The temporal and spatial destabilization patterns identified in the Turtmann Valley align with several key observations reported in other Alpine regions. While each case is shaped by local conditions, recurring mechanisms suggest shared dynamics that transcend individual sites. This section examines how the core findings of this study compare with documented examples in the literature.

10.4.1. Temporal sequence of destabilization

The temporal pattern observed in the Turtmann Valley, where localized kinematic anomalies typically precede surface disturbance following a delay after regionally coherent acceleration, is mirrored in several Alpine case studies and likely represents the most common trajectory. Marcer et al. (2021) report such a temporal decoupling in the French Alps, where acceleration began in the early 1990s, while surface ruptures only appeared years later. A similar sequence was observed at Tsaté-Moiry, where acceleration set in during the 1980s and morphological destabilization followed in the early 1990s (Lambiel, 2011). These cases support the interpretation that destabilization usually involves a preparatory phase during which internal conditions evolve before becoming visible at the surface.

Nevertheless, variations in this sequence exist. At Roti Ritze, for example, acceleration and surface cracking occurred almost simultaneously, suggesting a rapid surface response once internal thresholds were exceeded. Marcer et al. (2021) also document comparable cases, including examples where surface ruptures appear before measurable acceleration is detected. Such deviations indicate that the timing of destabilization features may differ, depending on site-specific factors such as topography or internal structure.

Despite these differences, it is unlikely that destabilization occurs entirely abruptly or without prior internal changes. Even in apparently sudden events, internal reorganization typically plays a key role. Kofler et al. (2021) show that a partial failure, although rapid in appearance, was preceded by a prolonged phase of increasing displacement and internal transformation. These findings suggest that while the order in which signs of destabilization emerge may vary, the process as a whole is a transformation initiated by external forcing and modulated by internal system dynamics.

10.4.2. Multi-phase development

Several rock glaciers in the Turtmann Valley show signs of temporally distinct phases of destabilization, separated by quieter intervals. The reappearance of kinematic anomalies at Gruob decades after earlier activity suggests a non-linear trajectory. This episodic character is also reported elsewhere in the Alps. Delaloye et al. (2013) describe such episodicity in the Grabengufer and Gugla rock glaciers, where activity peaks were separated by periods of apparent stabilization. Ghirlanda et al. (2016) characterize the destabilization of the Jegi rock glacier as a "pluri-decennial, multiphasic and complex process" with spatially shifting zones of activity. These examples indicate that destabilization can span decades and proceed in successive pulses, potentially triggered by combinations of climatic variability, internal reorganization, and external mechanical stress.

Such episodic behaviour challenges simplistic models of continuous degradation and highlights the need to consider feedback mechanisms and long-term system memory in interpreting rock glacier dynamics.

10.4.3. Spatial extent of destabilization

The studied Turtmann Valley rock glaciers exhibit considerable variation in the spatial expression of destabilization. Gruob and Furggwang are affected across nearly their entire extent, while Roti Ritze and Brändjispitz display destabilization confined to specific zones. This heterogeneity is also well documented in other Alpine regions. The Tsarmine rock glacier for example shows rapid displacement only in parts of the landform, with a potential decoupling between the rapidly moving front and the more stable upper section (Vivero et al., 2022). Similar observations are made by Delaloye et al. (2013) for Gugla and Dirru, where destabilization is limited to the terminal zones, whereas Grabengufer underwent a more pervasive transformation initiated in the rooting zone. Lambiel (2011) reports strong intra-glacier contrasts in kinematic activity at Tsaté-Moiry, with the central section being considerably more active than the margins or upper parts. Furthermore, Ghirlanda et al. (2016) emphasize that the spatial focus of destabilization may shift during different phases of the process.

These comparisons indicate that spatial patterns are shaped by a combination of internal and external controls. While topographic context, such as slope steepness or terrain confinement, can play a critical role, especially in valleys like the Matter Valley,

destabilization is more accurately described as the product of a complex interplay between structural, thermal, hydrological, and mechanical factors.

10.4.4. Aspect and elevation patterns

This study identified a tentative tendency for rock glaciers with northeast-facing aspects or lower-lying tongues to exhibit destabilization more frequently. Although this observation is based on a limited number of cases, it is partially corroborated by Marcer et al. (2019), who found a slight predominance of north-facing orientations among destabilized rock glaciers in the French Alps. A simple comparison of selected case studies suggests that this tendency may also apply to other regions. However, to derive meaningful and generalizable conclusions, a systematic and quantitative analysis would be required, based on a comprehensive inventory of a large number of rock glaciers. Such an analysis lies beyond the scope of this thesis but would be a valuable direction for future research.

In terms of elevation, no consistent threshold emerges across the literature. Scotti et al. (2016) suggest that low tongue elevation may increase the likelihood of destabilization, yet their studied example, the Plator rock glacier, lies at 2712 m a.s.l., which is higher than the maximum elevation of some stable rock glaciers in the Turtmann Valley. This example alone illustrates that defining fixed elevation thresholds is not meaningful, as permafrost conditions are strongly influenced by local climatic settings. As with aspect, a robust evaluation would require a regional, inventory-based approach combined with statistical analysis in order to produce more reliable and generalizable insights.

These considerations underline the need for caution when interpreting patterns in aspect or elevation, as current evidence remains anecdotal and lacks systematic validation in this study. Site-specific differences likely play a dominant role, and reliable insights will require regional inventories combined with statistical analysis.

10.4.5. Conclusion on the comparison with other cases

The comparison with other Alpine case studies shows that many of the temporal and spatial patterns identified in the Turtmann Valley reflect recurring trends observed elsewhere. This includes the frequent delay between acceleration and surface change,

the occurrence of episodic activity, and the heterogeneous spatial expression of destabilization. While tendencies in aspect and elevation remain inconclusive, they point to potentially relevant factors that merit further investigation. At the same time, the destabilization process remains highly site-specific. Almost every rock glacier displays its own combination of morphological, kinematic, and internal characteristics, shaped by local conditions. General patterns must therefore be interpreted in light of this variability. Overall, the findings of this study align well with established case studies and support the interpretation of local destabilization as part of a wider Alpine pattern.

10.5. Integration into climatic trends at alpine scale

To better contextualize the observed kinematic evolution, this section examines whether the velocity trends identified in the Turtmann Valley reflect localized dynamics or correspond to regional-scale developments across the Alps.

Several large-scale studies document an increase in rock glacier creep velocities across the Alps in recent decades. Delaloye et al. (2010) report a general acceleration in the Swiss Alps beginning in the 1980s, which they associate with rising permafrost temperatures due to increased air temperatures. Marcer et al. (2021) identify a similar acceleration trend for the French Alps since the early 1990s. On an alpine-wide scale, Kellerer-Pirklbauer et al. (2024) analyse velocity data from 1995 to 2022 and identify a general long-term warming induced trend of increasing velocities with three main acceleration phases from 2000–2004, 2008–2015, and 2018–2020 interrupted by intervals of relative stability or slight deceleration.

In this study, the onset of acceleration in the Turtmann Valley is observed between the mid-1980s and early 1990s. This timing is consistent with the trends described by Delaloye et al. (2010) for the Swiss Alps and by Marcer et al. (2021) for the French Alps. A comparison with the main acceleration phases identified by Kellerer-Pirklbauer et al. (2024) is less straightforward due to differences in temporal resolution. Nonetheless, the Turtmann dataset shows a first peak in velocities around 2005, followed by a deceleration and renewed increase during the period 2011–2017, thereby closely matching the second acceleration phase described in their study. The final phase between 2018 and 2020, however, is not evident in the Turtmann data, which instead show a general decrease in velocities after 2017.

Overall, the results from the Turtmann Valley correspond well with the regional trends reported in the literature and confirm that the observed acceleration is part of the broader warming-related kinematic response of rock glaciers in the Alps.

10.6. Methodological considerations and data limitations

The methods applied in this study enable a detailed analysis of long-term rock glacier kinematics and morphology. However, various sources of uncertainty arise at different stages of the workflow. This chapter systematically discusses the data basis, methodological challenges, and interpretation limitations to ensure a transparent assessment of the results and their reliability.

10.6.1. Data basis and co-registration

The analysis presented in this study is based on high-resolution true orthophotos, which were generated using temporally corresponding digital elevation models. This approach ensures high geometric accuracy in image alignment, particularly for more recent datasets. However, older orthophotos occasionally exhibit slight spatial offsets, which were addressed through image co-registration. After testing several approaches, an automated co-registration method was ultimately applied due to its ease of use and the promising performance observed in other study areas. Although both visual and quantitative assessments suggest enhancement in positioning precision of the images, minor residual misalignments remain detectable, especially in older images. While the residuals fall within a tolerable range, such deviations can still influence the calculated creep rates, particularly for small or slowly moving rock glaciers.

In terms of temporal resolution, the dataset is limited to image intervals of six years before 2011. This is sufficient to capture long-term trends but does not allow for detailed insight into intra-period dynamics. As a result, short-lived but potentially significant kinematic events may remain undetected. For instance, the sharp acceleration of Roti Ritze between 2011 and 2014 is only visible due to the availability of a three-year interval; such a development would likely have been missed with a longer observation window. It is therefore possible that other noteworthy episodes of acceleration or morphological transformation went unrecorded. Nevertheless, destabilization is typically a long-term process that is closely tied to surface

morphological change. Thes features are eventually detectable, even if the exact timing of their onset cannot be pinpointed with the available temporal resolution.

10.6.2. CIAS methodology and associated challenges

The CIAS algorithm offers an efficient and automated approach for measuring horizontal surface displacement between orthophotos. It enables a high point density across the entire surface and supports retrospective analysis over extended time periods. However, several limitations affect its reliability.

In areas affected by snow cover, shadow, or low surface contrast, CIAS often fails to generate reliable displacement vectors. While a systematic filtering strategy based on expected vector direction and magnitude helps to remove mismatches, the unintentional exclusion of valid vectors or the retention of undetected errors cannot be ruled out. This uncertainty is further compounded by the reduced spatial coverage resulting from the filtering process, which may bias mean creep rates if entire sections of the rock glacier (e.g. snow-covered zones) are systematically excluded. In highly active zones, such as the lower section of the Furggwang rock glacier, the method struggles to resolve displacement due to intense surface deformation. As a result, CIAS likely underestimates mean creep rates of the rock glacier and maximum displacement rates in these areas. Moreover, comparisons between different years are inherently difficult, as the number and spatial distribution of valid vectors vary across periods, potentially affecting the consistency of derived velocity values.

Another limitation is that CIAS detects only horizontal displacement. Vertical surface changes remain unaccounted for and must be analysed using complementary approaches such as DoD (DEM of Difference) analysis. However, vertical processes cannot be integrated into the kinematic assessment with the same level of detail.

A further source of uncertainty lies in the parameter selection used during the CIAS matching process. Despite extensive testing during this study, it is unlikely that a globally optimal parameter set was found, particularly given the strong variability between individual rock glaciers and across different time periods. The applied parameters represent a compromise that performs well across most settings, but local mismatches and suboptimal correlation in specific areas or periods may still affect the results.

Finally, the delineation of rock glacier outlines influences the calculated mean creep rates, as these values directly depend on which areas are included as part of the active rock glacier. In morphologically complex settings or at sites with multiple lobes, distinguishing between active and inactive sections is often challenging. If other studies define the active extent differently, direct comparison of results becomes difficult.

10.6.3. Validation against independent data and literature

To evaluate the plausibility of the CIAS-derived results, comparisons are made with existing in situ measurements and published studies.

At the regional scale, Roer et al. (2005) identify a trend of rock glacier acceleration in the Turtmann Valley between 1993 and 2001. In the present study, the onset of increasing creep rates is placed slightly earlier, around 1987. The acceleration prior to 1993 is still relatively modest and becomes more pronounced only in the following years. It is therefore likely that both studies are based on comparable kinematic developments but interpret the onset of effective acceleration slightly differently.

For Furggwang, in-situ observations by Buchli et al. (2013, 2018) report displacement rates between 2.6 and up to 7 m/year for the period 2010–2015. These values match well with the maximum creep rates derived in this study. The spatial patterns of deformation also align closely. Also compared with the study from Roer et al. (2008) the spatial deformation pattern from 1993-2001 is very similar. However, the results from this study show slightly lower mean creep velocities, which potentially can be explained that the CIAS output show fewer vectors in the most active zones.

For Brändjispitz and Hungerlihorli, a comparison with data from PERMOS (2024) for the period 2005 to 2023 is possible. The PERMOS measurements have annual resolution, whereas the intervals in this study often encompass years with both increasing and decreasing creep velocities. A direct comparison is therefore limited. However, the general trends observed with CIAS are consistent with those recorded by PERMOS. CIAS-derived mean velocities are generally around 0.5 m/year lower than the PERMOS measurements. This difference may result from the inclusion of the entire glacier surface in the CIAS analysis, which also covers very slow-moving areas, whereas PERMOS surveys are point based on the rock glacier. It is also possible that

missing values in the most active areas contribute to a slight underestimation of mean creep velocities by CIAS.

These comparisons indicate that the CIAS-derived values are generally plausible and align well with existing studies. However, a slight underestimation of creep rates is likely, particularly at sites with highly active zones.

10.6.4. Interpretation uncertainty and lack of threshold criteria

A central methodological challenge of this study lies in the interpretation of CIAS-derived kinematic data. Applying fixed thresholds for specific velocity parameters would simplify classification but is unsuitable for reliably distinguishing destabilized from non-destabilized rock glaciers. Displacement values must always be interpreted in the context of regional trends and the temporal development of each site. Moreover, a single kinematic indicator, such as mean creep, is often insufficient to characterize destabilization, as the relevant changes may affect different parameters, such as maximum displacement or spatial pattern of acceleration, depending on the site. This interpretative uncertainty increases the demands placed on classification and requires comprehensive contextual analysis. In the absence of clearly defined thresholds, ambiguous cases such as Hungerlihorli remain open to multiple interpretations depending on how individual indicators are weighted. However, this ambiguity reflects the inherent complexity of destabilization processes and points to the existence of transitional forms between stable and fully destabilized states.

This complexity extends to the morphological assessment. Although the decision tree provides a systematic framework, surface disturbances are not always clearly identifiable or unambiguously linked to destabilization, particularly in marginal or early-stage cases.

10.6.5. Lack of internal process observations

The surface-based nature of the applied methodology limits the analysis to observable horizontal displacement and surface morphology. Neither the CIAS approach nor the morphological analysis provides insight into internal characteristics such as ice content, the presence and depth of shear zones, or subsurface hydrological dynamics. Assumptions regarding internal processes are inferred from the assigned destabilization type, as each category in the typology is linked to characteristic internal

behaviours and destabilization mechanisms described in the literature. These process-structure relationships are transferred to the rock glaciers in the study area based on their surface expression. However, such inferences remain unverified and are subject to considerable uncertainty. Given the complexity and site-specific variability of destabilized rock glaciers, all interpretations concerning internal dynamics should therefore be approached with caution.

10.6.6. Hazard potential as related but untreated aspect

While destabilized rock glaciers are increasingly recognized for their potential role in alpine hazard cascades, such as debris flows or sudden mass movements, this study did not include a systematic assessment of associated hazard potential. The methodological focus on horizontal surface displacement and surface morphology does not capture parameters relevant for hazard evaluation, such as sediment availability, drainage patterns, or downstream connectivity. Although none of the investigated rock glaciers show clear indications of active involvement in hazard cascades, this observation should be interpreted with caution, as the required indicators were not explicitly analysed. Future studies that aim to assess hazard potential would require a broader methodological framework including hydrological modelling, downstream geomorphological analysis, or high-frequency monitoring of volume changes.

10.6.7. Summary of methodological considerations

In summary, the applied methods provide a valuable and efficient means of analysing long-term rock glacier kinematics across multiple sites. The results are generally consistent with independent measurements and established trends. Nonetheless, the analysis is subject to important limitations: image co-registration uncertainties, reduced vector coverage in critical zones, parameter sensitivity, and the lack of direct information on internal processes all introduce potential inaccuracies. Moreover, the absence of threshold criteria makes interpretation dependent on contextual judgement. These constraints do not invalidate the findings, but they highlight the need for cautious interpretation and underscore the importance of integrating surface-based observations with complementary data sources where possible.

10.7. Potential simplified destabilization assessment

The combined analysis of kinematic and morphological development has proven effective for detecting and classifying rock glacier destabilization. However, it requires long-term orthophotos and DEMs with high spatial and temporal resolution—data that are not universally available. In view of this limitation, simplified approaches with lower data requirements may be useful for preliminary assessments, particularly in areas where destabilized rock glaciers may interact with hazard cascades and pose a potential risk.

The findings of this study suggest that the combined presence of pronounced surface disturbances and long-term elevation change may already serve as a rough indicator of destabilization, even without detailed kinematic analysis. All rock glaciers classified as destabilized exhibit both deep crevasses or scarps and clear signs of mass redistribution, whereas none of the stable rock glaciers show similar features. This implies that a first-order assessment may be feasible using DoD analysis in combination with systematic visual inspection of surface morphology (e.g. orthophotos, hillshades or field observations). While such an approach cannot replace comprehensive kinematic investigations, it may support the identification and prioritization of sites for further monitoring or analysis.

Nevertheless, this suggestion is preliminary and based on a small number of study sites. It lacks systematic validation and should be interpreted accordingly. In particular, surface morphology alone offers no information on the timing or progression of destabilization, as visible features may result from past phases and persist long after activity has subsided.

11. Conclusion

This study investigates the destabilization of rock glaciers in the Turtmann Valley by developing a classification framework and applying it to a set of nine active rock glaciers. The typology proposed is based on topographic criteria and integrates kinematic and morphological indicators to distinguish between different stages and expressions of destabilization. It serves as a baseline for systematically assessing and comparing rock glacier behaviour within a defined region or across multiple case studies.

The analysis shows that destabilization affects a substantial portion of the studied rock glaciers. Four out of nine exhibit clear indicators of destabilization, including elevated and spatially variable creep velocities, structural surface disturbances and signs of mass redistribution. These findings support the first hypothesis: the number of rock glaciers showing signs of destabilization has increased over time. However, the intensity and timing of destabilization activity differ among the individual rock glaciers.

Comparison with documented cases from other Alpine regions reveals partial alignment with previously observed trends. At the same time, local conditions appear to influence the specific manifestations and timing of destabilization. The early onset and prolonged activity at Gruob or the spatial confinement of destabilization at Roti Ritze illustrate this variability. These findings confirm the second hypothesis, which assumed partial consistency with external patterns but limited generalisability.

The results underscore that destabilization is not a uniform process. It varies in timing, magnitude and spatial distribution and is likely shaped by both internal and external factors. The classification framework developed in this study provides a useful tool for analysing this complexity. However, its simplifying character must be acknowledged, particularly when applied to borderline cases. The framework is transferable to other regions and may be extended by incorporating additional parameters such as ground temperature, ice content or subsurface deformation derived from geophysical surveys or borehole observations.

In addition, the study highlights the potential of DEMs of Difference as a preliminary screening method for identifying areas of recent morphological change. While not sufficient for detailed interpretation, this approach proves promising in detecting

spatial patterns and guiding further analysis. Its broader applicability for identifying destabilized rock glaciers should be further evaluated. Continued monitoring of the Turtmann Valley is recommended to assess whether the identified destabilization processes persist or develop episodically, as suggested by some of the observed timelines. The integration of climate data could further help clarify whether short-term temperature fluctuations or longer-term trends play a more dominant role in driving destabilization.

The classification results from this study also offer a basis for systematically comparing destabilized and stable rock glaciers under comparable environmental conditions. Such comparisons may help identify key morphological or topographic factors that promote or inhibit destabilization and support the development of more robust indicators for anticipating rock glacier behaviour. A more differentiated understanding of these dynamics is essential for assessing landscape evolution in periglacial environments and anticipating related natural hazards.

12. Acknowledgements

I would like to thank my supervisor, Dr. Isabelle Gärtner-Roer, who introduced me to the topic and supported me throughout the different stages of this thesis with her broad expertise on rock glaciers.

My thanks also go to Holger Heisig from the Federal Office of Topography swisstopo, who provided support through the swisstopoEDU programme. Holger prepared the data used in this thesis and offered valuable insights into the work at swisstopo.

In addition, I would like to thank Mohd. Ataullah Raza Khan for his assistance with the co-registration process and Thomas Renggli for his help in illustrating the classification schemes.

13. References

Abdullah, Q., Munjy, R., Nimetz, J., Zoltek, M., & Lee, C. (2024). ASPRS Positional Accuracy Standards for Digital Geospatial Data. *Photogramm. Eng. Remote Sens*, *81*, 1–26. https://doi.org/10.14358/ASPRS.PAS.2024

Agüera-Vega, F., Carvajal-Ramírez, F., & Martínez-Carricondo, P. (2017). Assessment of photogrammetric mapping accuracy based on variation ground control points number using unmanned aerial vehicle. *Measurement*, *98*, 221–227. https://doi.org/10.1016/J.MEASUREMENT.2016.12.002

Arenson, L., Hoelzle, M., & Springman, S. (2002). Borehole deformation measurements and internal structure of some rock glaciers in Switzerland. *Permafrost and Periglacial Processes*, *13*(2), 117–135. https://doi.org/10.1002/ppp.414

Arenson, L., & Springman, S. (2005). Mathematical descriptions for the behaviour of ice-rich frozen soils at temperatures close to 0 °C. *Canadian Geotechnical Journal*, *42*(2), 431–442. https://doi.org/10.1139/t04-109

Arenson, L., Springman, S., & Sego, D. (2007). The rheology of frozen soils. *Applied Rheology*, *17*(1). https://doi.org/10.1515/arh-2007-0003

Bagheri, H., & Sadeghian, S. (2013). Ortho image and DTM generation with intelligent methods. *The International Archives of the Photogrammetry, Remote Sensing and Spatial Information Sciences*, *XL-1-W3*(1W3), 475–480. https://doi.org/10.5194/ISPRSARCHIVES-XL-1-W3-475-2013

Barsch, D. (1992). Permafrost creep and rockglaciers. *Permafrost and Periglacial Processes*, *3*(3), 175–188. https://doi.org/10.1002/PPP.3430030303

Barsch, D. (1996). *Rockglaciers: Indicators for the Present and Former Geoecology in High Mountain Environments*. Springer.

Bearzot, F., Garzonio, R., Colombo, R., Crosta, G. B., Di Mauro, B., Fioletti, M., Di Cella, U. M., & Rossini, M. (2022). Flow Velocity Variations and Surface Change of the Destabilised Plator Rock Glacier (Central Italian Alps) from Aerial Surveys. *Remote Sensing*, *14*(3). https://doi.org/10.3390/rs14030635

Berthling, I. (2011). Beyond confusion: Rock glaciers as cryo-conditioned landforms. *Geomorphology*, *131*(3–4), 98–106. https://doi.org/10.1016/j.geomorph.2011.05.002

Bodin, X., Krysiecki, J. M., Schoeneich, P., Le Roux, O., Lorier, L., Echelard, T., Peyron, M., & Walpersdorf, A. (2017). The 2006 Collapse of the Bérard Rock Glacier (Southern French Alps). *Permafrost and Periglacial Processes*, *28*(1), 209–223. https://doi.org/10.1002/ppp.1887

Bodin, X., Krysiecki, J.-M., & Anacona, P. I. (2012). Recent collapse of rock glaciers: two study cases in the Alps and in the Andes. *12th Congress, Protection of Living Spaces from Natural Hazards, Interpraevent 2012*.

Buchli, T., Kos, A., Limpach, P., Merz, K., Zhou, X., & Springman, S. M. (2018). Kinematic investigations on the Furggwanghorn Rock Glacier, Switzerland. *Permafrost and Periglacial Processes*, *29*(1), 3–20. https://doi.org/10.1002/PPP.1968

Buchli, T., Merz, K., Zhou, X., Kinzelbach, W., & Springman, S. M. (2013). Characterization and Monitoring of the Furggwanghorn Rock Glacier, Turtmann Valley, Switzerland: Results from 2010 to 2012. *Vadose Zone Journal*, *12*(1), 1–15. https://doi.org/10.2136/vzj2012.0067

Bundesamt für Landestopografie swisstopo. (2024, January 8). *Fotogrammetrie und Landeskarten*. https://www.swisstopo.admin.ch/de/neue-verfahren

Cicoira, A. (2020). *On the Dynamics of Rock Glaciers*. University of Zurich.

Cicoira, A., Marcer, M., Gärtner-Roer, I., Bodin, X., Arenson, L. U., & Vieli, A. (2021). A general theory of rock glacier creep based on in-situ and remote sensing observations. *Permafrost and Periglacial Processes*, *32*(1), 139–153. https://doi.org/10.1002/PPP.2090

Davies, M., Hamza, O., & Harris, C. (2001). The Effect of Rise in Mean Annual Temperature on the Stability of Rock Slopes Containing Ice-Filled Discontinuities. *Permafrost and Periglacial Processes*, *12*, 137–144. https://doi.org/10.1002/ppp

Delaloye, R., & Lambiel, C. (2005). Evidence of winter ascending air circulation throughout talus slopes and rock glaciers situated in the lower belt of alpine discontinuous permafrost (Swiss Alps). *Norsk Geografisk Tidsskrift*, *59*(2), 194–203. https://doi.org/10.1080/00291950510020673

Delaloye, R., Lambiel, C., & Gärtner-Roer, I. (2010). Overview of rock glacier kinematics research in the Swiss Alps. *Geogr. Helv.*, *65*, 135–145. https://doi.org/https://doi.org/10.5194/gh-65-135-2010

Delaloye, R., & Morard, S. (2011). Le glacier rocheux déstabilisé du Petit-Vélan (Val d'En-tremont, Valais) : morphologie de surface, vitesses de déplacement et structure interne. In *La géomorphologique alpine: entre patrimoine et contrainte. Actes du colloque de la Société Suisse de Géomorphologie*. Institut de géographie, Université de Lausanne.

Delaloye, R., Morard, S., Barboux, C., Abbet, D., Gruber, V., Riedo, M., & Gachet, S. (2013). Rapidly moving rock glaciers in Mattertal. In C. Graf (Ed.), *Mattertal-ein Tal in Bewegung, Publikation zur Jahrestagung der Schweizerischen Geomorphologischen Gesellschaft* (pp. 21–31).

Durisch, F. (2023). *Long-term evolution of different permafrost landforms on the northern slope of Piz Corvatsch, Engadin* [MSc-Thesis]. University of Zurich.

Eriksen, H., Rouyet, L., Lauknes, T. R., Berthling, I., Isaksen, K., Hindberg, H., Larsen, Y., & Corner, G. D. (2018). Recent Acceleration of a Rock Glacier Complex, Ádjet, Norway, Documented by 62 Years of Remote Sensing Observations. *Geophysical Research Letters*, *45*(16), 8314–8323. https://doi.org/10.1029/2018GL077605

Ghirlanda, A., Braillard, L., Delaloye, R., Kummert, M., & Staub, B. (2016). The complex pluri-decennial and multiphasic destabilization of the Jegi rock glacier (western Swiss Alps): historical development and ongoing crisis. *XI. International Conference On Permafrost, Potsdam, Germany*, 20–24. https://doi.org/10.1016/j.isprsjprs.2015.09.010

Gnägi, C., & Labhart, T. P. (2017). *Geologie der Schweiz* (10th ed.). Ott.

Güngör, R., Uzar, M., Atak, B., Yilmaz, O. S., & Gümüs, E. (2022). Orthophoto production and accuracy analysis with UAV photogrammetry. *Mersin Photogrammetry Journal*, *4*(1), 1–6. https://doi.org/10.53093/MEPHOJ.1122615

Haeberli, W. (1985). Creep of mountain permafrost: internal structure and flow of alpine rock glaciers. *Mitteilungen Der Versuchsanstalt Fur Wasserbau, Hydrologie Und Glaziologie an Der Eidgenossischen Technischen Hochschule Zurich*, *77*.

Haeberli, W., Haeberli, W., Huder, J., Keusen, H.-R., Pika, J., & Rathlisberger, H. (1988). Core drilling through rock glacier permafrost. *Proceedings of the Fifth International Conference on Permafrost*, 937–942.

Haeberli, W., Hallet, B., Arenson, L., Elconin, R., Humlum, O., Kääb, A., Kaufmann, V., Ladanyi, B., Matsuoka, N., Springman, S., & Mühll, D. V. (2006). Permafrost creep and rock glacier dynamics. In *Permafrost and Periglacial Processes* (Vol. 17, Issue 3, pp. 189–214). John Wiley and Sons Ltd. https://doi.org/10.1002/ppp.561

Haeberli, W., & Vonder Mühll, D. (1996). On the characteristics and origin of ice in rock glacier permafrost. *Zeitschrift Für Geomorphologie*, 43–57.

Hanson, S., & Hoelzle, M. (2004). The thermal regime of the active layer at the Murtèl rock glacier based on data from 2002. *Permafrost and Periglacial Processes*, *15*(3), 273–282. https://doi.org/10.1002/ppp.499

Hartl, L., Fischer, A., Stocker-Waldhuber, M., & Abermann, J. (2016). Recent speed-up of an alpine rock glacier: an updated chronology of the kinematics of outer hochebenkar rock glacier based on geodetic measurements. *Geografiska Annaler: Series A, Physical Geography*, *98*(2), 129–141. https://doi.org/10.1111/GEOA.12127

Hashim, K. A., Darwin, N. H., Ahmad, A., & Samad, A. M. (2013). Assessment of low altitude aerial data for large scale urban environmental mapping. *Proceedings - 2013 IEEE 9th International Colloquium on Signal Processing and Its Applications, CSPA 2013*, 229–234. https://doi.org/10.1109/CSPA.2013.6530047

Hausmann, H., Krainer, K., Brückl, E., & Mostler, W. (2007). Internal structure and ice content of Reichenkar rock glacier (Stubai Alps, Austria) assessed by geophysical investigations. *Permafrost and Periglacial Processes*, *18*(4), 351–367. https://doi.org/10.1002/ppp.601

Hausmann, H., Krainer, K., Brückl, E., & Wien, T. U. (2012). Internal structure, ice content and dynamics of Ölgrube and Kaiserberg rock glaciers (Ötztal Alps, Austria) determined from geophysical surveys. *Austrian Journal of Earth Sciences*, *105*(2), 12–31. https://www.researchgate.net/publication/291210077

Heid, T., & Kääb, A. (2012). Evaluation of existing image matching methods for deriving glacier surface displacements globally from optical satellite imagery. *Remote Sensing of Environment*, *118*, 339–355. https://doi.org/10.1016/j.rse.2011.11.024

Heisig, H., & Simmen, J. L. (2021). Re-engineering the Past: Countrywide Geo-referencing of Archival Aerial Imagery. *PFG - Journal of Photogrammetry, Remote Sensing and Geoinformation Science*, *89*(6), 487–503. https://doi.org/10.1007/S41064-021-00162-Z

Ikeda, A., Matsuoka, N., & Kääb, A. (2008). Fast deformation of perennially frozen debris in a warm rock glacier in the Swiss Alps: An effect of liquid water. *Journal of Geophysical Research: Earth Surface*, *113*(F1). https://doi.org/10.1029/2007JF000859

IPCC. (2023). Summary for Policimakers. In Core Writing Team, H. Lee, & J. Romero (Eds.), *Climate Change 2023: Syntehsis Report. Contribution of Working Groups I, II and III to the Sixth Assessment Report of the Intergovernmental Panel on Climate Change* (pp. 1–34). IPCC. https://doi.org/10.59327/IPCC/AR6-9789291691647.001

Kääb, A. (2005). *Remote sensing of mountain glaciers and permafrost creep* (W. Haeberli & M. Maisch, Eds.). Geographisches Institut der Universität Zürich.

Kääb, A., Frauenfelder, R., & Roer, I. (2007). On the response of rockglacier creep to surface temperature increase. *Global and Planetary Change*, *56*(1–2), 172–187. https://doi.org/10.1016/J.GLOPLACHA.2006.07.005

Kääb, A., & Reichmuth, T. (2005). Advance mechanisms of rock glaciers. *Permafrost and Periglacial Processes*, *16*(2), 187–193. https://doi.org/10.1002/ppp.507

Kääb, A., & Vollmer, M. (2000). Surface Geometry, Thickness Changes and Flow Fields on Creeping Mountain Permafrost: Automatic Extraction by Digital Image Analysis. *PROCESSES Permafrost Periglac. Process*, *11*, 315–326. https://doi.org/10.1002/1099-1530(200012)11:4

Kaufmann, V., & Ladstädter, R. (2002). Spatio-temporal analysis of the dynamic behaviour of the Hochebenkar rock glaciers (Oetztal Alps, Austria) by means of digital photogrammetric methods. *6th International Symposium on High Mountain Remote Sensing Cartography 2000*.

Kellerer-Pirklbauer, A., Bodin, X., Delaloye, R., Lambiel, C., Gärtner-Roer, I., Bonnefoy-Demongeot, M., Carturan, L., Damm, B., Eulenstein, J., Fischer, A., Hartl, L., Ikeda, A., Kaufmann, V., Krainer, K., Matsuoka, N., Di Cella, U. M., Noetzli, J., Seppi, R., Scapozza, C., … Zumiani, M. (2024). Acceleration and interannual variability of creep rates in mountain permafrost landforms (rock glacier velocities) in the European Alps in 1995-2022. *Environmental Research Letters*, *19*(3). https://doi.org/10.1088/1748-9326/AD25A4

Kofler, C., Mair, V., Gruber, S., Todisco, M. C., Nettleton, I., Steger, S., Zebisch, M., Schneiderbauer, S., & Comiti, F. (2021). When do rock glacier fronts fail? Insights from two case studies in South Tyrol (Italian Alps). *Earth Surface Processes and Landforms*, *46*(7), 1311–1327. https://doi.org/10.1002/ESP.5099

Korumaz, S. A. G., & Yildiz, F. (2021). Positional Accuracy Assessment of Digital Orthophoto Based on UAV Images: An Experience on an Archaeological Area. *Heritage 2021, Vol. 4, Pages 1304-1327*, *4*(3), 1304–1327. https://doi.org/10.3390/HERITAGE4030071

Kummert, M., Delaloye, R., & Braillard, L. (2017). Erosion and sediment transfer processes at the front of rapidly moving rock glaciers: Systematic observations with automatic cameras in the western Swiss Alps. *Permafrost and Periglacial Processes*, *29*(1), 21–33. https://doi.org/10.1002/PPP.1960

Lambiel, C. (2011). Le glacier rocheux déstabilisé de Tsaté-Moiry (VS) : caractéristiques morphologiques et vitesses de déplacement. *La Géomorphologie Alpine: Entre Patri- Moine et Contrainte. Actes Du Colloque de La Société Suisse de Géomorphologie*.

Marcer, M., Cicoira, A., Cusicanqui, D., Bodin, X., Echelard, T., Obregon, R., & Schoeneich, P. (2021). Rock glaciers throughout the French Alps accelerated and destabilised since 1990 as air temperatures increased. *Communications Earth & Environment 2021 2:1*, *2*(1), 1–11. https://doi.org/10.1038/s43247-021-00150-6

Marcer, M., Ringsø Nielsen, S., Ribeyre, C., Kummert, M., Duvillard, P. A., Schoeneich, P., Bodin, X., & Genuite, K. (2020). Investigating the slope failures at the Lou rock glacier front, French Alps. *Permafrost and Periglacial Processes*, *31*(1), 15–30. https://doi.org/10.1002/PPP.2035

Marcer, M., Serrano, C., Brenning, A., Bodin, X., Goetz, J., & Schoeneich, P. (2019). Evaluating the destabilization susceptibility of active rock glaciers in the French Alps. *The Cryosphere*, *13*(1), 141–155. https://doi.org/10.5194/tc-13-141-2019

Moore, P. L. (2014). Deformation of debris-ice mixtures. In *Reviews of Geophysics* (Vol. 52, Issue 3, pp. 435–467). Blackwell Publishing Ltd. https://doi.org/10.1002/2014RG000453

Nuth, C., & Kääb. (2011). Co-registration and bias corrections of satellite elevation data sets for quantifying glacier thickness change. *Cryosphere*, *5*(1), 271–290. https://doi.org/10.5194/TC-5-271-2011

Nyenhuis, M., Hoelzle, M., & Dikau, R. (2005). Rock glacier mapping and permafrost distribution modelling in the Turtmanntal, Valais, Switzerland. *Zeitschrift Fur Geomorphologie*, *49*(3), 275–292.

Otto, J. C., & Dikau, R. (2004). Geomorphologic system analysis of a high mountain valley in the Swiss Alps. *Zeitschrift Für Geomorphologie*, *48*(3), 323–341. https://doi.org/10.1127/zfg/48/2004/323

PERMOS. (2019). *Permafrost in Switzerland 2014/2015 to 2017/2018*. https://doi.org/10.13093/permos-rep-2019-16-19

PERMOS. (2024). *Swiss Permafrost Bulletin 2023* (J. Noetzli & C. Pellet, Eds.; No 5). https://doi.org/10.13093/permos-bull-24

Redpath, T. A. N., Sirguey, P., Fitzsimons, S. J., & Kääb, A. (2013). Accuracy assessment for mapping glacier flow velocity and detecting flow dynamics from ASTER satellite imagery: Tasman Glacier, New Zealand. *Remote Sensing of Environment*, *133*, 90–101.

Reynard, E., Lambiel, C., Delaloye, R., Devaud, G., Baron, L., Chapellier, D., Marescot, L., & Monnet, R. (2003). Glacier/permafrost relationships in recently deglaciated forefields of small alpine glaciers, Penninic Alps, Valais, Western Switzerland. *Proceedings of the 8th International Conference on Permafrost*, 947–952.

RGIK. (2023). *Guidelines for inventorying rock glaciers: baseline and practical concepts (version 1.0)*. IPA Action Group Rock glacier inventories and kinematics. https://doi.org/10.51363/unifr.srr.2023.002

Roer, I., Haeberli, W., Avian, M., Kaufmann, V., Delaloye, R., Lambiel, C., & Kääb, A. (2008). Observations and considerations on destabilizing active rock glaciers in the European Alps. *9th International Conference on Permafrost*, 1505–1510. https://doi.org/10.5167/uzh-6082

Roer, I., Kääb, A., & Dikau, R. (2005). Rockglacier acceleration in the Turtmann valley (Swiss Alps): Probable controls. *Norsk Geografisk Tidsskrift - Norwegian Journal of Geography*, *59*(2), 157–163. https://doi.org/10.1080/00291950510020655

Scheffler, D., Hollstein, A., Diedrich, H., Segl, K., & Hostert, P. (2017). AROSICS: An automated and robust open-source image co-registration software for multi-sensor satellite data. *Remote Sensing*, *9*(7). https://doi.org/10.3390/rs9070676

Schoeneich, P., Bodin, X., Echelard, T., & Kaufmann, V. (2015). Velocity Changes of Rock Glaciers and Induced Hazards. *Engineering Geology for Society and Territory - Volume 1: Climate Change and Engineering Geology*, 223–227. https://doi.org/10.1007/978-3-319-09300-0_42

Scotti, R., Crosta, G. B., & Villa, A. (2016). Destabilisation of Creeping Permafrost: The Plator Rock Glacier Case Study (Central Italian Alps). *Permafrost and Periglacial Processes*, *28*(1), 224–236. https://doi.org/10.1002/ppp.1917

Springman, S. M., Yamamoto, Y., Buchli, T., Hertrich, M., Maurer, H., Merz, K., Gärtner-Roer, I., & Seward, L. (2013). Rock glacier degradation and instabilities in the European Alps: a characterisation and monitoring experiment in the Turtmanntal, CH. In C. Margottini, P. Canuti, & K. Sassa (Eds.), *Landslide Science and Practice* (pp. 5–13). Springer. https://doi.org/10.1007/978-3-642-31337-0_1

Tatenhove, F. van, & Dikau, R. (1990). Past and Present Permafrost Distribution in the Turtmanntal, Wallis, Swiss Alps. *Arctic and Alpine Research*, *22*(3), 302–316. https://doi.org/10.1080/00040851.1990.12002794

Tsai, C. H., & Lin, Y. C. (2017). An accelerated image matching technique for UAV orthoimage registration. *ISPRS Journal of Photogrammetry and Remote Sensing*, *128*, 130–145. https://doi.org/10.1016/J.ISPRSJPRS.2017.03.017

Vivero, S., Hendrickx, H., Frankl, A., Delaloye, R., & Lambiel, C. (2022). Kinematics and geomorphological changes of a destabilising rock glacier captured from close-range sensing techniques (Tsarmine rock glacier, Western Swiss Alps). *Frontiers in Earth Science*, *10*, 1017949. https://doi.org/10.3389/FEART.2022.1017949/BIBTEX

Vollmer, M. (1999). *Kriechender alpiner Permafrost: Digitale photogrammetrische Bewegungsmessung* [Thesis]. University of Zurich.

Wangensteen, B., Gudmundsson, Á., Eiken, T., Kääb, A., Farbrot, H., & Etzelmüller, B. (2006). Surface displacements and surface age estimates for creeping slope landforms in Northern and Eastern Iceland using digital photogrammetry. *Geomorphology*, *80*(1–2), 59–79. https://doi.org/10.1016/j.geomorph.2006.01.034

Wicky, J., & Hauck, C. (2017). Numerical modelling of convective heat transport by air flow in permafrost talus slopes. *Cryosphere*, *11*(3), 1311–1325. https://doi.org/10.5194/tc-11-1311-2017

14. Appendix

Displacement vectors

Brändjitelli

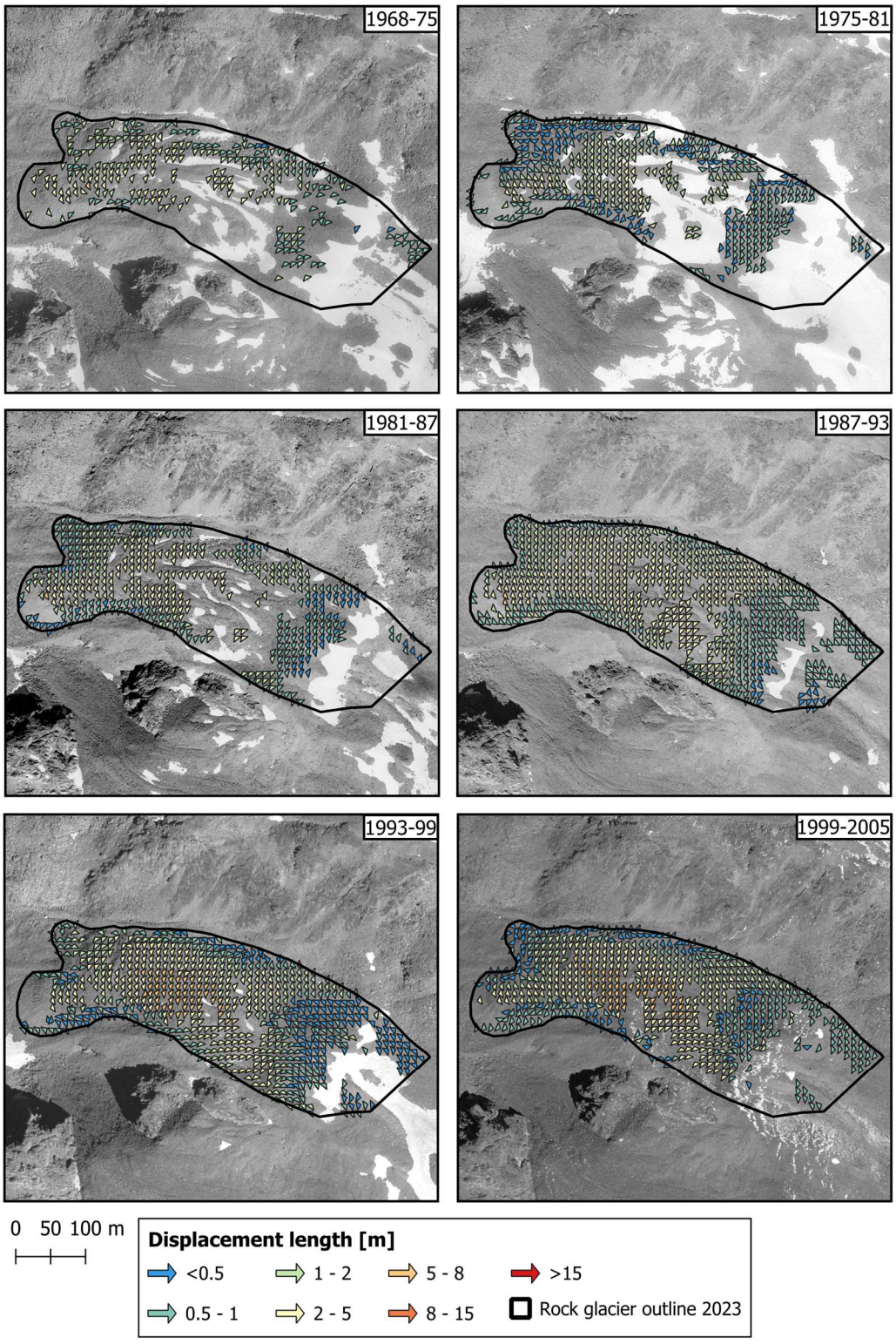

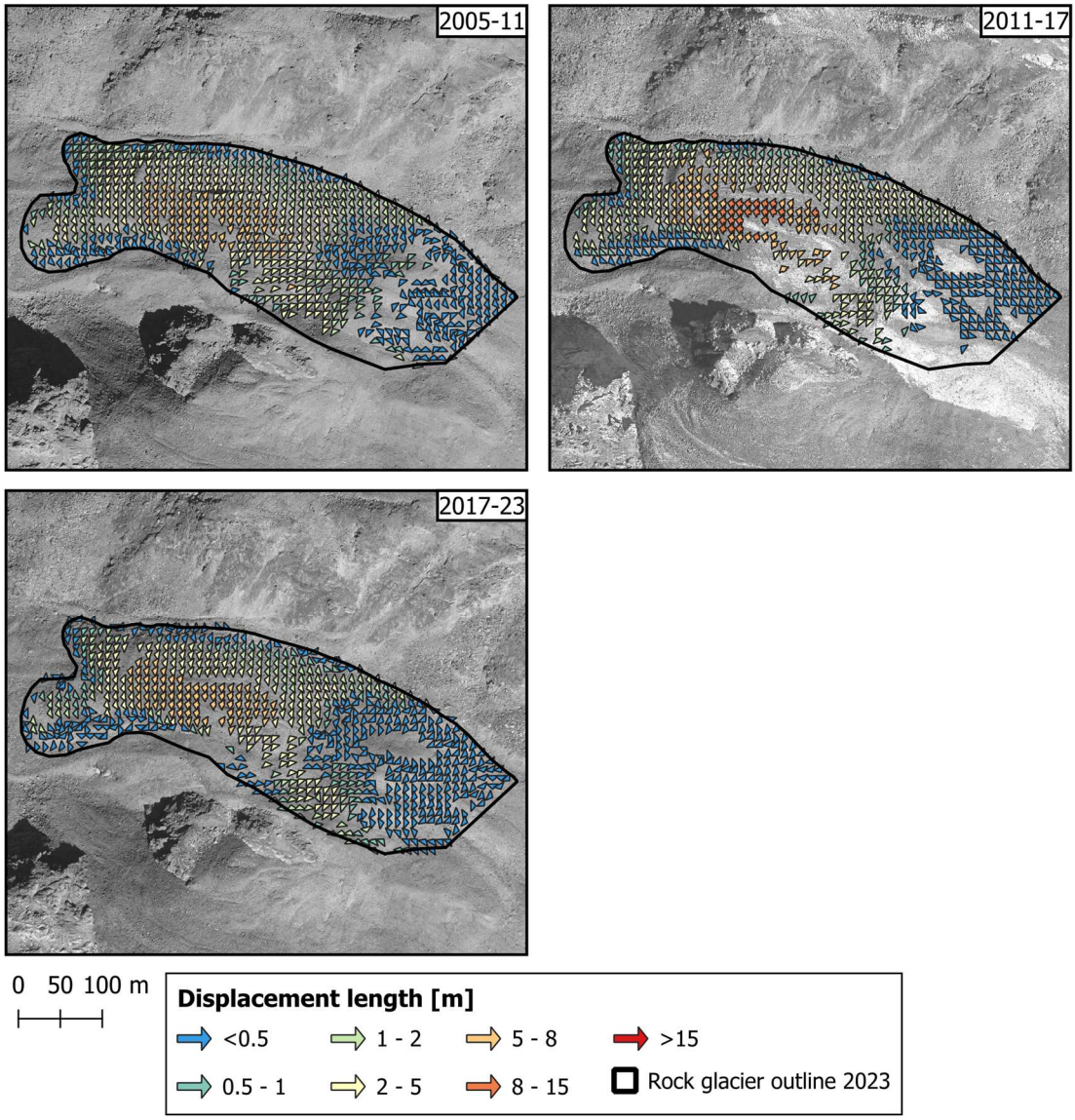
2005-11
2011-17
2017-23
0 50 100 m
Displacement length [m]
<0.5
0.5 - 1
1 - 2
2 - 5
5 - 8
8 - 15
>15
Rock glacier outline 2023

Furggwang

For the 6-year intervals, no meaningful results could be generated in recent years. Therefore, the 3-year intervals are displayed instead. However, it must be noted that a direct comparison between data with different interval lengths is not recommended, as the displayed values represent absolute displacement values.

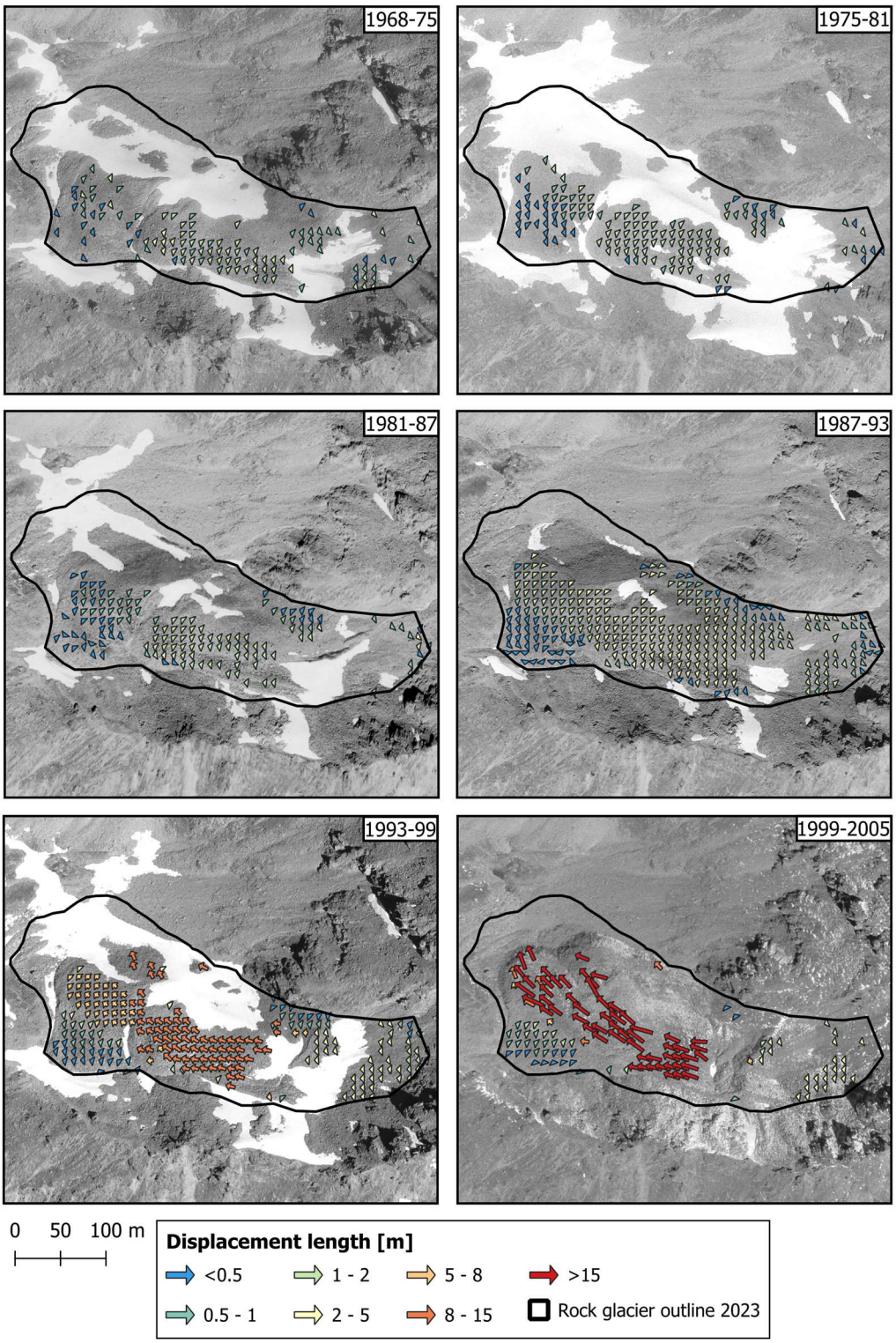

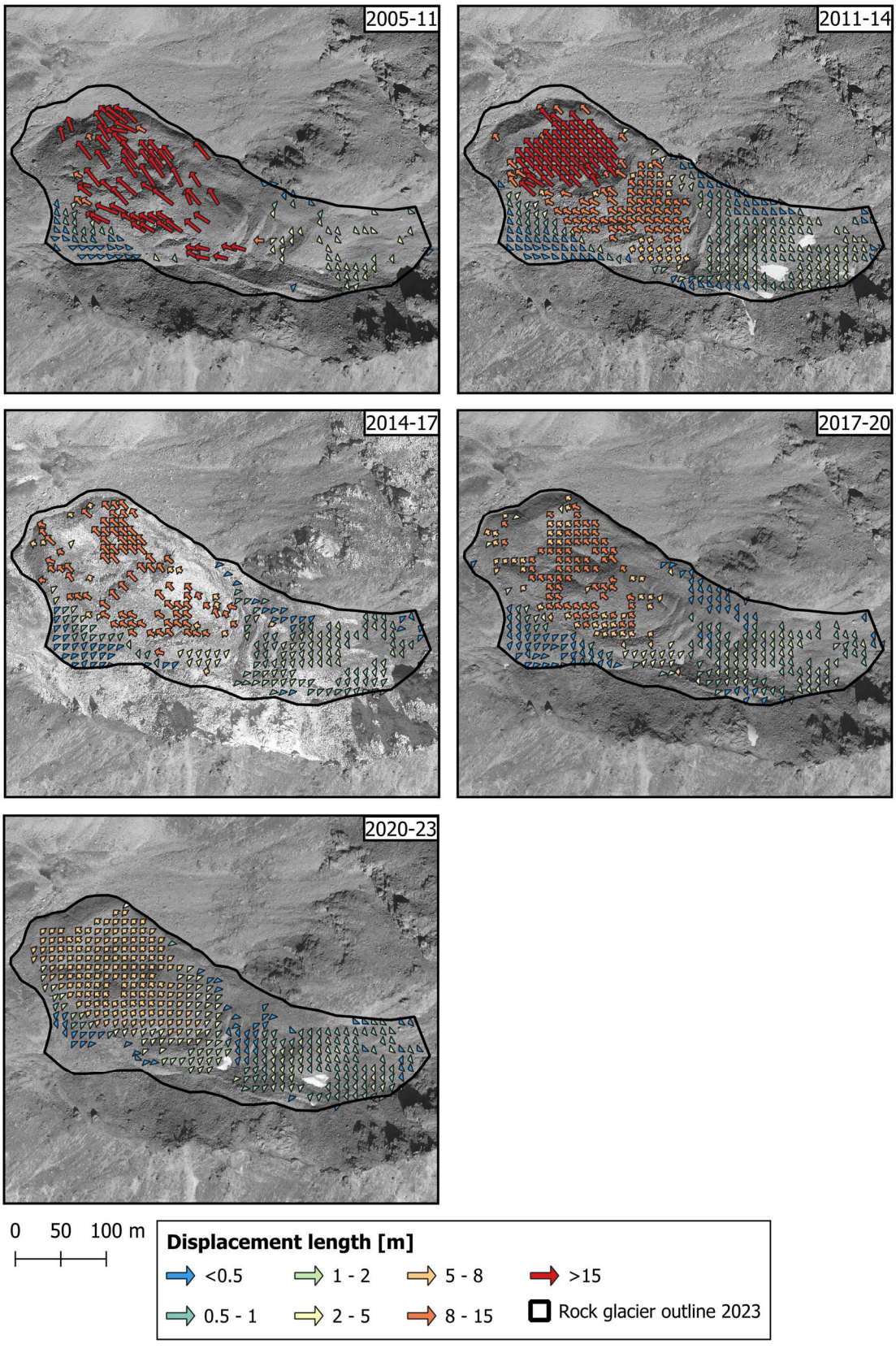
2005-11
2011-14
2014-17
2017-20
2020-23
0 50 100 m
Displacement length [m]
<0.5
0.5 - 1
1 - 2
2 - 5
5 - 8
8 - 15
>15
Rock glacier outline 2023

Gruob

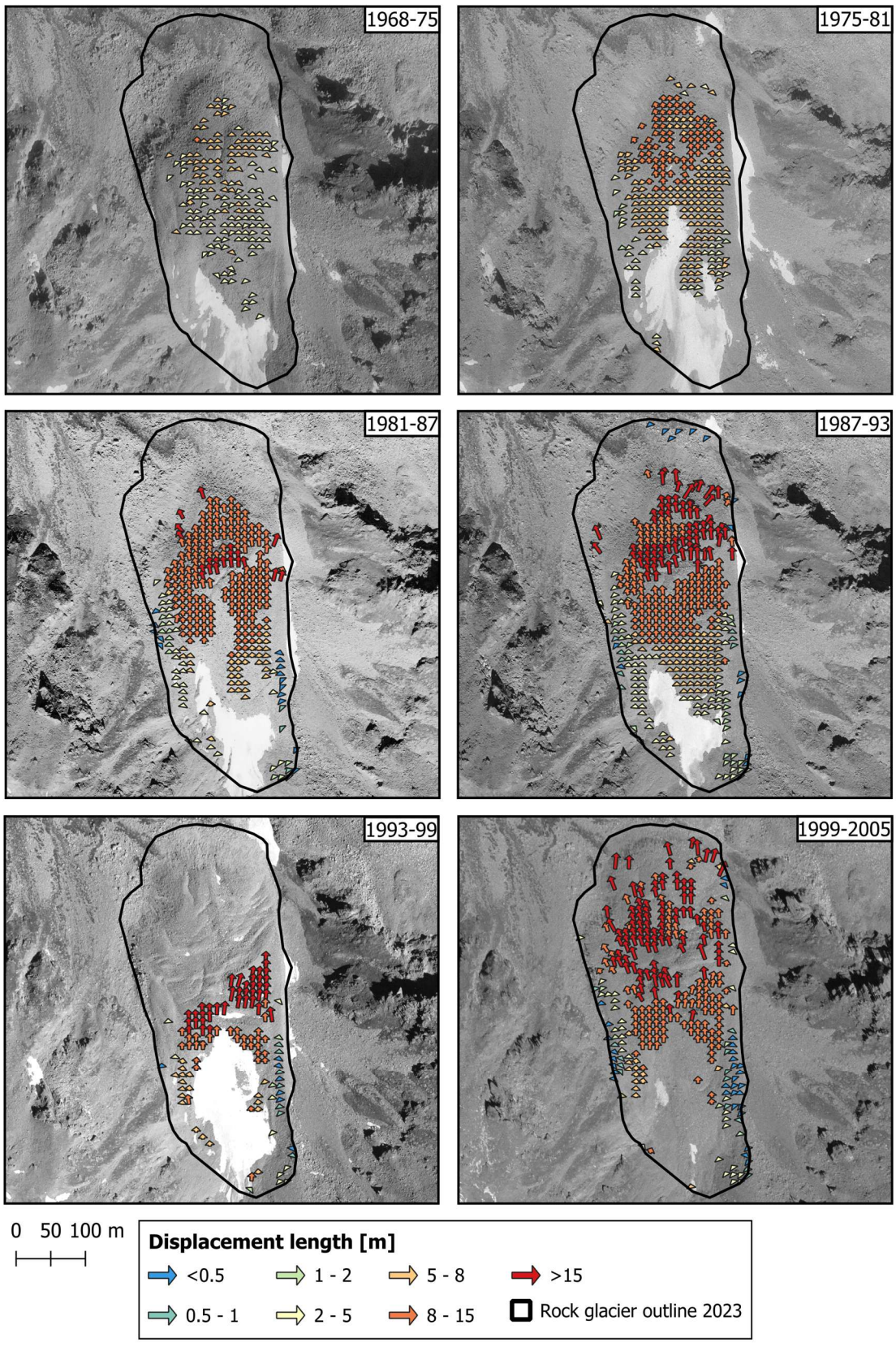
1968-75
1975-81
1981-87
1987-93
1993-99
1999-2005
0 50 100 m
Displacement length [m]
<0.5
0.5 - 1
1 - 2
2 - 5
5 - 8
8 - 15
>15
Rock glacier outline 2023

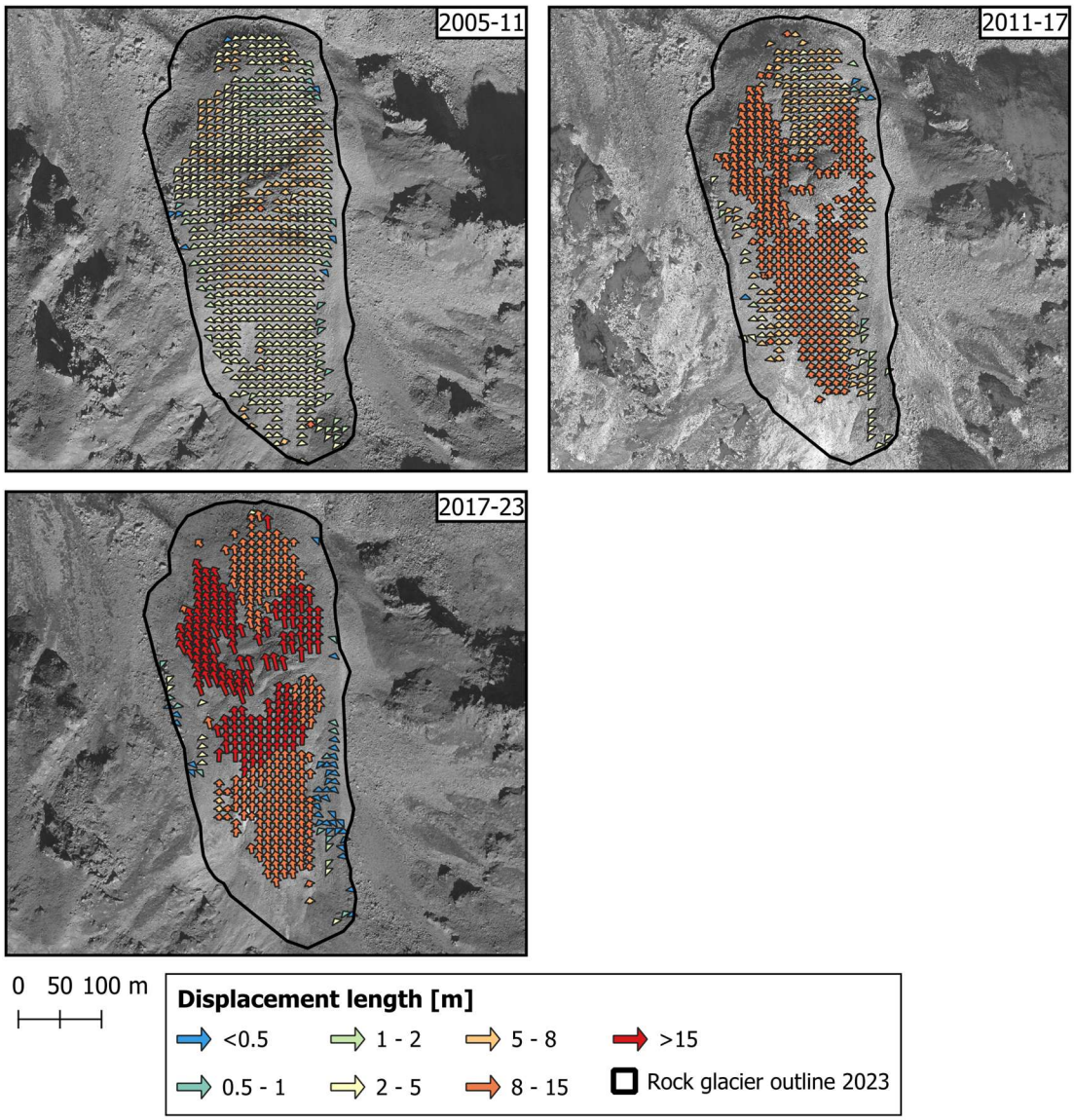
2005-11
2011-17
2017-23
0 50 100 m
Displacement length [m]
<0.5
0.5 - 1
1 - 2
2 - 5
5 - 8
8 - 15
>15
Rock glacier outline 2023

Gruobtälli

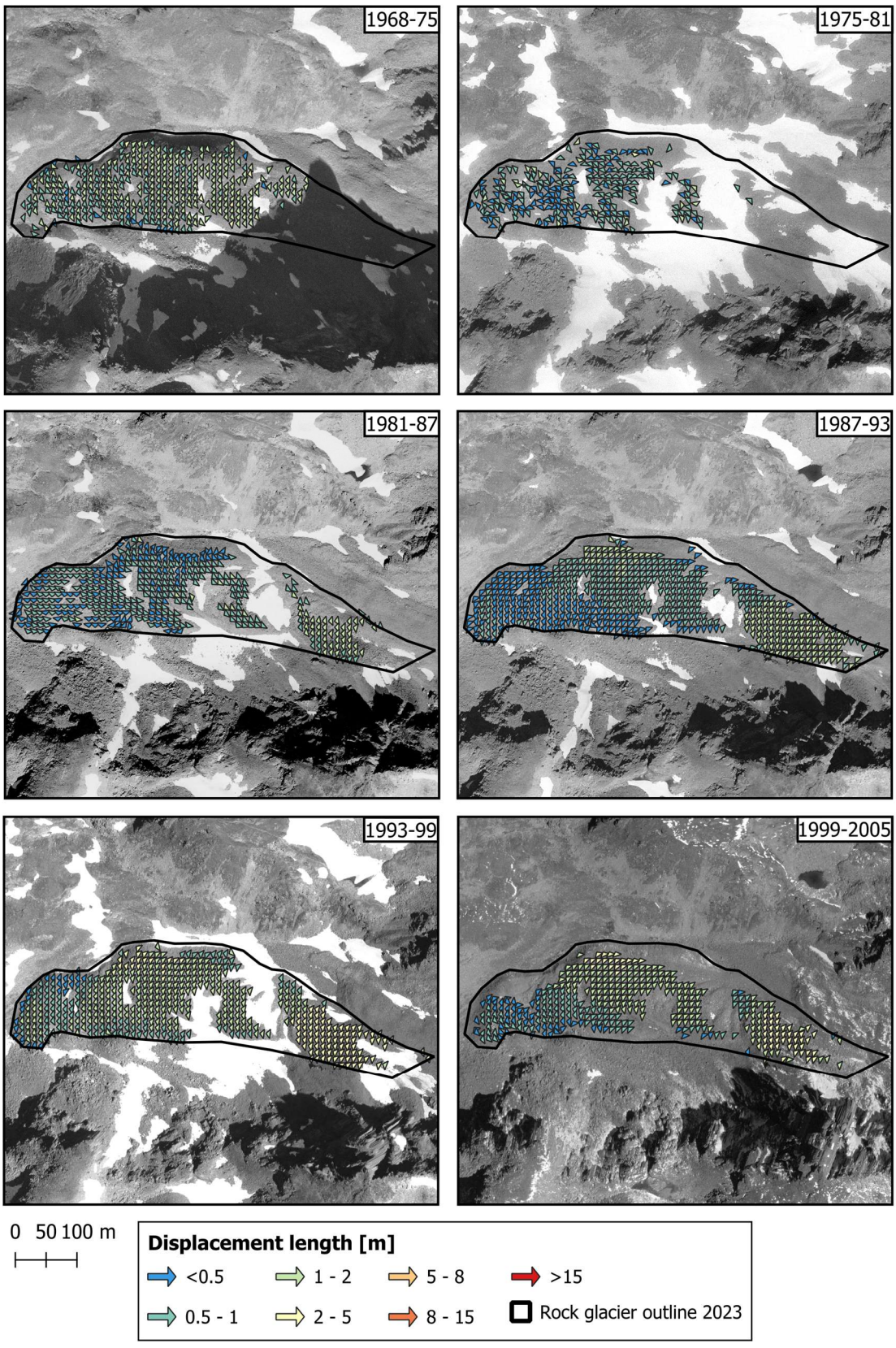
1968-75
1975-81
1981-87
1987-93
1993-99
1999-2005
0 50 100 m
Displacement length [m]
<0.5
0.5 - 1
1 - 2
2 - 5
5 - 8
8 - 15
>15
Rock glacier outline 2023

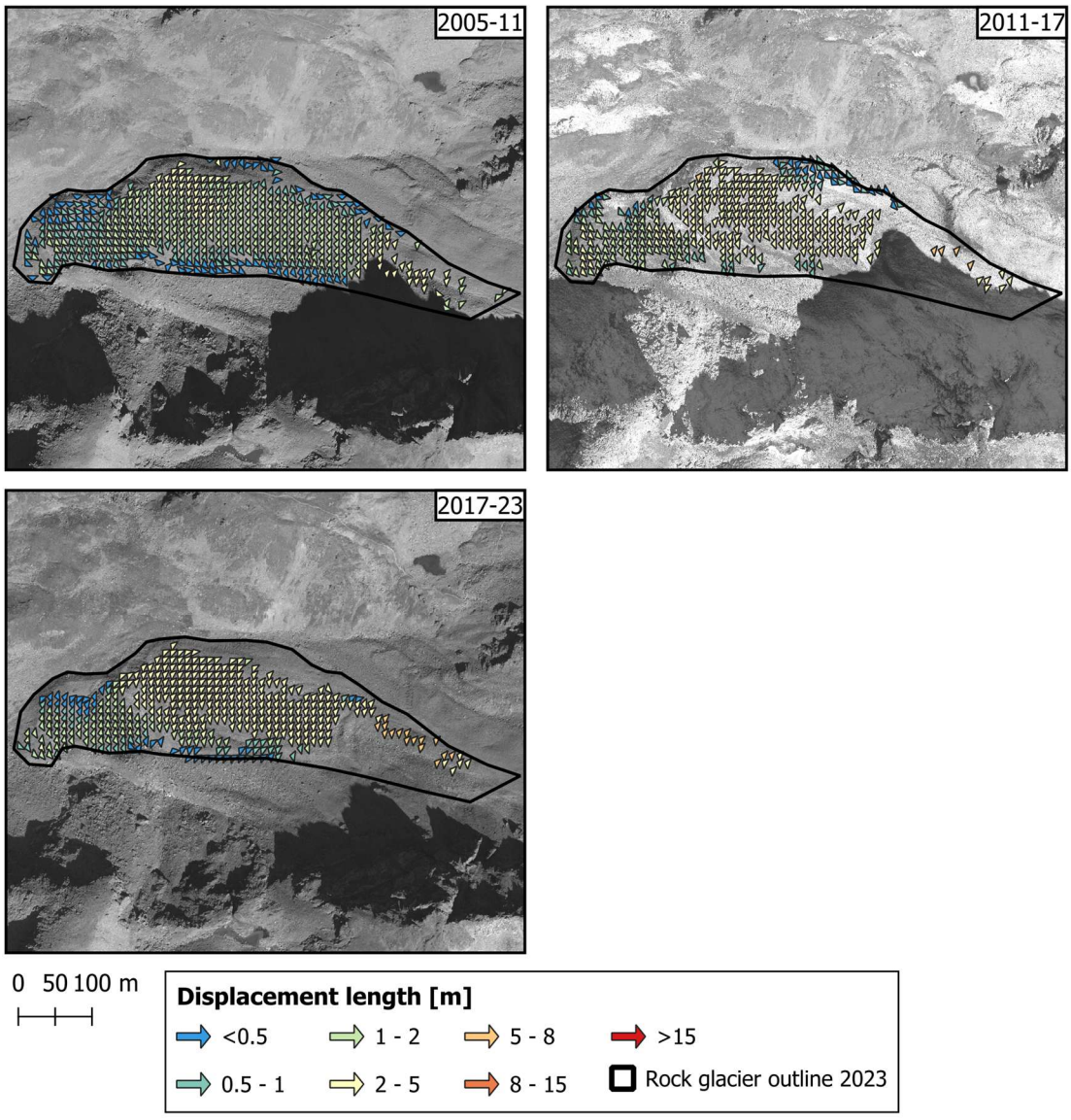
2005-11
2011-17
2017-23
0 50 100 m
Displacement length [m]
<0.5
0.5 - 1
1 - 2
2 - 5
5 - 8
8 - 15
>15
Rock glacier outline 2023

Hungerlihorli

Here, as for Brändjispitz, no values could be generated for the 1968–1975 period due to insufficient optical contrast.

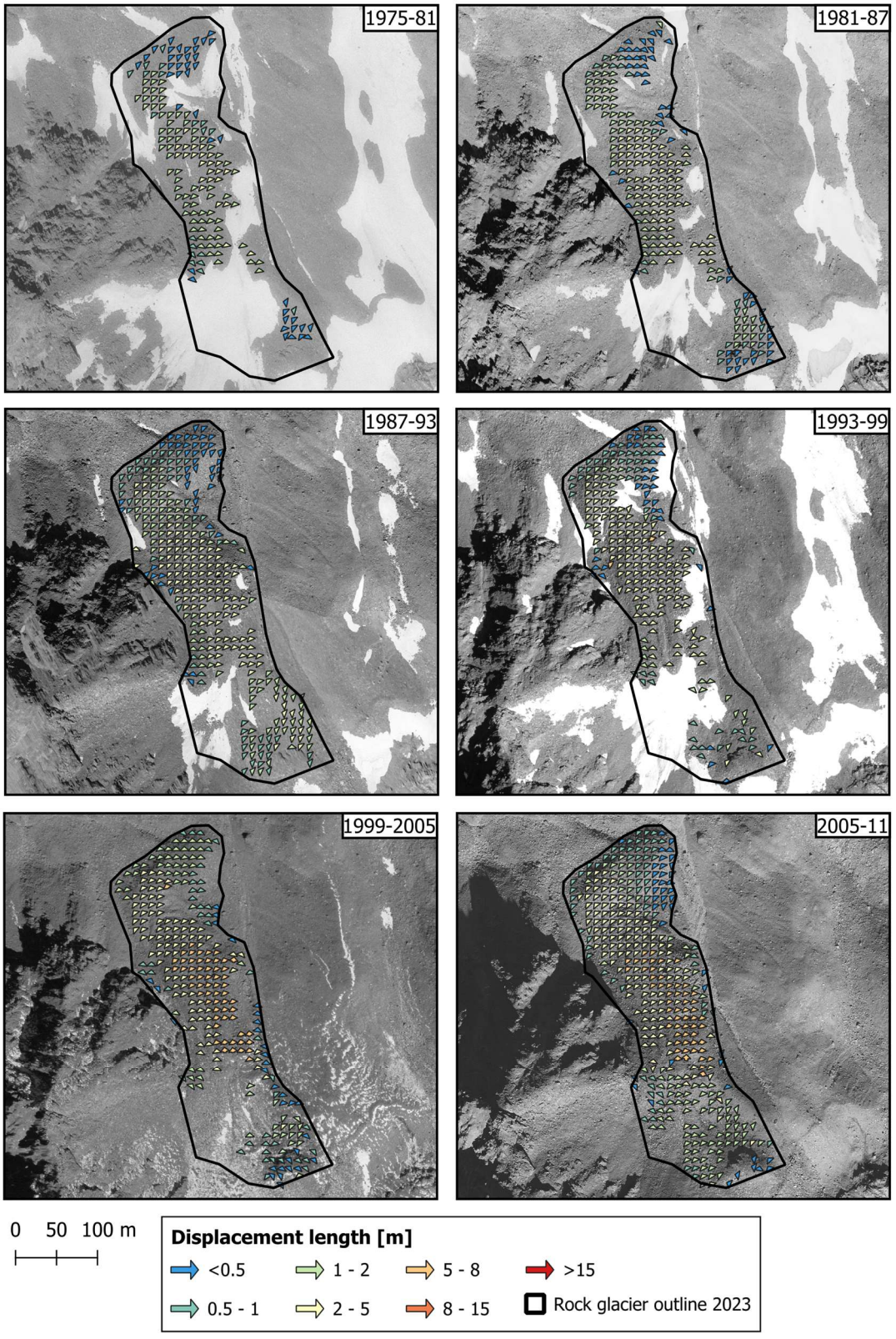

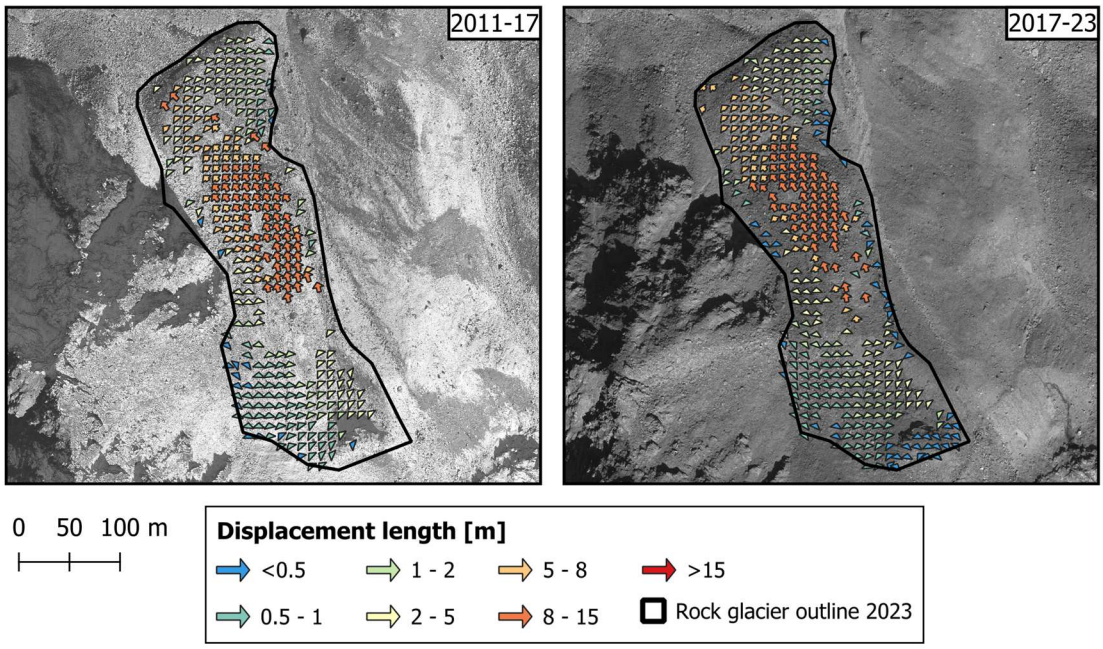
2011-17
2017-23
0 50 100 m
Displacement length [m]
<0.5
0.5 - 1
1 - 2
2 - 5
5 - 8
8 - 15
>15
Rock glacier outline 2023

Ritzuegg

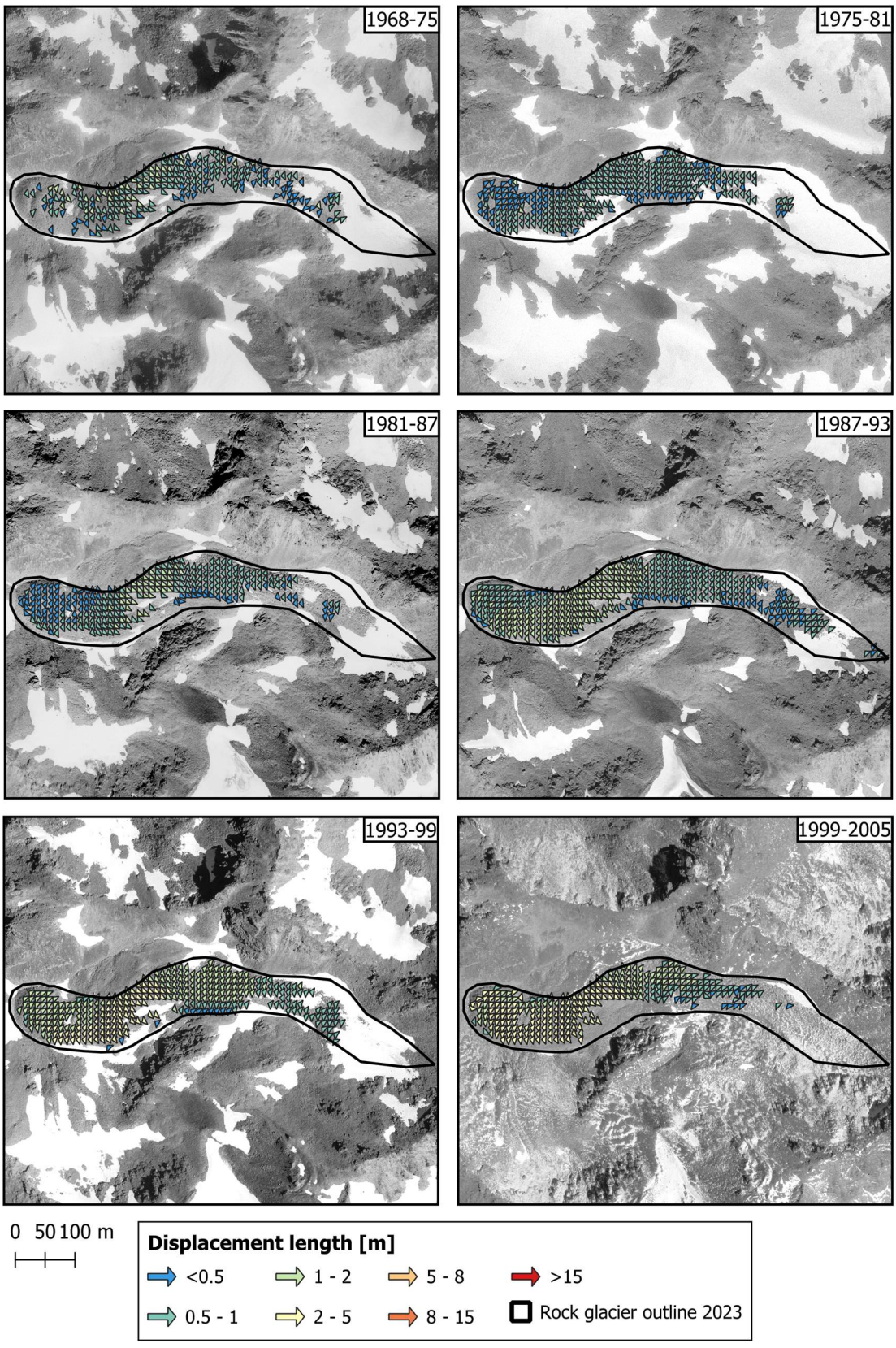
1968-75
1975-81
1981-87
1987-93
1993-99
1999-2005
0 50 100 m
Displacement length [m]
<0.5
0.5 - 1
1 - 2
2 - 5
5 - 8
8 - 15
>15
Rock glacier outline 2023

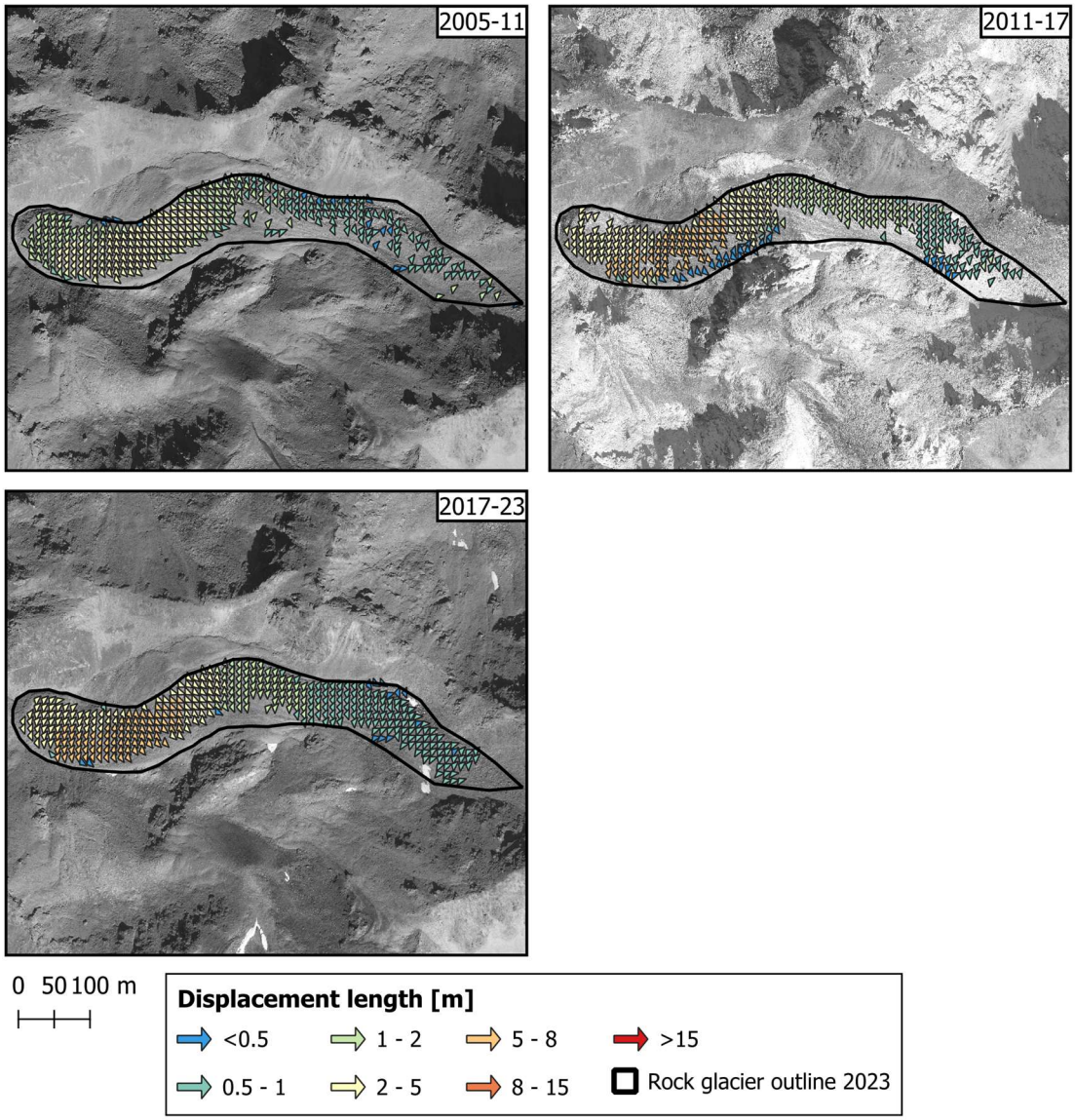
2005-11
2011-17
2017-23
0 50 100 m
Displacement length [m]
<0.5
0.5 - 1
1 - 2
2 - 5
5 - 8
8 - 15
>15
Rock glacier outline 2023

Roti Ritze

Also here, the 3-year intervals had to be used in the recent periods instead of 6-year intervals.

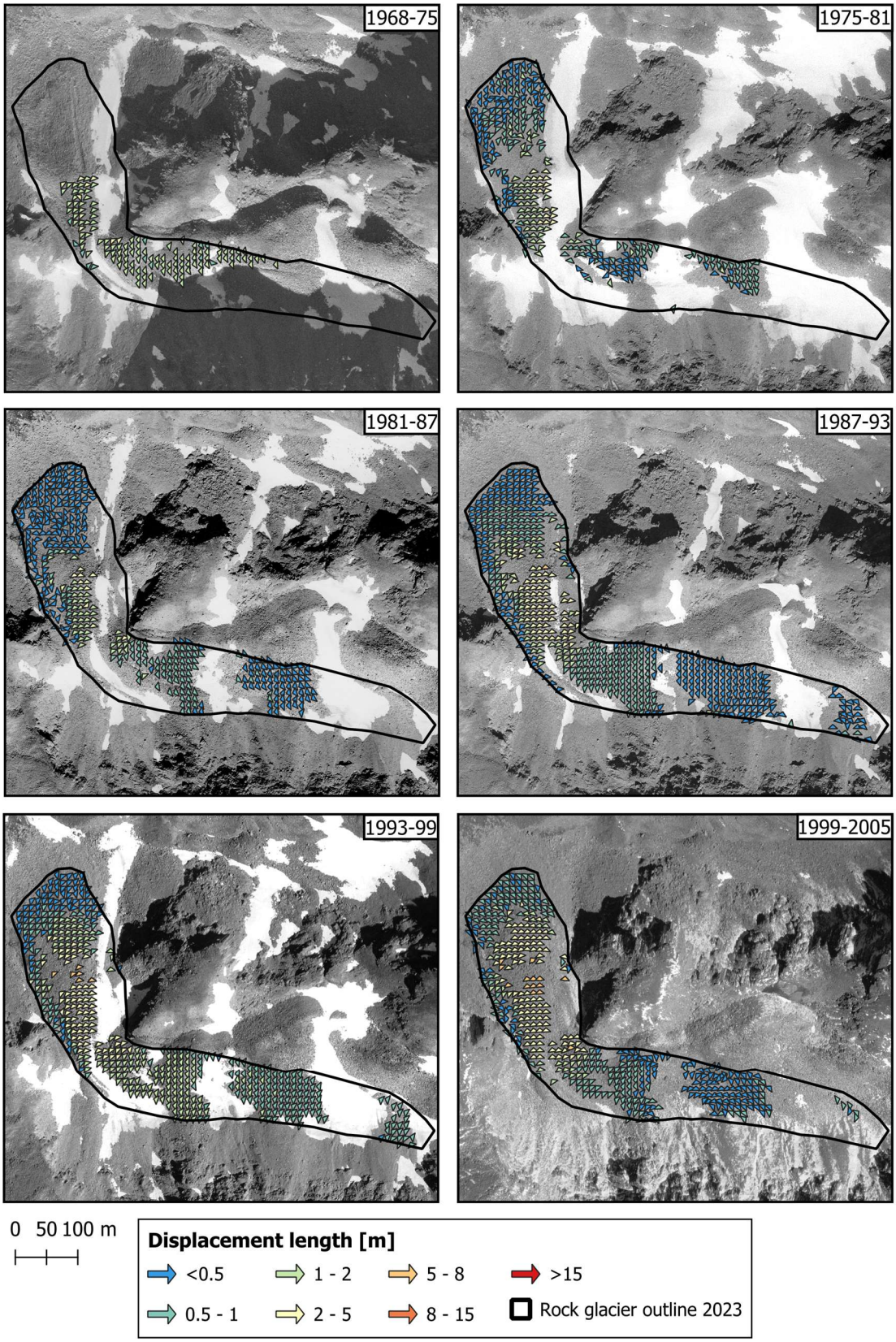

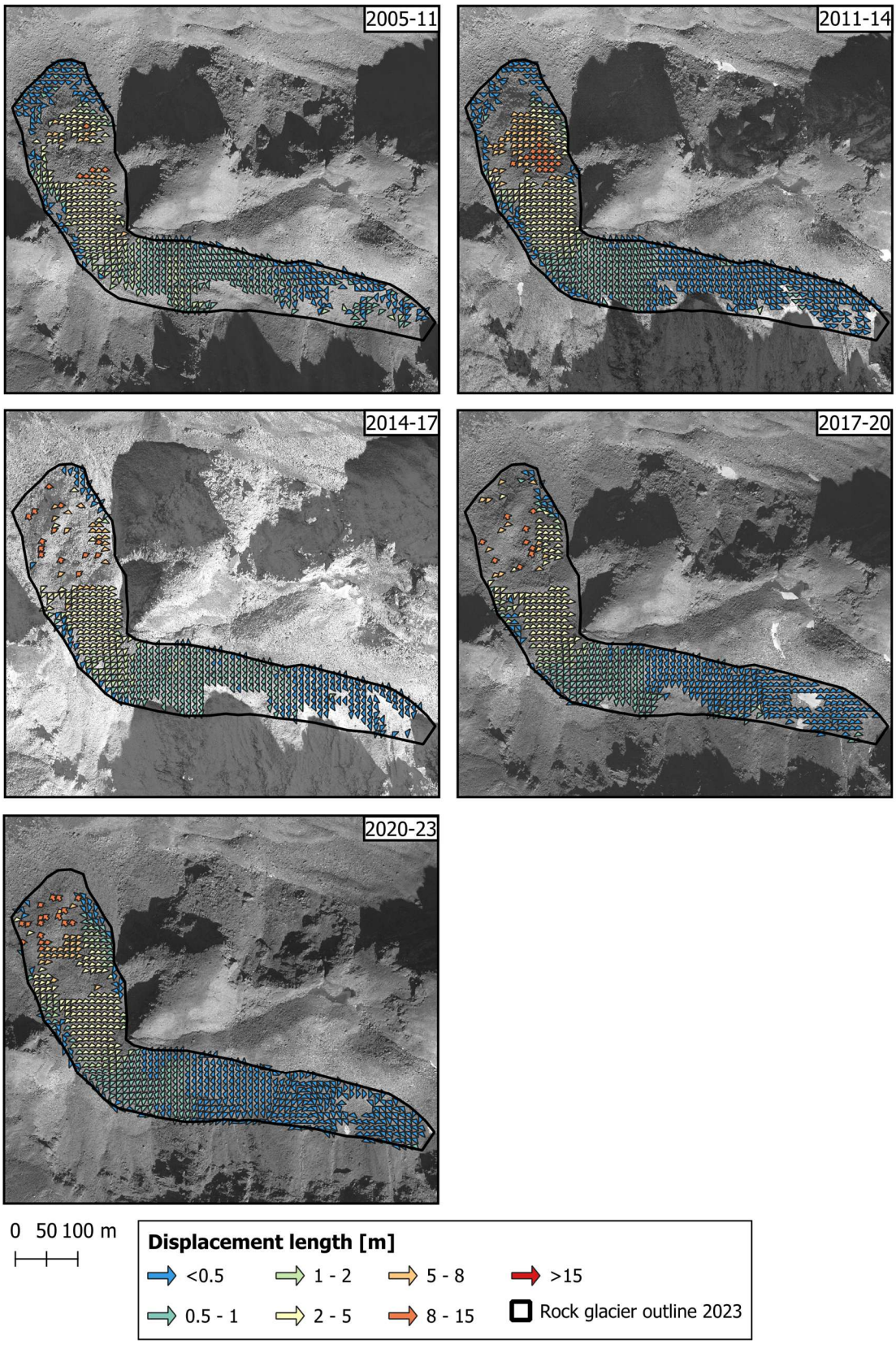
2005-11
2011-14
2014-17
2017-20
2020-23
0 50 100 m
Displacement length [m]
<0.5
0.5 - 1
1 - 2
2 - 5
5 - 8
8 - 15
>15
Rock glacier outline 2023

15. Personal declaration

I hereby declare that the submitted thesis is the result of my own, independent work. All external sources are explicitly acknowledged in the thesis.

During the preparation of this thesis, I used generative AI tools to assist with specific tasks such as language refinement and code implementation. The content, structure and interpretation presented are entirely my own and I take full responsibility for the submitted work.

Zurich, April 2025

Claudio Steffen